Electronic Supplementary Information I

tert – Butylnitrite promoted one – component based direct synthesis of 2- cyano substituted maleimide probes and their fluorescence turn – off sensing towards Fe^{3+}

Prabhat Sarkar[a], Shuba Paul[+a], Supratim Das[+a], Tania Chowdhury[b], Subham Mandal[c], Sanchita Goswami[a], Asim Bhaumik[b] and Chhanda Mukhopadhyay[a]*

[a]Department of Chemistry, University of Calcutta, 92 APC Road, Kolkata-700009, India.

*Corresponding author e-mail: cmukhop@yahoo.co.in

[b]School of Materials Sciences, Indian Association for the Cultivation of Science, 2A & 2B Raja S. C Mullick Road, Kolkata-700032, India

[c]School of Chemical Sciences, Indian Association for the Cultivation of Science, 2A & 2B Raja S. C Mullick Road, Kolkata-700032, India

[+]These authors contributed equally to this work.

Table of contents

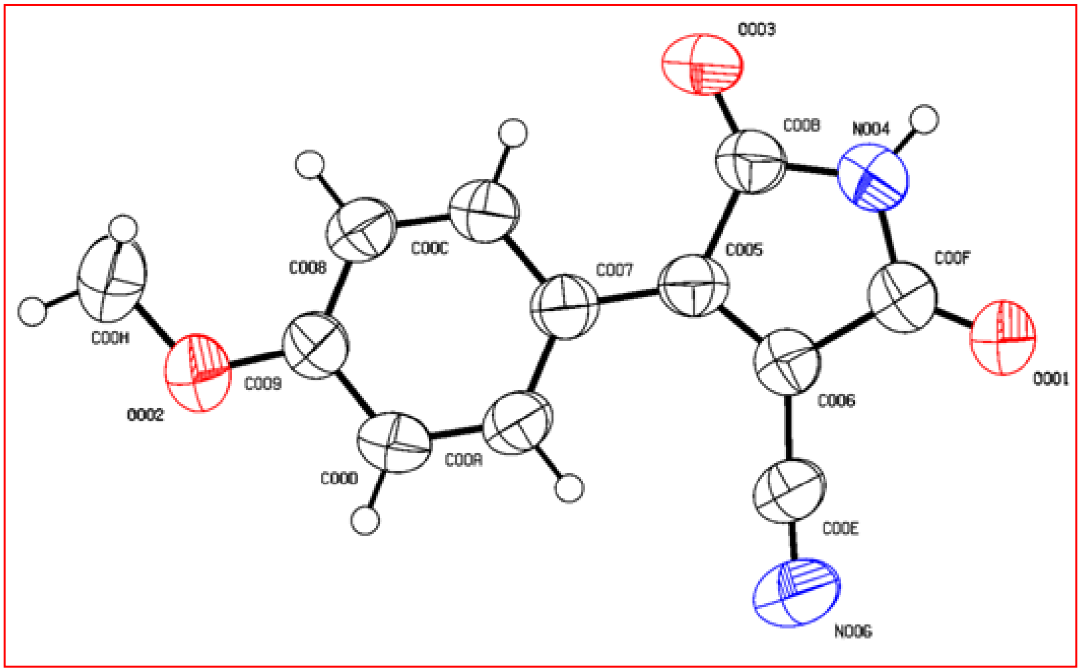

Figure 1: Molecular structure of compound **3c** with ellipsoids at the 50% probability level

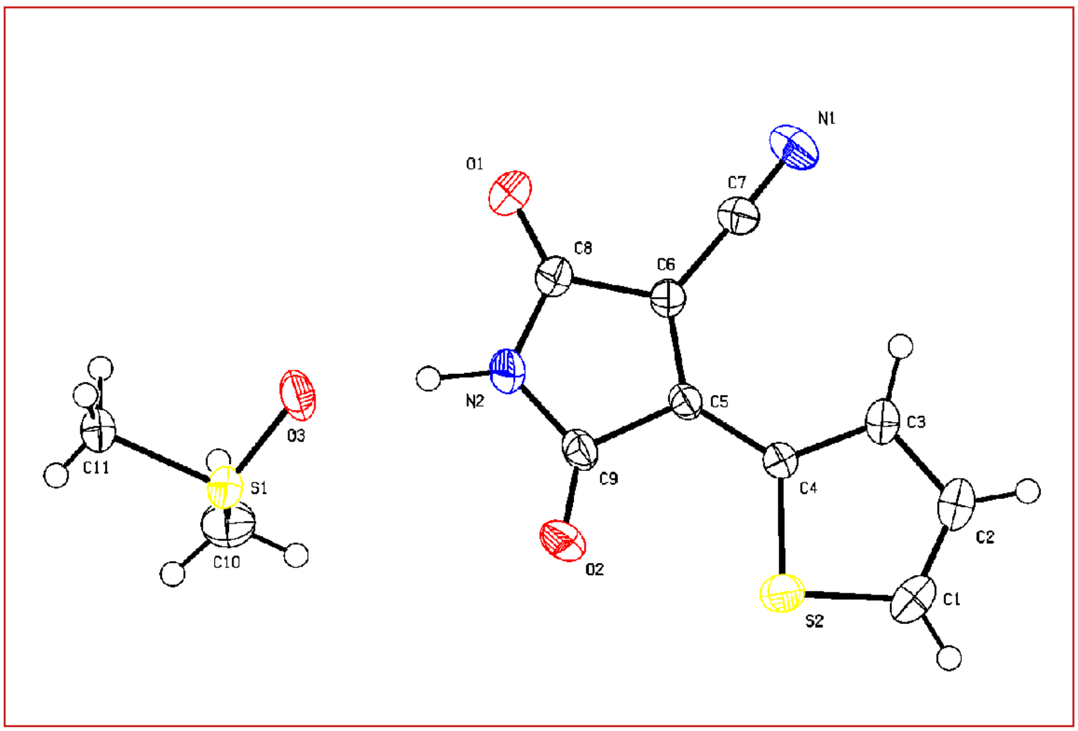

Figure 2: Molecular structure of compound **3k** with ellipsoids at the 50% probability level

Table 1. *Detailed analysis data of the X-ray crystal structures of compounds **3c** and **3k***

Complex	**3c**	**3k**
CCDC	2403601	2380170
Formula	$C_{12}H_8N_2O_3$	$C_9H_4N_2O_2S$
Fw	228.20	204.20
crystal color	yellow	Clear yellowish yellow
crystal system	triclinic	triclinic
space group	P-1	P-1
a (Å)	7.1679(4)	7.6557 (16)
b (Å)	7.7218(4)	9.1009 (2)
c (Å)	10.2127(5)	10.049 (2)
α (°)	96.893(2)	80.505 (8)
β (°)	90.608(2)	69.600 (7)
γ (°)	107.975(2)	78.742 (7)
V (Å^3)	533.11(5)	640.6 (2)
Z	2	2
T (K)	273.15	161.60
2θ range	8.74 to 135.82	2.99 to 34.42
ρ_{calc}g/cm^3	1.422	1.464
unique reflections	1949	2909
reflection (I>2σ(I))	1763	2616
λ (Å)/μ (mm^{-1})	1.54178/0.879	0.71073/0.416
F(000)	236	292
R1^a[I>2σ(I)]/GOF ^{b}	0.0608/1.034	0.0751/ 1.066
R1^a (all data)	0.0640	0.0788
*w*R2^c (I>2σ (I))	0.1907	0.2096
no. of para-meters/restr.	156/0	192/2
residual density (eÅ^{-3})	0.391	0.480

Observation criterion: ^{a}R1 = $\Sigma||F_o|-|F_c||/\Sigma|F_o|$. ^{b}GOF = $\{\Sigma[w(F_o^2-F_c^2)^2]/(n-p)\}^{1/2}$,
^{c}*w*R2 = $[\Sigma[w(F_o^2-F_c^2)^2]/\Sigma[w(F_o^2)^2]]^{1/2}$ where $w = 1/[\sigma^2(F_o^2)+(aP)^2+bP]$, $P = (F_o^2+2F_c^2)/3$.

2,5-dioxo-4-phenyl-2,5-dihydro-1H-pyrrole-3-carbonitrile (3a) :

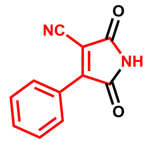

White solid; Yield : 80 % (159 mg); m.p: 178 - 179^{o} C; R_f [20 % EtOAc / Petroleum ether (60 - 80 ^{o}C)]: 0.4; ^{1}H NMR (DMSO-d_6, 300 MHz); δ_H = 7.60 – 7.71 (m, 3H), 7.98 – 8.01 (m, 2H), 11.85 (s, 1H) ppm. ^{13}C NMR (DMSO-d_6, 75 MHz); δ_C = 109.0, 112.3, 126.9, 129.2, 129.8, 133.1, 149.7, 166.3, 169.3 ppm. HRMS (ESI/TOF-Q) M/Z: $[M+H]^+$ Calcd. For $C_{11}H_7N_2O_2$: 199.0508, Found: 199.0506

2,5-dioxo-4-(p-tolyl)-2,5-dihydro-1H-pyrrole-3-carbonitrile (3b) :

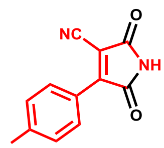

Yellow solid; Yield : 82 % (170 mg); m.p: 180 - 182^{o} C; R_f [20 % EtOAc / Petroleum ether (60 - 80 ^{0}C)]: 0.5; ^{1}H NMR (DMSO-d_6, 300 MHz); δ_H = 2.42 (s, 3H), 7.46 (d, J = 8.1 Hz, 2H), 7.95 (d, J = 8.4 Hz, 2H), 11.80 (s, 1H) ppm. ^{13}C NMR (DMSO-d_6, 75 MHz); δ_C = 21.4, 107.5, 112.5, 124.3, 129.9, 144.1, 149.4, 166.4, 169.4 ppm. HRMS (ESI/TOF-Q) M/Z: $[M+H]^+$ Calcd. For $C_{12}H_9N_2O_2$: 213.0664, Found: 213.0660

4-(4-methoxyphenyl)-2,5-dioxo-2,5-dihydro-1H-pyrrole-3-carbonitrile (3c) :

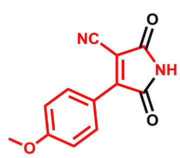

Light green solid; Yield : 84 % (192 mg); m.p: 170 - 172^{o} C; R_f [20 % EtOAc / Petroleum ether (60 - 80 ^{o}C)]: 0.25; ^{1}H NMR (DMSO-d_6, 300 MHz); δ_H = 3.88 (s, 3H), 7.21 (d, J = 9.2 Hz, 2H), 8.12 (d, J = 8.8 Hz, 2H), 11.73 (s, 1H) ppm. ^{13}C NMR (DMSO-d_6, 75 MHz); δ_C = 55.8, 104.7, 112.9, 115.1, 119.6, 132.3, 148.7, 163.4, 166.7, 169.7 ppm. HRMS (ESI/TOF-Q) M/Z: $[M+H]^+$ Calcd. For $C_{12}H_9N_2O_3$: 229.0613, Found: 229.0615

4-(2-methoxyphenyl)-2,5-dioxo-2,5-dihydro-1H-pyrrole-3-carbonitrile (3d) :

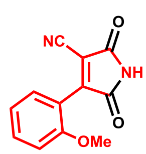

Light green solid; Yield : 74 % (169 mg); m.p: 167 - 168^{o} C; R_f [20 % EtOAc / Petroleum ether (60 - 80 ^{o}C)]: 0.2; ^{1}H NMR (DMSO-d_6, 400 MHz); δ_H = 3.90 (s, 3H), 7.10 – 7.14 (m, 1H), 7.24 – 7.26 (m, 1H), 7.61 – 7.64 (m, 2H), 11.83 (s, 1H) ppm. ^{13}C NMR (DMSO-d_6, 100 MHz); δ_C = 55.3, 111.3, 111.6, 112.0, 115.3, 120.3, 132.2, 134.5, 147.0, 158.6, 166.8, 169.3 ppm. HRMS (ESI/TOF-Q) M/Z: $[M+H]^+$ Calcd. For $C_{12}H_9N_2O_3$: 229.0613, Found: 229.0610

4-(4-chlorophenyl)-2,5-dioxo-2,5-dihydro-1H-pyrrole-3-carbonitrile (3e) :

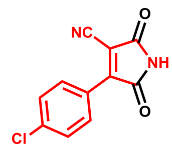

White solid; Yield : 78 % (181 mg); m.p: 195 - 197^{o} C; R_f [20 % EtOAc / Petroleum ether (60 - 80 ^{o}C)]: 0.3; ^{1}H NMR (DMSO-d$_6$, 300 MHz); δ_H = 7.74 (d, *J* = 8.7 Hz, 2H), 8.00 (d, *J* = 8.7 Hz, 2H), 11.9 (s, 1H) ppm. ^{13}C NMR (DMSO-d$_6$, 75 MHz); δ_C = 109.2, 112.1, 125.7, 128.8, 129.5, 131.2, 131.6, 138.0, 148.5, 166.2, 169.2 ppm. HRMS (ESI/TOF-Q) M/Z: [M+H]$^+$ Calcd. For $C_{11}H_6ClN_2O_2$: 233.0118, Found: 233.0117

4-(2-chlorophenyl)-2,5-dioxo-2,5-dihydro-1H-pyrrole-3-carbonitrileitrile (3f) :

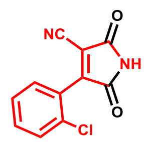

White solid; Yield : 62 % (144 mg); m.p: 186 - 188^{o} C; R_f [20 % EtOAc / Petroleum ether (60 - 80 ^{o}C)]: 0.3; ^{1}H NMR (DMSO-d$_6$, 300 MHz); δ_H = 7.19 – 7.20 (m, 1H), 7.23 – 7.52 (m, 3H), 12.05 (s, 1H) ppm. ^{13}C NMR (DMSO-d$_6$, 75 MHz); δ_C = 110.9, 115.7, 127.4, 129.4, 130.3, 130.9, 131.3, 133.4, 151.0, 165.6, 168.3 ppm. HRMS (ESI/TOF-Q) M/Z: [M+H]$^+$ Calcd. For $C_{11}H_6ClN_2O_2$: 233.0118, Found: 233.0114

4-(2,4-dichlorophenyl)-2,5-dioxo-2,5-dihydro-1H-pyrrole-3-carbonitrile (3g) :

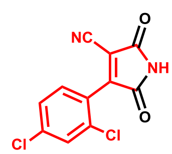

White solid; Yield : 60 % (159 mg); m.p: 176 - 178^{o} C; R_f [20 % EtOAc / Petroleum ether (60 - 80 ^{o}C)]: 0.32; ^{1}H NMR (DMSO-d$_6$, 300 MHz); δ_H = 7.56 – 7.58 (m, 2H), 7.80 – 7.81 (m, 1H), 14.07 (s, 1H) ppm. ^{13}C NMR (DMSO-d$_6$, 75 MHz); δ_C = 111.6, 115.6, 127.7, 129.1, 131.9, 132.2, 133.0, 135.2, 150.0, 164.1 ppm. HRMS (ESI/TOF-Q) M/Z: [M+H]$^+$ Calcd. For $C_{11}H_5Cl_2N_2O_2$: 266.9728, Found: 266.9725

4-(4-bromophenyl)-2,5-dioxo-2,5-dihydro-1H-pyrrole-3-carbonitrile (3h) :

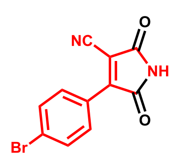

White solid; Yield : 80 % (220 mg); m.p: 204 - 205^{o} C; R_f [20 % EtOAc / Petroleum ether (60 - 80 ^{o}C)]: 0.3; ^{1}H NMR (DMSO-d$_6$, 300 MHz); δ_H = 7.42 (d, *J* = 8.7 Hz, 2H), 7.64 (d, *J* = 8.1 Hz, 2H), 12.05 (s, 1H) ppm. ^{13}C NMR (DMSO-d$_6$, 75 MHz); δ_C = 109.3, 112.1, 126.1, 131.3, 131.6, 131.7, 132.4, 148.7, 166.2, 169.2 ppm. HRMS (ESI/TOF-Q) M/Z: [M+H]$^+$ Calcd. For $C_{11}H_6BrN_2O_2$: 276.9813, Found: 276.9815

4-(3-bromophenyl)-2,5-dioxo-2,5-dihydro-1H-pyrrole-3-carbonitrile (3i) :

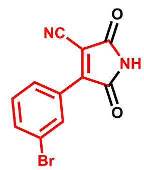

Light yellow solid; Yield : 72 % (198 mg); m.p: 178 - 179^{o} C; R_f [20 % EtOAc / Petroleum ether (60 - 80 ^{o}C)]: 0.35; ^{1}H NMR (DMSO-d_6, 300 MHz); δ_H = 7.45 – 7.51 (m, 1H), 7.62 – 7.64 (m, 1H), 7.83 – 7.88 (m, 2H), 11.95 (s, 1H) ppm. ^{13}C NMR (DMSO-d_6, 100 MHz); δ_C = 110.2, 111.9, 122.0, 128.7, 131.4, 132.1, 135.4, 135.6, 148.2, 166.0, 169.0 ppm. HRMS (ESI/TOF-Q) M/Z: $[M+H]^+$ Calcd. For $C_{11}H_6BrN_2O_2$: 276.9813, Found: 276.9814

2,5-dioxo-4-(4-(trifluoromethyl)phenyl)-2,5-dihydro-1H-pyrrole-3-carbonitrile (3j) :

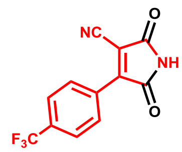

White solid; Yield : 75 % (200 mg); m.p: 207 - 208^{o} C; R_f [20 % EtOAc / Petroleum ether (60 - 80 ^{o}C)]: 0.25; ^{1}H NMR (DMSO-d_6, 400 MHz); δ_H = 8.03 (d, J = 8.4 Hz, 2H), 8.13 (d, J = 8.4 Hz, 2H), 11.99 (s, 1H) ppm. ^{13}C NMR (DMSO-d_6, 100 MHz); δ_C = 111.3, 111.8, 123.7 (C-F, $^{1}J_{C\text{-}F}$ = 270 Hz), 125.7, 126.1 (C-F, $^{3}J_{C\text{-}F}$ = 4 Hz), 127.7, 130.1, 131.5, 132.0 (C-F, $^{2}J_{C\text{-}F}$ = 33 Hz), 132.5, 134.6, 148.5, 165.9, 168.9 ppm. HRMS (ESI/TOF-Q) M/Z: $[M+H]^+$ Calcd. For $C_{12}H_6F_3N_2O_2$: 267.0381, Found: 267.0383

2,5-dioxo-4-(thiophen-2-yl)-2,5-dihydro-1H-pyrrole-3-carbonitrile (3k) :

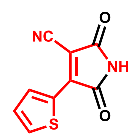

Brown solid; Yield : 77 % (157 mg); m.p: 215 - 217^{o} C; R_f [20 % EtOAc / Petroleum ether (60 - 80 ^{o}C)]: 0.5; ^{1}H NMR (DMSO-d_6, 300 MHz); δ_H = 7.44 – 7.47 (m, 1H), 8.29 – 8.30 (m, 1H), 8.35 – 8.37 (m, 1H), 11.82 (s, 1H) ppm. ^{13}C NMR (DMSO-d_6, 75 MHz); δ_C = 101.0, 112.8, 128.8, 129.8, 135.7, 139.5, 143.2, 166.9, 168.9 ppm. HRMS (ESI/TOF-Q) M/Z: $[M+H]^+$ Calcd. For $C_9H_5N_2O_2S$: 205.0072, Found: 205.0070

2,5-dioxo-4-(thiophen-3-yl)-2,5-dihydro-1H-pyrrole-3-carbonitrile (3l) :

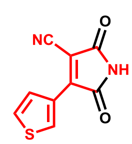

Yellow solid; Yield : 72 % (147 mg); m.p: 220 - 222^{o} C; R_f [20 % EtOAc / Petroleum ether (60 - 80 ^{o}C)]: 0.5; ^{1}H NMR (DMSO-d_6, 400 MHz); δ_H = 7.83 – 7.85 (m, 1H), 7.88 – 7.90 (m, 1H), 8.78 – 8.79 (m, 1H), 11.76 (s, 1H) ppm. ^{13}C NMR (DMSO-d_6, 100 MHz); δ_C = 104.2, 112.7, 126.4, 128.3, 129.2, 136.4, 143.7, 166.9, 169.3 ppm. HRMS (ESI/TOF-Q) M/Z: $[M+H]^+$ Calcd. For $C_9H_5N_2O_2S$: 205.0072, Found: 205.0075

4-(furan-2-yl)-2,5-dioxo-2,5-dihydro-1H-pyrrole-3-carbonitrile (3m) :

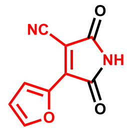

Brown solid; Yield : 70 % (132 mg); m.p: 185 - 187^{o} C; R_f [20 % EtOAc / Petroleum ether (60 - 80 ^{o}C)]: 0.35; ^{1}H NMR (DMSO-d$_6$, 400 MHz); δ_H = 6.95 – 6.96 (m, 1H), 7.67 – 7.68 (m, 1H), 8.39 (s, 1H), 11.75 (s, 1H) ppm. ^{13}C NMR (DMSO-d$_6$, 100 MHz); δ_C = 100.1, 112.2, 114.9, 123.2, 137.3, 143.9, 151.5, 167.0, 167.5 ppm. HRMS (ESI/TOF-Q) M/Z: $[M+H]^+$ Calcd. For $C_9H_5N_2O_3$: 189.0300, Found: 189.0302

4-(9H-fluoren-2-yl)-2,5-dioxo-2,5-dihydro-1H-pyrrole-3-carbonitrile (3n) :

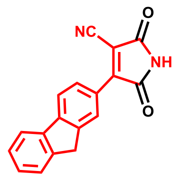

White solid; Yield : 63 % (180 mg); m.p: 213 - 215^{o} C; R_f [20 % EtOAc / Petroleum ether (60 - 80 ^{o}C)]: 0.5; ^{1}H NMR (DMSO-d$_6$, 400 MHz); δ_H = 4.00 (s, 1H), 7.38 – 7.45 (m, 2H), 7.63 – 7.65 (m, 1H), 7.98 – 8.00 (m, 3H), 8.15 – 8.17 (m, 1H), 12.87 (s, 1H) ppm. ^{13}C NMR (DMSO-d$_6$, 100 MHz); δ_C = 36.4, 107.1, 112.8, 119.9, 121.0, 125.4, 126.1, 127.0, 128.0, 128.4, 128.9, 129.1, 140.0, 143.2, 144.3, 145.5, 149.5, 166.6, 169.6 ppm. HRMS (ESI/TOF-Q) M/Z: $[M+H]^+$ Calcd. For $C_{18}H_{11}N_2O_2$: 287.0821, Found: 287.0820

1-ethyl-2,5-dioxo-4-phenyl-2,5-dihydro-1H-pyrrole-3-carbonitrile (5a) :

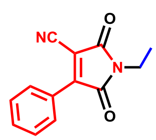

White solid; Yield : 85 % (192 mg); m.p: 110 - 112^{o} C; R_f [20 % EtOAc / Petroleum ether (60 - 80 ^{o}C)]: 0.7; ^{1}H NMR (DMSO-d$_6$, 300 MHz); δ_H = 1.27 (t, J = 7.2 Hz, 3H), 3.73 (q, J = 7.2 Hz, 2H), 7.54 – 7.66 (m, 3H), 8.20 – 8.23 (m, 2H) ppm. ^{13}C NMR (DMSO-d$_6$, 75 MHz); δ_C = 13.4, 34.6, 108.0, 111.6, 126.9, 129.6, 130.5, 134.0, 149.2, 164.7, 167.9 ppm. HRMS (ESI/TOF-Q) M/Z: $[M+H]^+$ Calcd. For $C_{13}H_{11}N_2O_2$: 227.0821, Found: 227.0824

1-benzyl-2,5-dioxo-4-(p-tolyl)-2,5-dihydro-1H-pyrrole-3-carbonitrile (5b) :

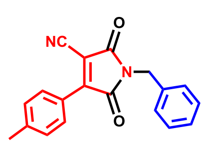

White solid; Yield : 90 % (272 mg); m.p: 120 - 122^{o} C; R_f [20 % EtOAc / Petroleum ether (60 - 80 ^{o}C)]: 0.7; ^{1}H NMR (DMSO-d$_6$, 300 MHz); δ_H = 4.77 (s, 2H), 7.30 – 7.36 (m, 5H), 7.39 – 7.42 (m, 2H), 8.16 (d, J = 8.4 Hz, 2H) ppm. ^{13}C NMR (DMSO-d$_6$, 75 MHz); δ_C = 22.1, 42.8, 106.2, 111.8, 124.3, 128.4, 128.9, 129.0, 130.3, 130.6, 135.3, 145.8, 148.8, 164.8, 167.9 ppm. HRMS (ESI/TOF-Q) M/Z: $[M+H]^+$ Calcd. For $C_{19}H_{15}N_2O_2$: 303.1134, Found: 303.1136

1-allyl-4-(2-methoxyphenyl)-2,5-dioxo-2,5-dihydro-1H-pyrrole-3-carbonitrile (5c) :

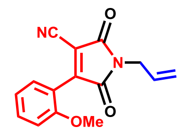

Yellow solid; Yield : 78 % (209 mg); m.p: 117 - 119^o C; R_f [20 % EtOAc / Petroleum ether (60 - 80 ^{o}C)]: 0.8; ^{1}H NMR (DMSO-d_6, 400 MHz); δ_H = 3.87 (s, 3H), 4.42 (d, J = 5.6 Hz, 2H), 5.30 (d, J = 10.4 Hz, 1H), 5.42 (d, J = 16 Hz, 1H), 5.98 – 6.07 (m, 1H), 7.02 – 7.06 (m, 2H), 7.26 – 7.28 (m, 1H), 7.40 – 7.45 (m, 1H) ppm. ^{13}C NMR (DMSO-d_6, 100 MHz); δ_C = 48.7, 55.6, 98.4, 111.5, 117.0, 118.1, 120.9, 122.6, 127.0, 130.6, 131.0, 134.1, 148.5, 152.5, 156.5 ppm. HRMS (ESI/TOF-Q) M/Z: $[M+H]^+$ Calcd. For $C_{15}H_{13}N_2O_3$: 269.0926, Found: 269.0928

1-benzyl-4-(4-chlorophenyl)-2,5-dioxo-2,5-dihydro-1H-pyrrole-3-carbonitrile (5d) :

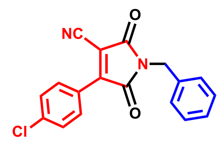

Green solid; Yield : 92 % (297 mg); m.p: 130 - 132^o C; R_f [20 % EtOAc / Petroleum ether (60 - 80 ^{o}C)]: 0.75; ^{1}H NMR (DMSO-d_6, 400 MHz); δ_H = 4.78 (s, 2H), 7.31 – 7.36 (m, 3H), 7.38 – 7.43 (m, 2H), 7.51 – 7.54 (m, 2H), 8.19 (d, J = 8.8 Hz, 2H) ppm. ^{13}C NMR (DMSO-d_6, 100 MHz); δ_C = 42.9, 107.9, 111.3, 125.2, 128.6, 128.9, 129.0, 130.0, 131.7, 135.1, 140.9, 147.7, 164.3, 167.5 ppm. HRMS (ESI/TOF-Q) M/Z: $[M+H]^+$ Calcd. For $C_{18}H_{12}ClN_2O_2$: 323.0587, Found: 323.0584

4-(4-bromophenyl)-1-methyl-2,5-dioxo-2,5-dihydro-1H-pyrrole-3-carbonitrile (5e) :

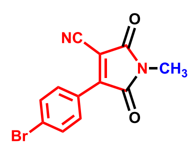

Yellow solid; Yield : 65 % (188 mg); m.p: 104 - 106^o C; R_f [20 % EtOAc / Petroleum ether (60 - 80 ^{o}C)]: 0.65; ^{1}H NMR (DMSO-d_6, 300 MHz); δ_H = 3.30 (s, 3H), 7.29 (d, J = 8.7 Hz, 2H), 7.63 (d, J = 7.8 Hz, 2H) ppm. ^{13}C NMR (DMSO-d_6, 75 MHz); δ_C = 26.2, 107.3, 116.3, 124.7, 129.3, 129.6, 130.5, 132.4, 148.2, 170.0, 171.9 ppm. HRMS (ESI/TOF-Q) M/Z: $[M+H]^+$ Calcd. For $C_{12}H_8BrN_2O_2$: 290.9769, Found: 290.9766

4-(3-bromophenyl)-2,5-dioxo-1-propyl-2,5-dihydro-1H-pyrrole-3-carbonitrile (5f) :

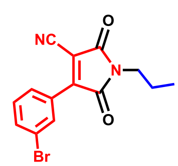

Yellow solid; Yield : 75 % (239 mg); m.p: 120 - 121^o C; R_f [20 % EtOAc / Petroleum ether (60 - 80 ^{o}C)]: 0.8; ^{1}H NMR (DMSO-d_6, 400 MHz); δ_H = 0.93 – 0.97 (m, 3H), 1.66 – 1.75 (m, 2H), 3.60 (t, J = 7.2 Hz, 2H), 7.42 – 7.46 (m, 1H), 7.73 – 7.75 (m, 1H), 8.11 – 8.14 (m, 1H), 8.33 – 8.34 (m, 1H) ppm. ^{13}C NMR (DMSO-d_6, 100 MHz); δ_C = 11.3, 21.7, 41.1, 109.2, 111.1, 123.6, 128.5, 128.8, 131.0, 133.2, 136.7, 147.3, 164.4, 167.6 ppm. HRMS (ESI/TOF-Q) M/Z: $[M+H]^+$ Calcd. For $C_{14}H_{12}BrN_2O_2$: 319.0082, Found: 319.0080

2,5-dioxo-4-(*p*-tolyl)-2,5-dihydro-1H-pyrrole-3-carboxylic acid (6) :

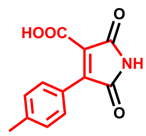

Yellow solid; Yield : 60 % (139 mg); m.p: 134 - 136^{o} C; R_f [40 % EtOAc / Petroleum ether (60 - 80 ^{o}C)]: 0.7; ^{1}H NMR (DMSO-d$_6$, 300 MHz); δ_H = 2.35 (s, 3H), 7.30 (d, *J* = 8.1 Hz, 2H), 7.64 (d, *J* = 8.1 Hz, 2H), 11.27 (s, 1H) ppm. ^{13}C NMR (DMSO-d$_6$, 75 MHz); δ_C = 21.1, 125.3, 129.1, 129.4, 132.8, 137.1, 140.7, 163.0, 170.0, 171.5 ppm. HRMS (ESI/TOF-Q) M/Z: [M+H]$^+$ Calcd. For $C_{12}H_{10}N_2O_4$: 232.0610, Found: 232.0612

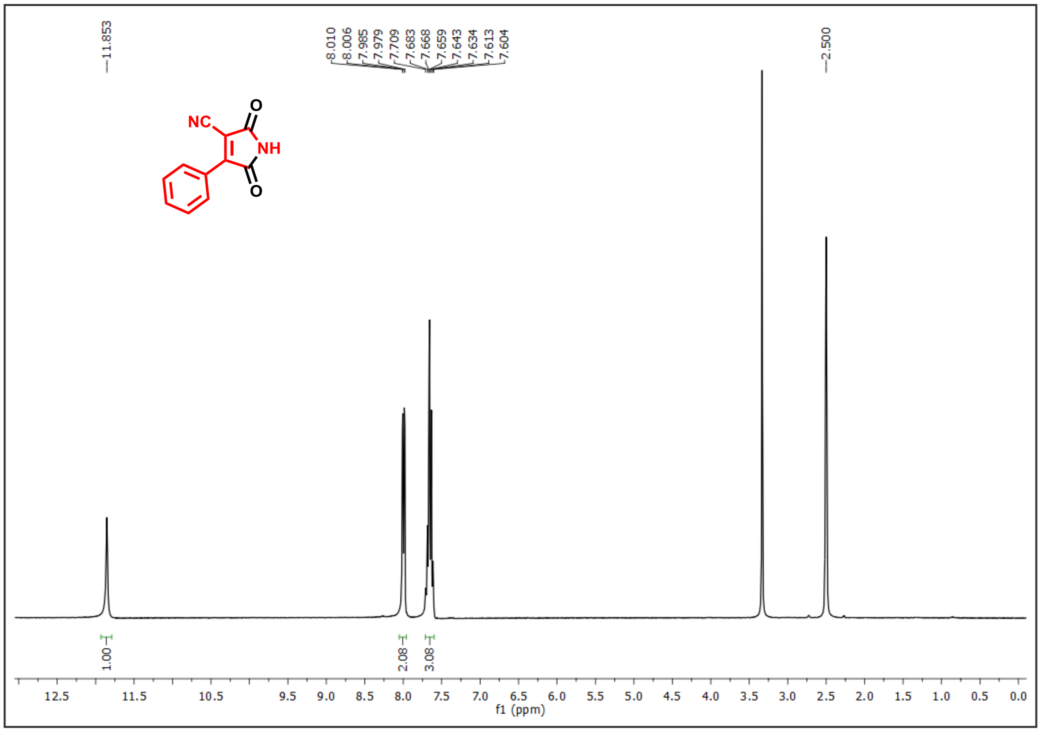

[1]H NMR spectrum of compound **3a** (300 MHz, DMSO-d_6)

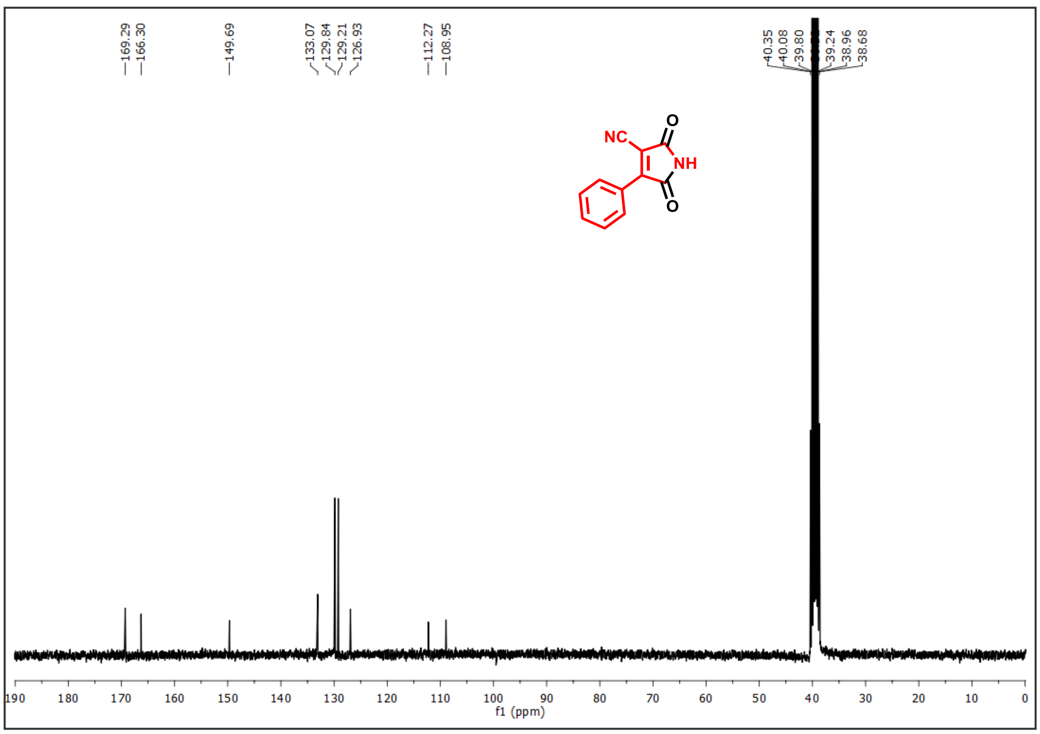

[13]C NMR spectrum of compound **3a** (75 MHz, DMSO-d_6)

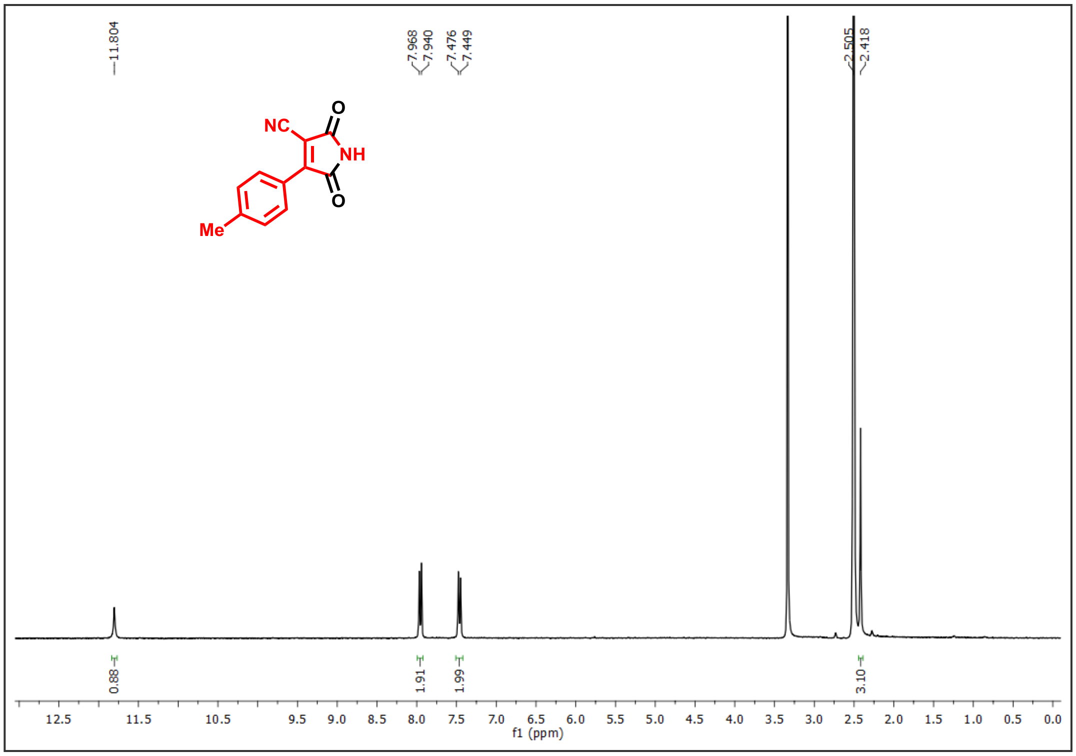

^{1}H NMR spectrum of compound **3b** (300 MHz, DMSO-d$_6$)

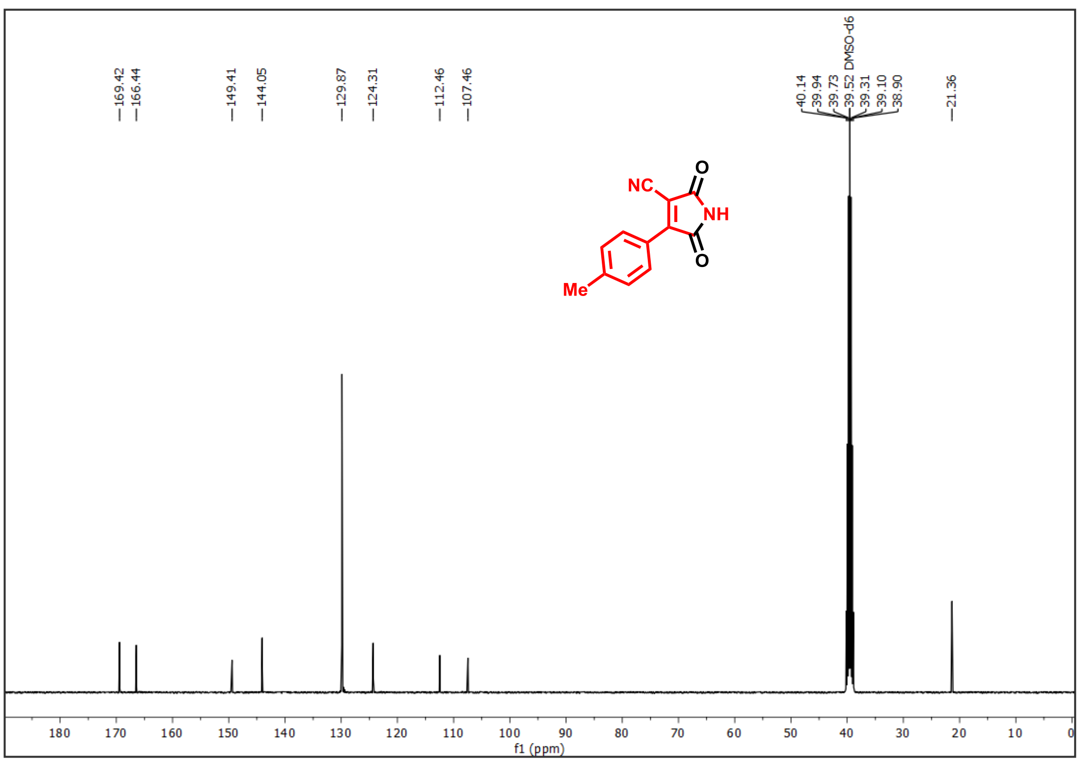

^{13}C NMR spectrum of compound **3b** (100 MHz, DMSO-d$_6$)

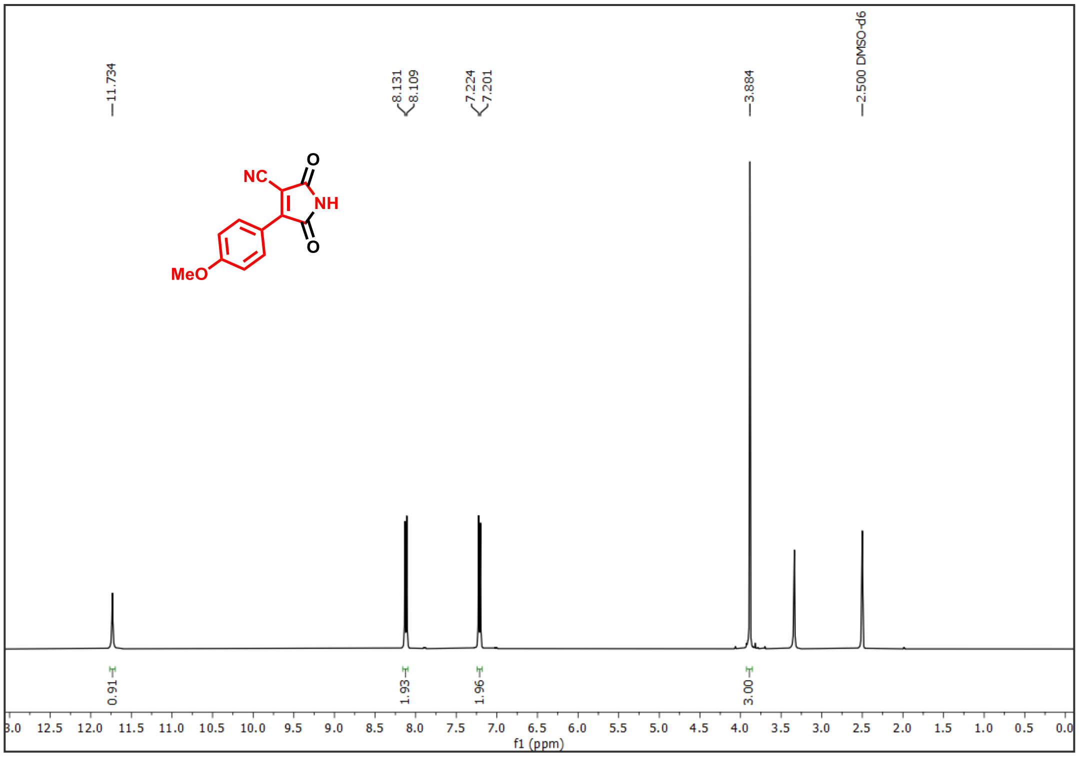

^{1}H NMR spectrum of compound **3c** (400 MHz, DMSO-d_6)

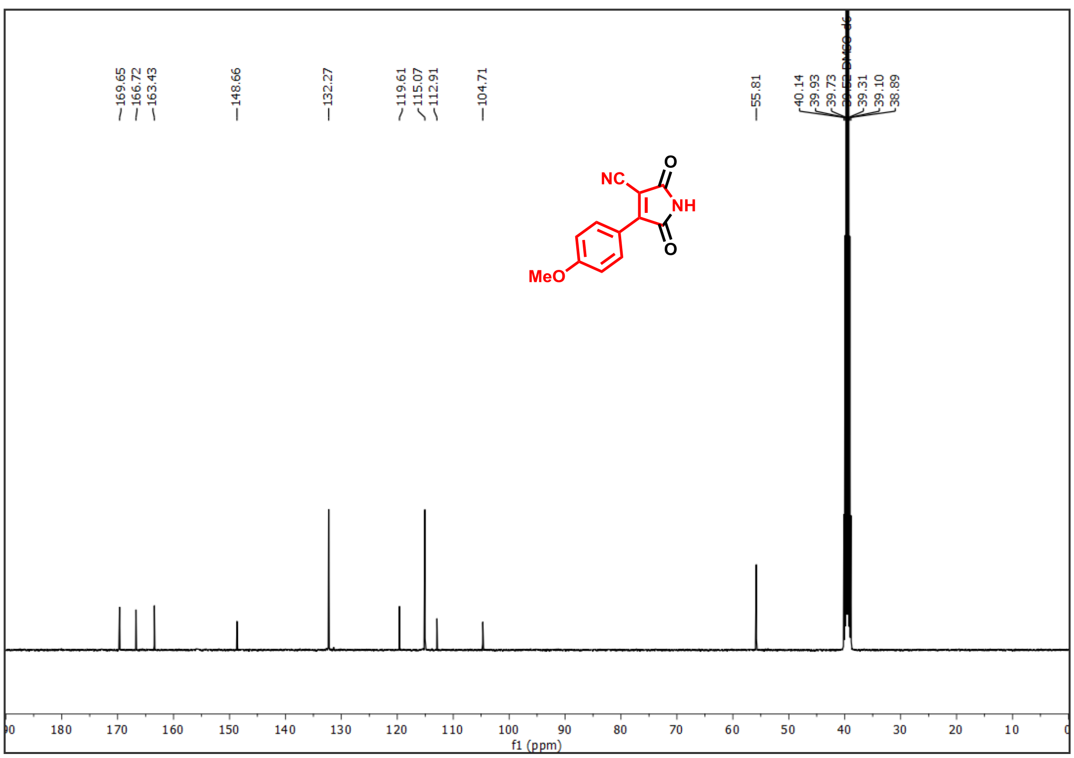

^{13}C NMR spectrum of compound **3c** (100 MHz, DMSO-d_6)

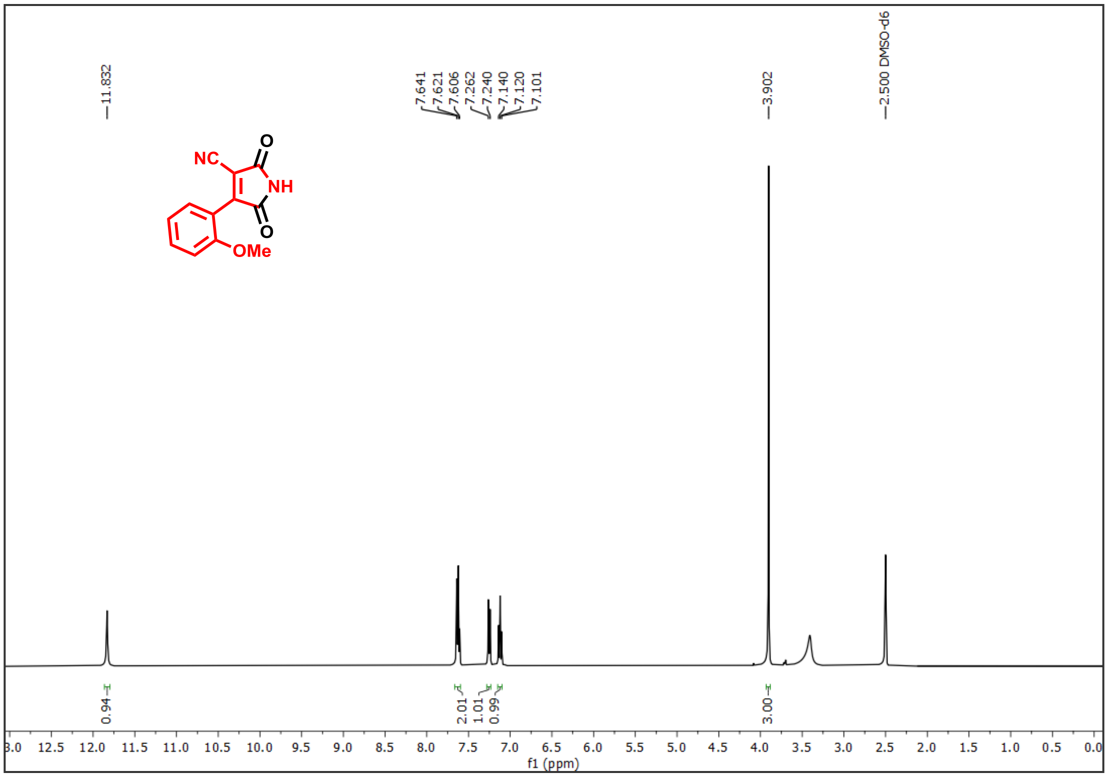

^{1}H NMR spectrum of compound **3d** (400 MHz, DMSO-d$_6$)

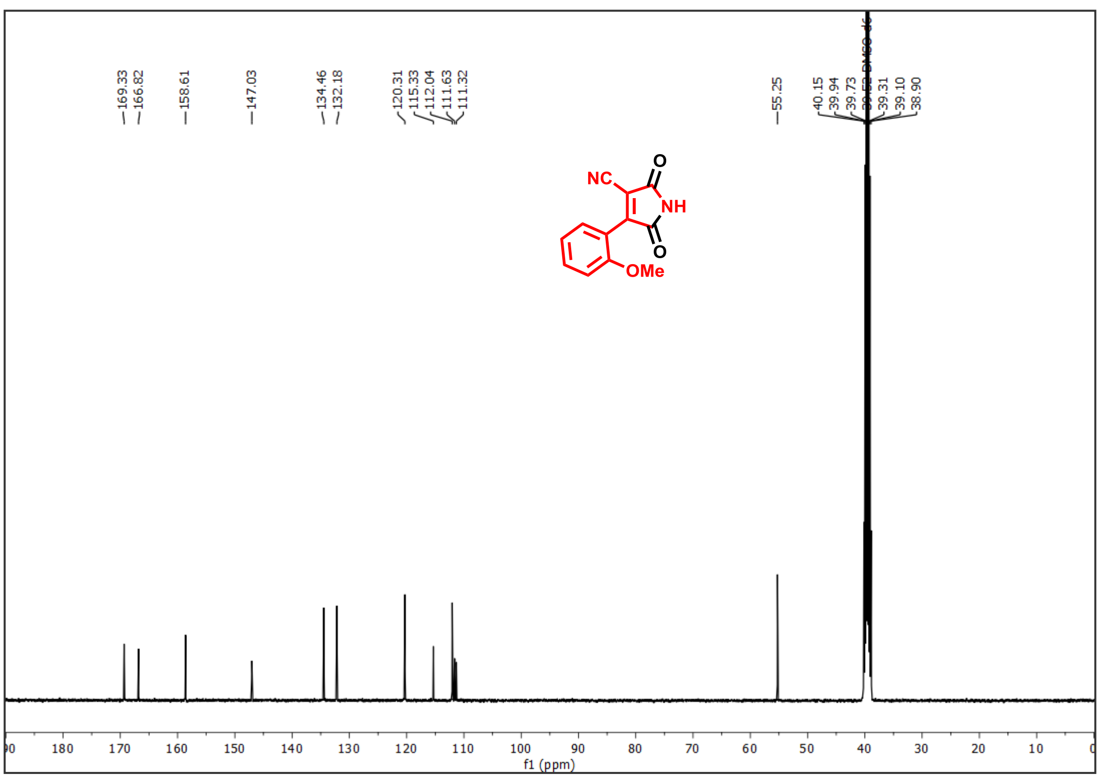

^{13}C NMR spectrum of compound **3d** (100 MHz, DMSO-d$_6$)

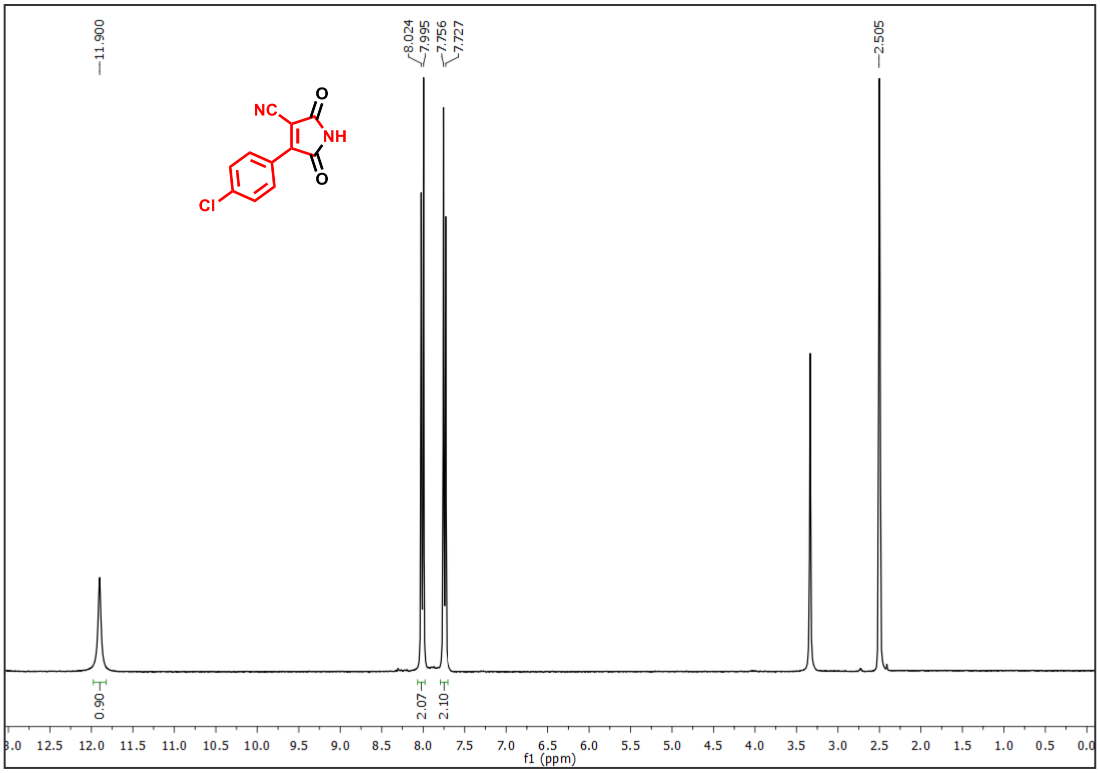

^{1}H NMR spectrum of compound **3e** (300 MHz, DMSO-d_6)

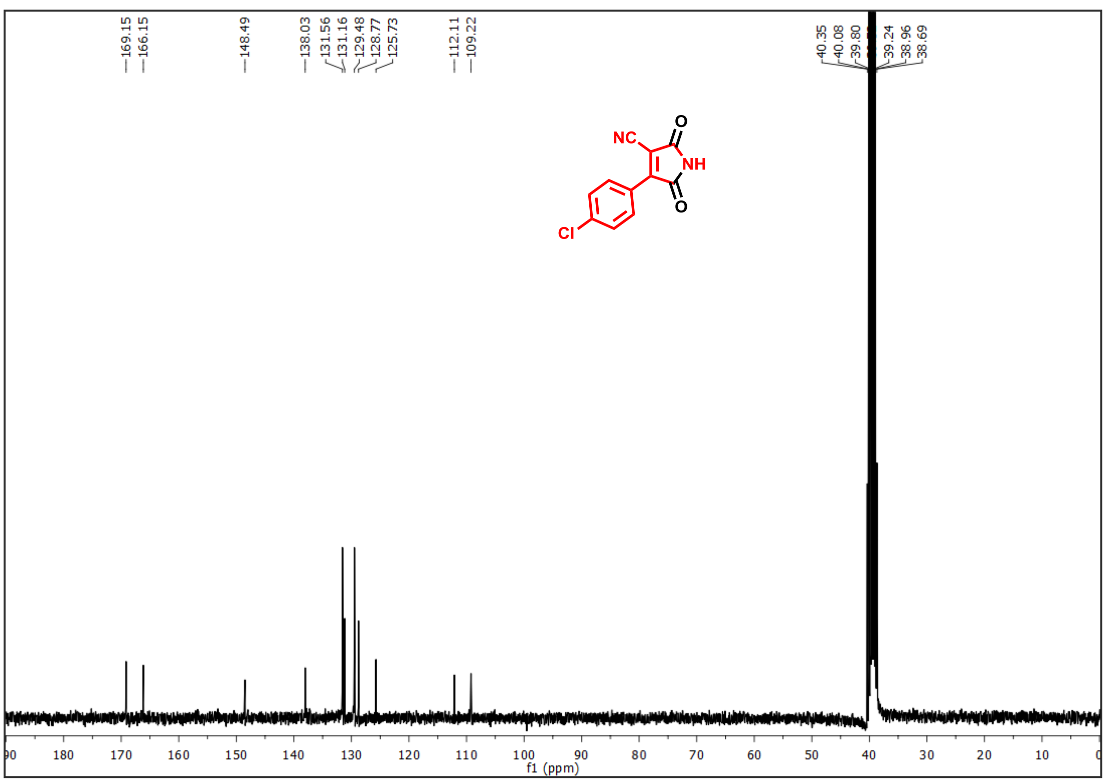

^{13}C NMR spectrum of compound **3e** (75 MHz, DMSO-d_6)

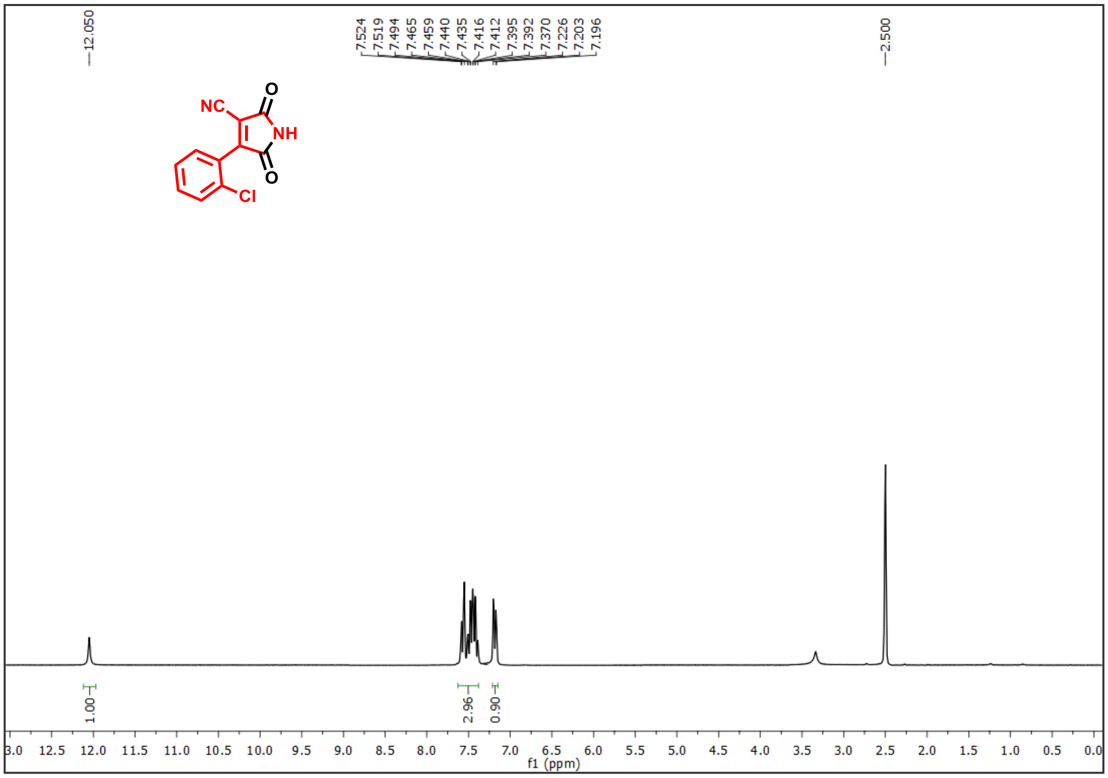

^{1}H NMR spectrum of compound **3f** (300 MHz, DMSO-d_6)

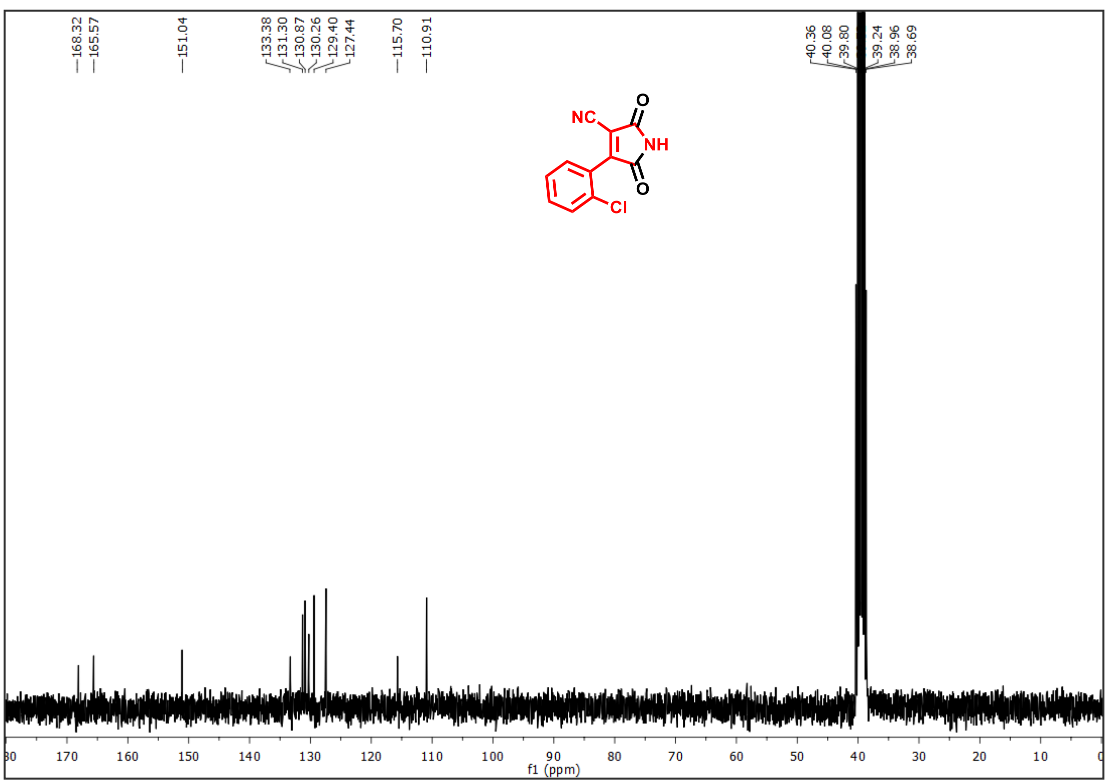

^{13}C NMR spectrum of compound **3f** (75 MHz, DMSO-d_6)

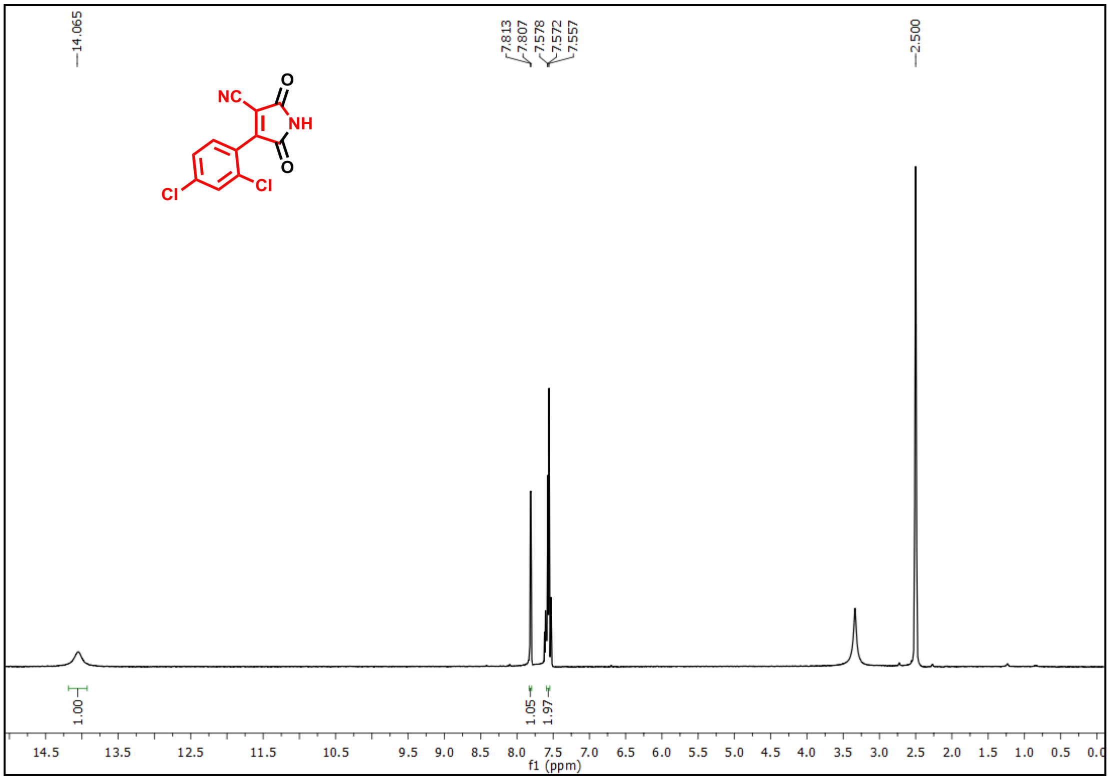

^{1}H NMR spectrum of compound **3g** (300 MHz, DMSO-d_6)

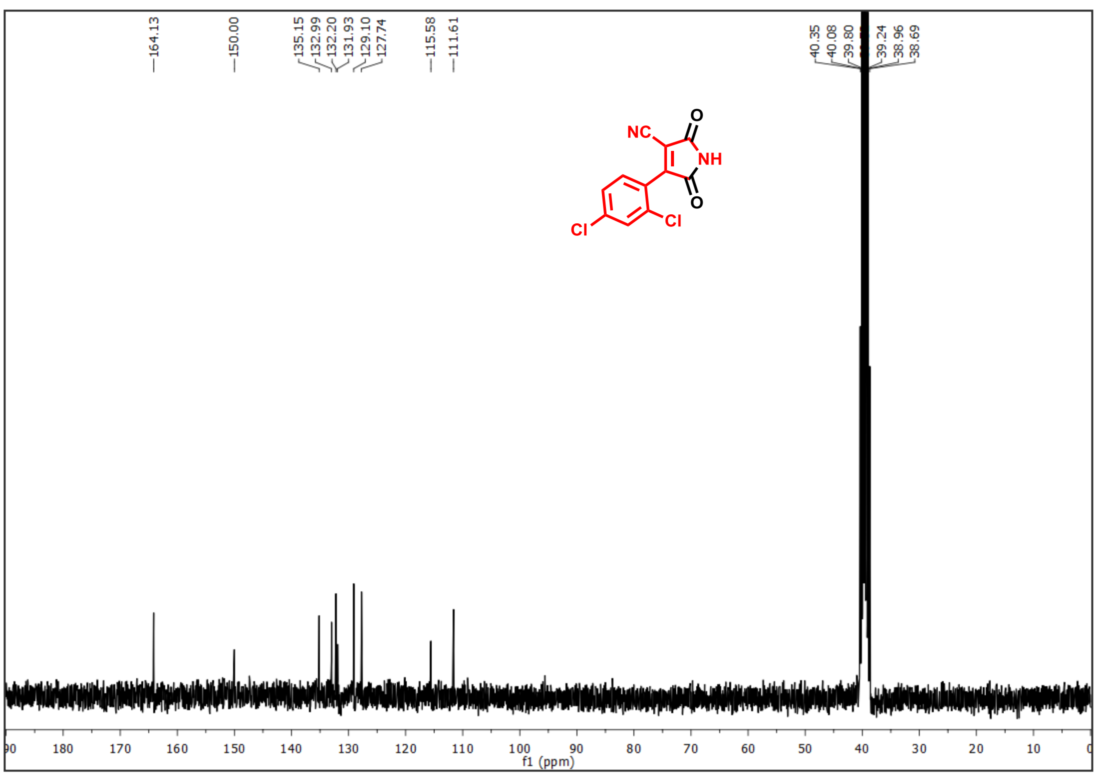

^{13}C NMR spectrum of compound **3g** (75 MHz, DMSO-d_6)

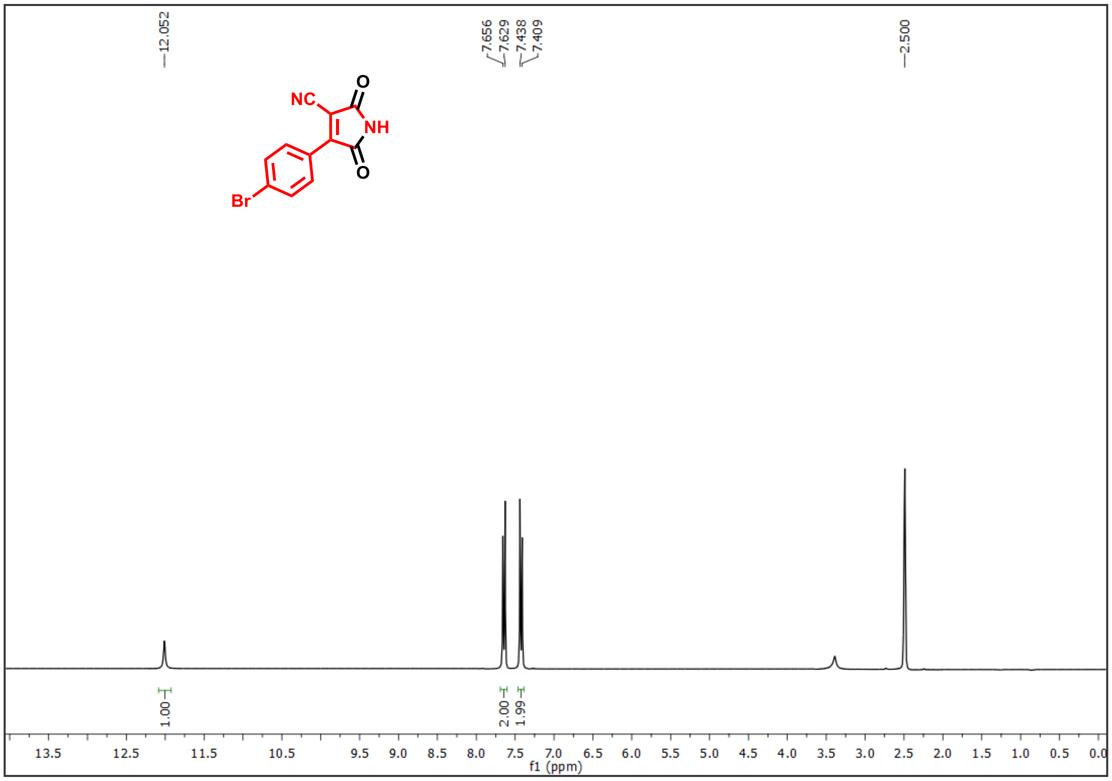

^{1}H NMR spectrum of compound **3h** (300 MHz, DMSO-d_6)

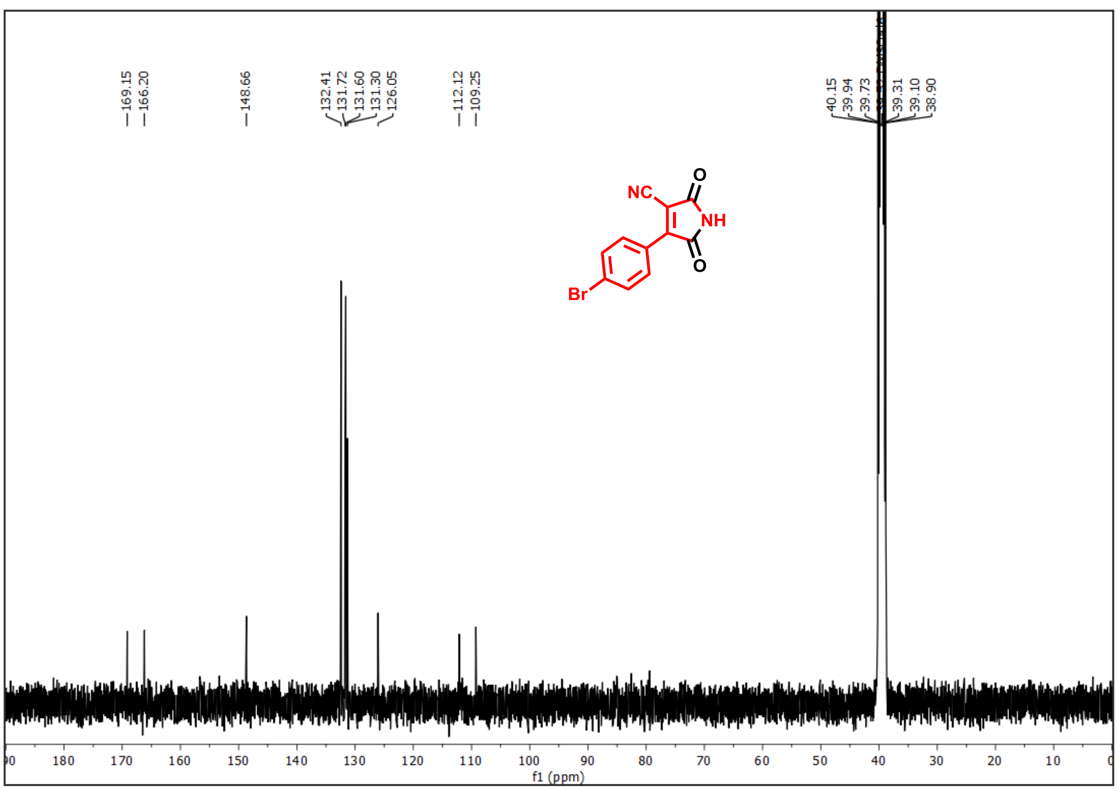

^{13}C NMR spectrum of compound **3h** (100 MHz, DMSO-d_6)

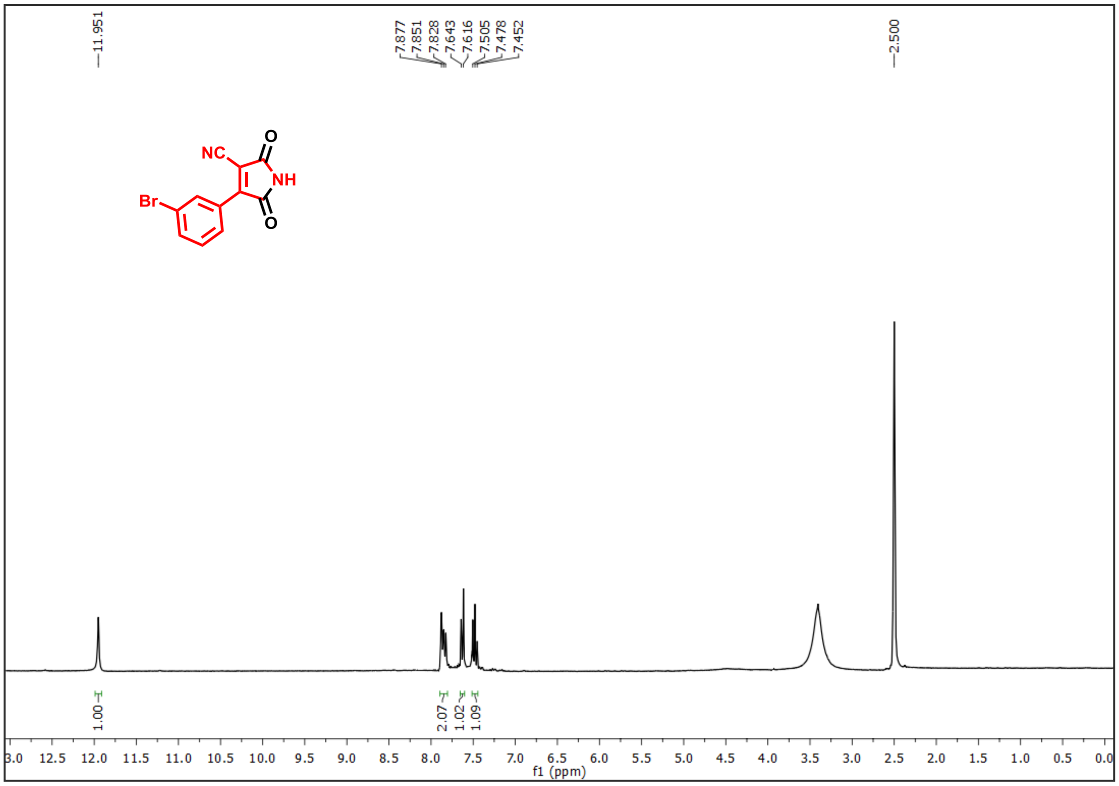

[1]H NMR spectrum of compound **3i** (300 MHz, DMSO-d_6)

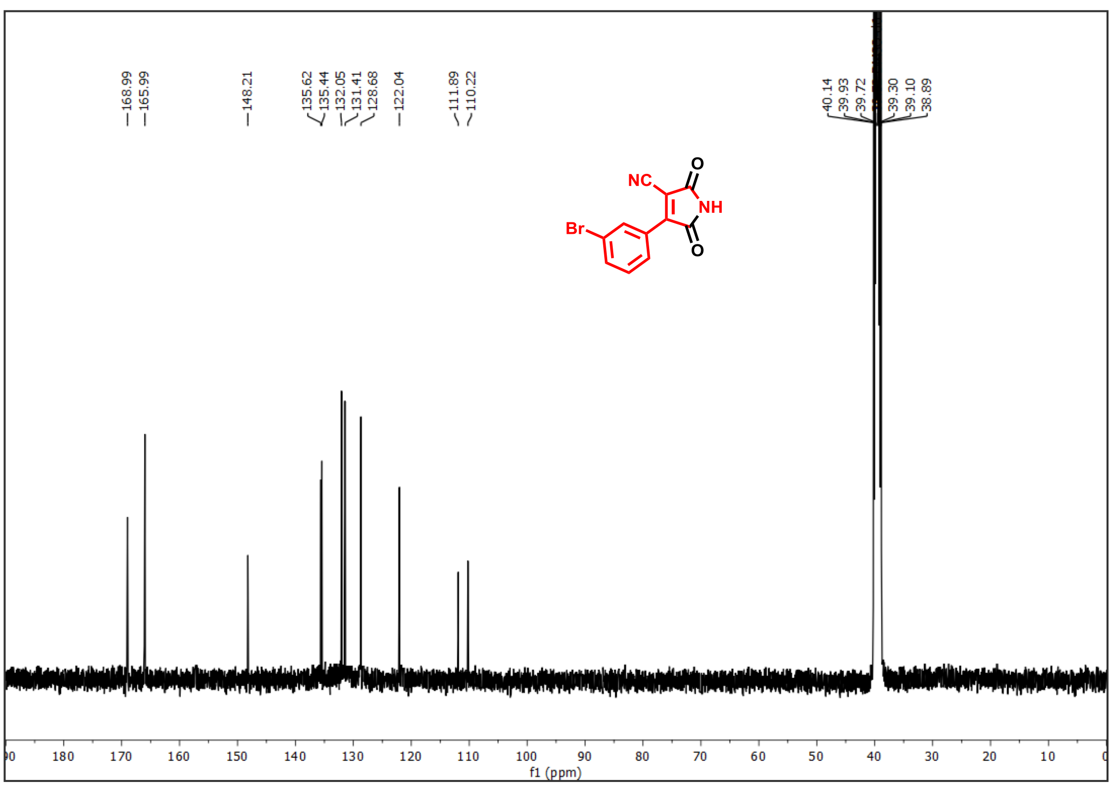

[13]C NMR spectrum of compound **3i** (100 MHz, DMSO-d_6)

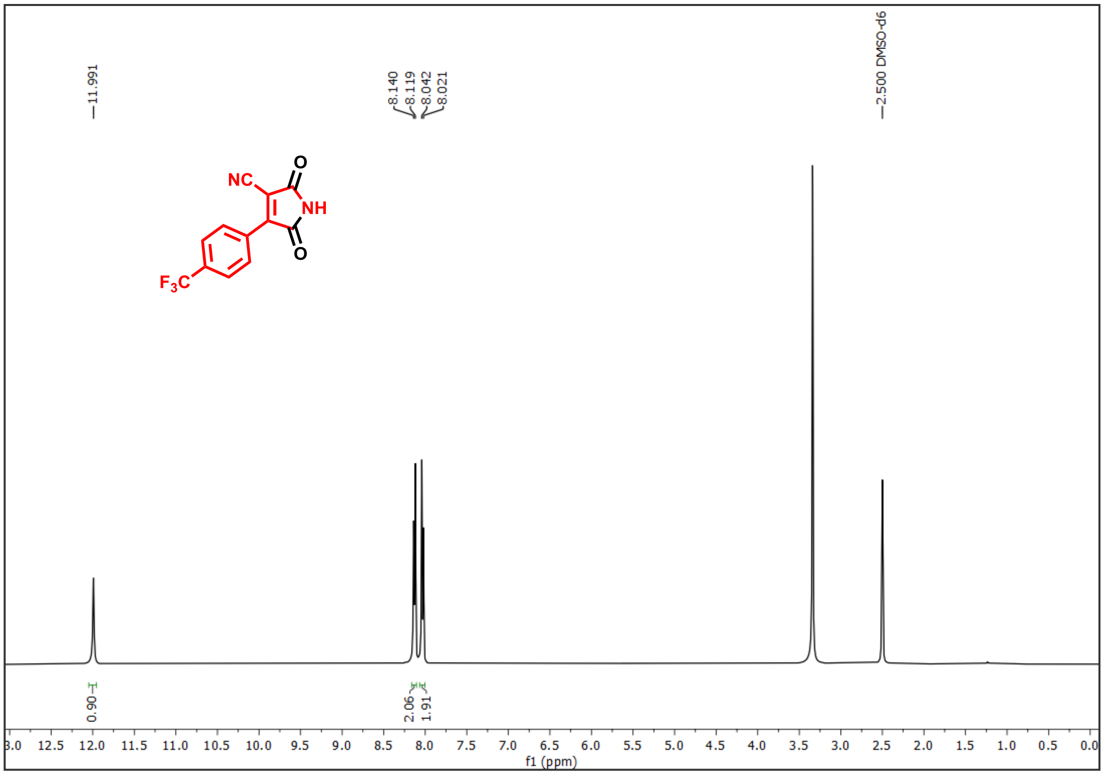

[1]H NMR spectrum of compound **3j** (400 MHz, DMSO-d_6)

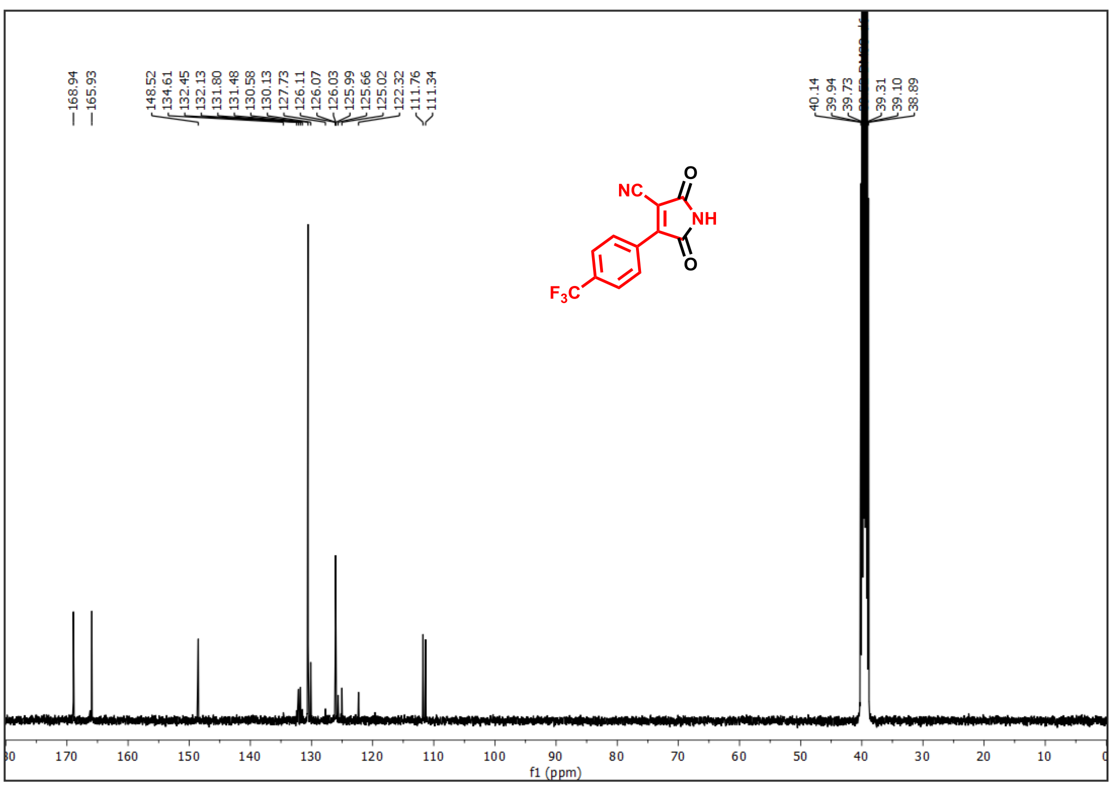

[13]C NMR spectrum of compound **3j** (100 MHz, DMSO-d_6)

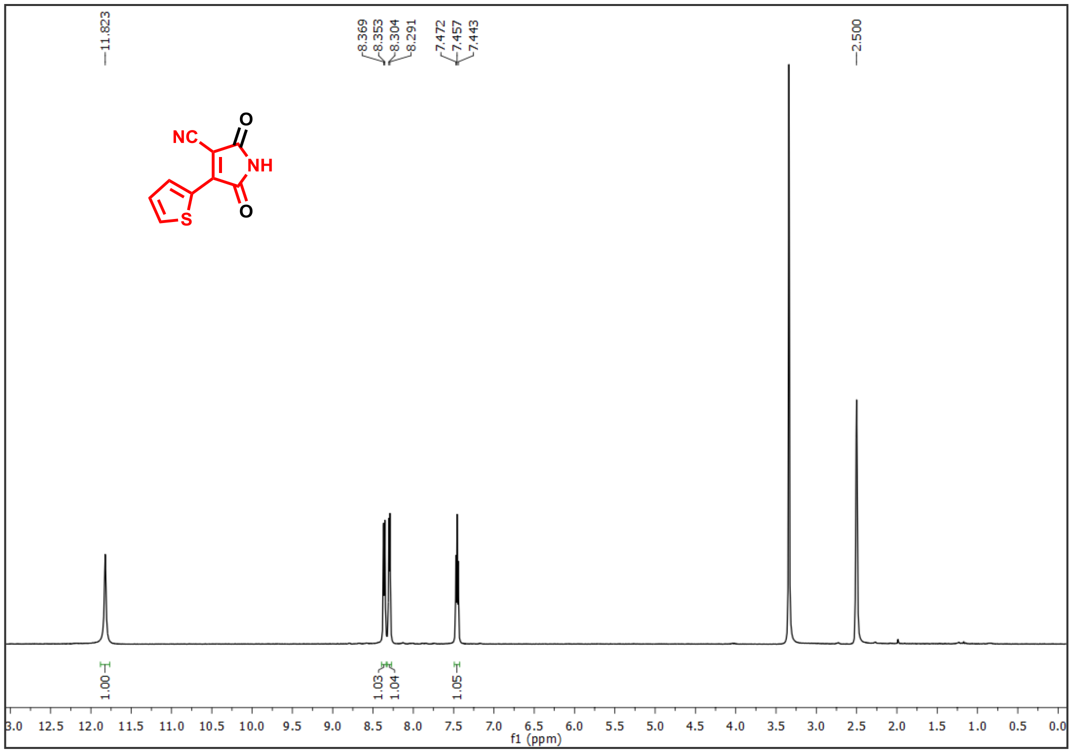

^{1}H NMR spectrum of compound **3k** (300 MHz, DMSO-d_6)

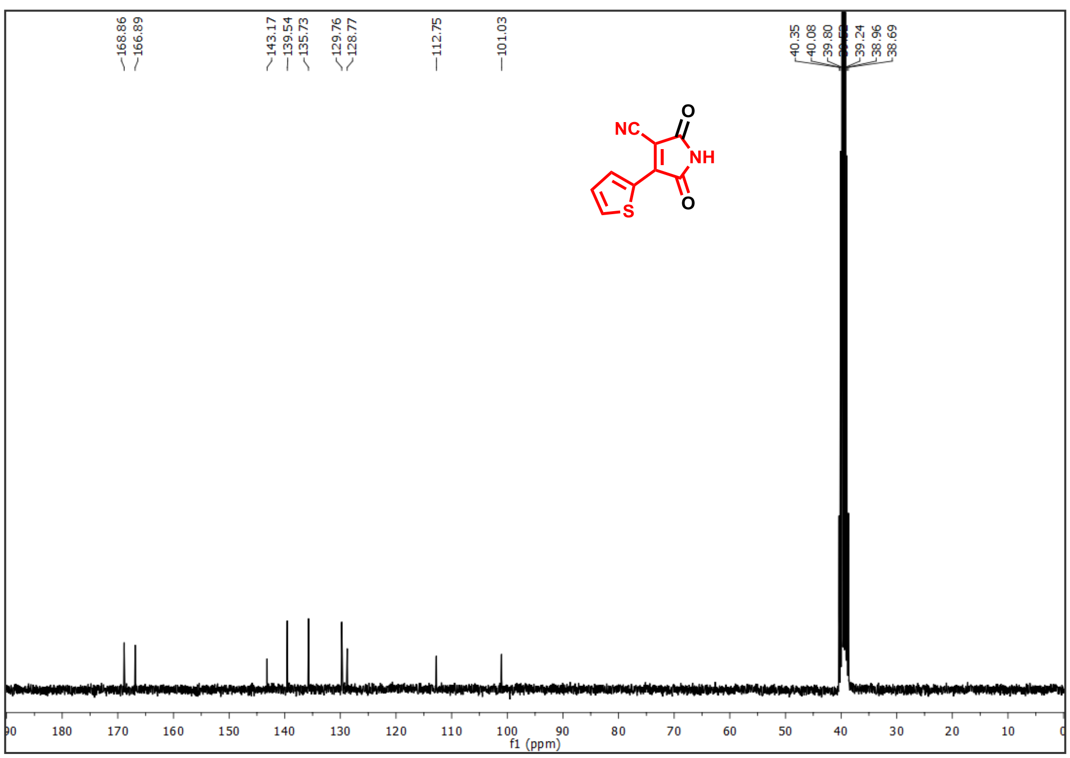

^{13}C NMR spectrum of compound **3k** (75 MHz, DMSO-d_6)

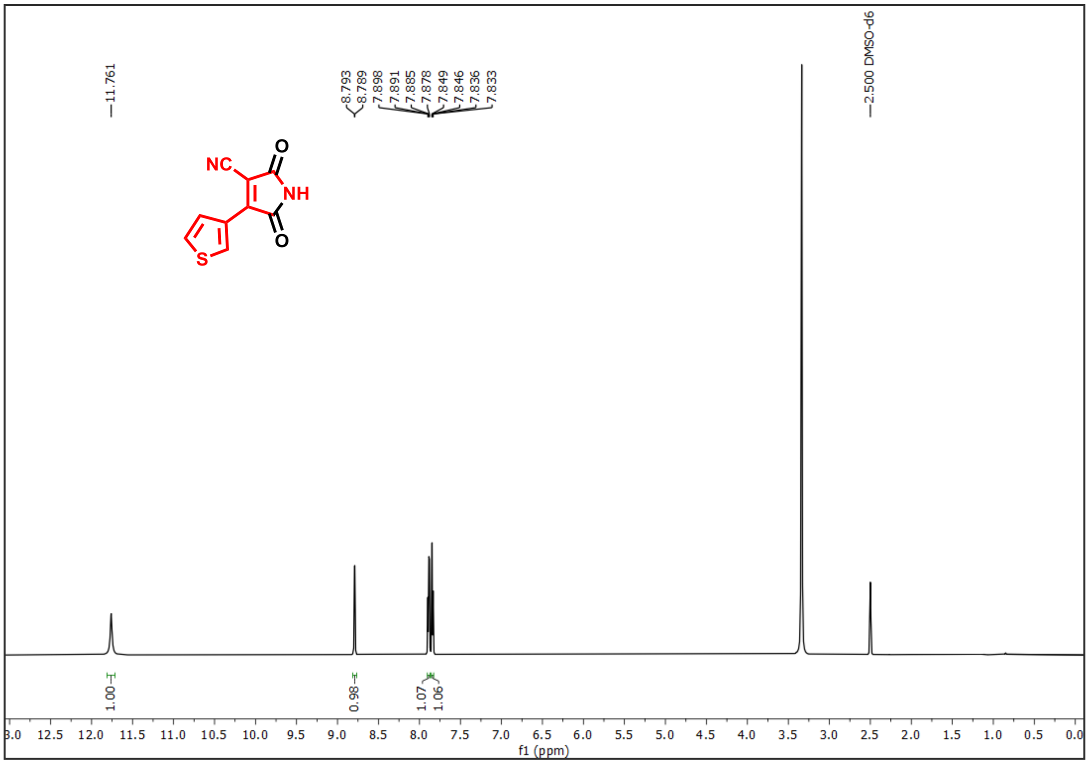

^{1}H NMR spectrum of compound **3l** (400 MHz, DMSO-d_6)

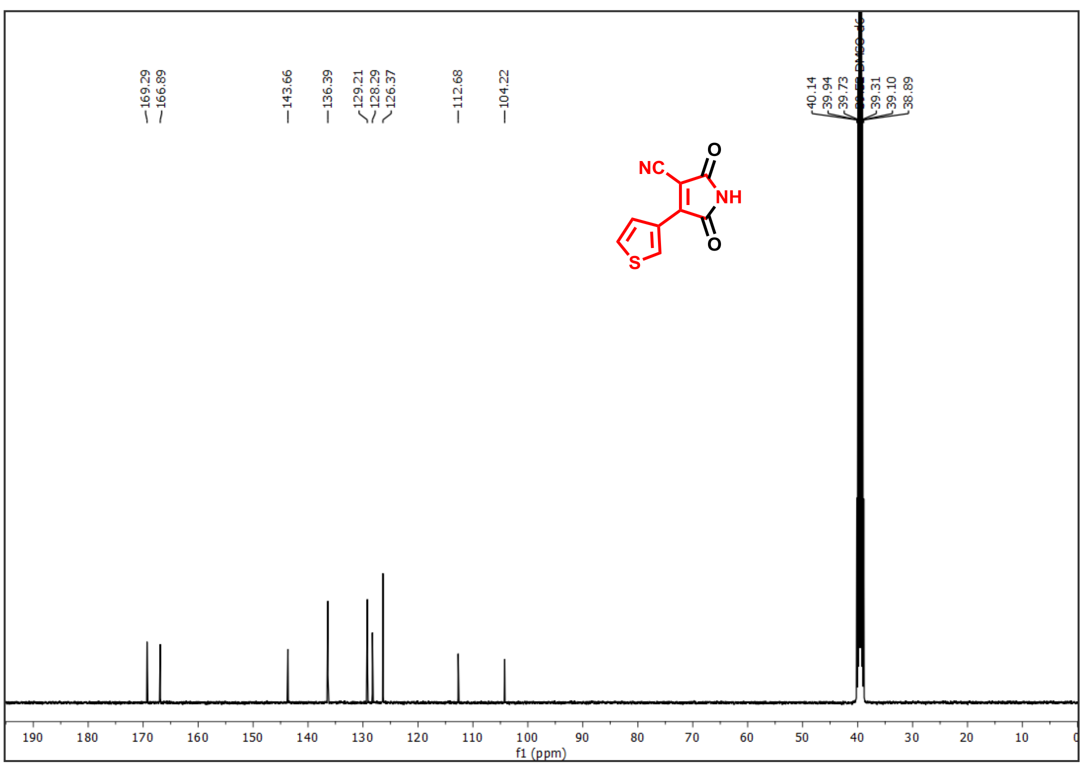

^{13}C NMR spectrum of compound **3l** (100 MHz, DMSO-d_6)

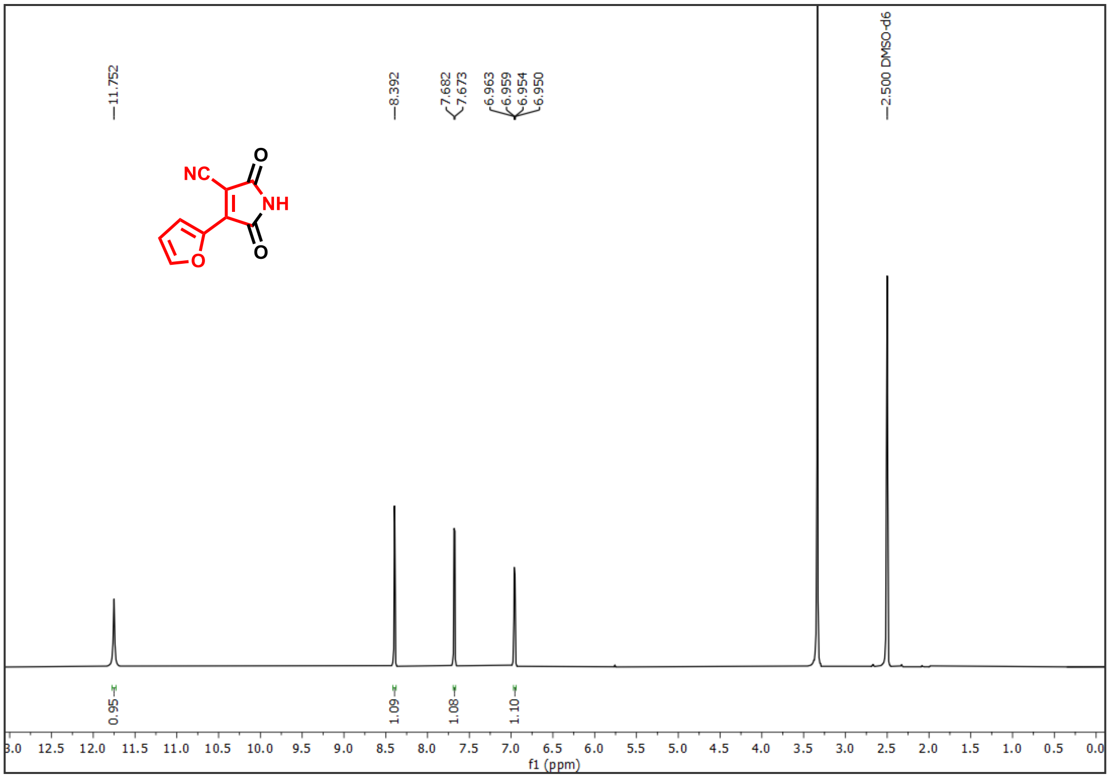

^{1}H NMR spectrum of compound **3m** (400 MHz, DMSO-d_6)

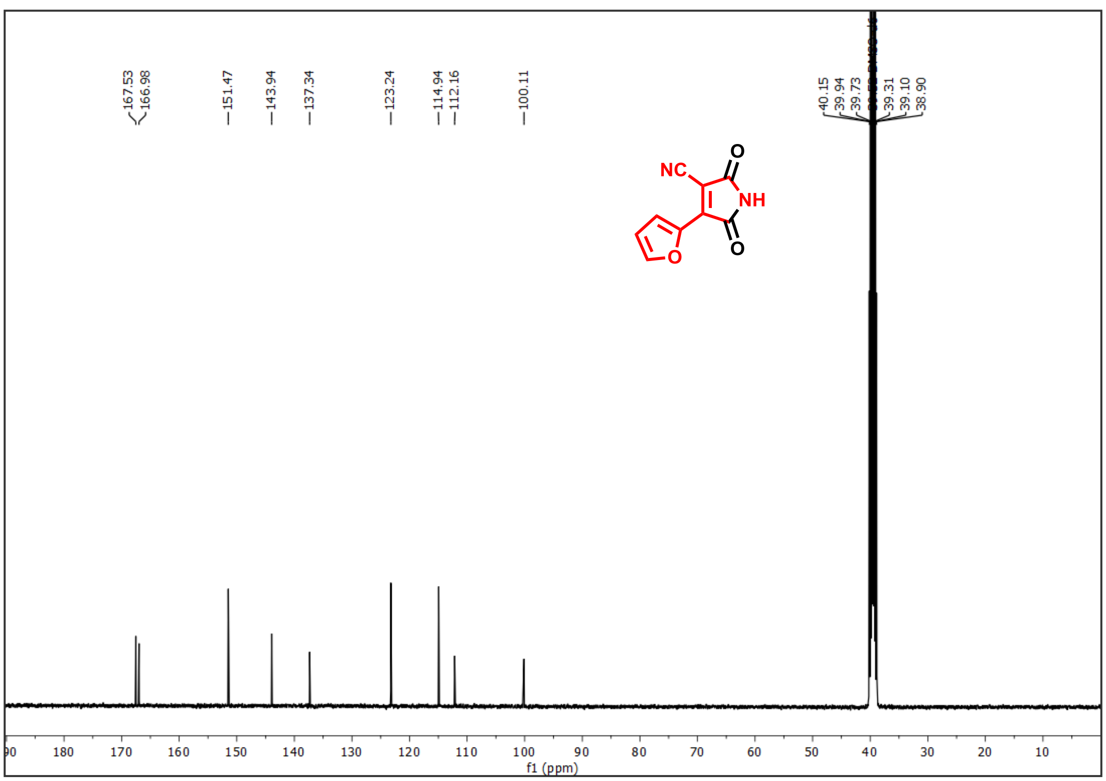

^{13}C NMR spectrum of compound **3m** (100 MHz, DMSO-d_6)

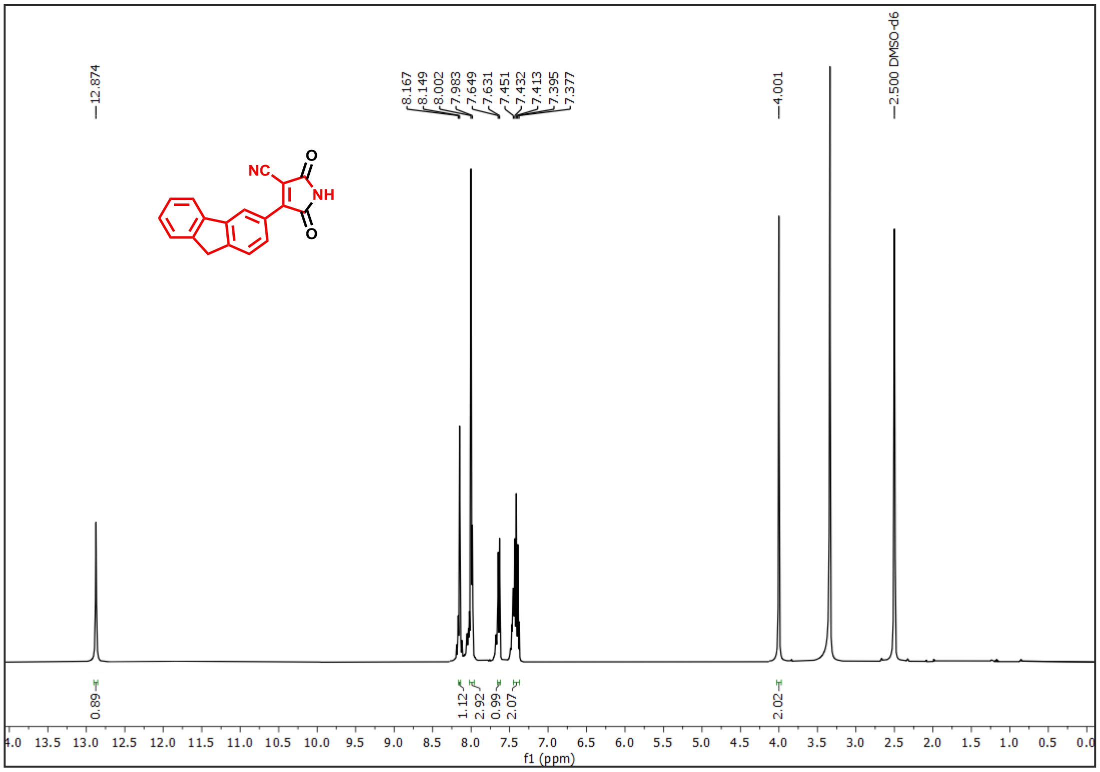

^{1}H NMR spectrum of compound **3n** (400 MHz, DMSO-d_6)

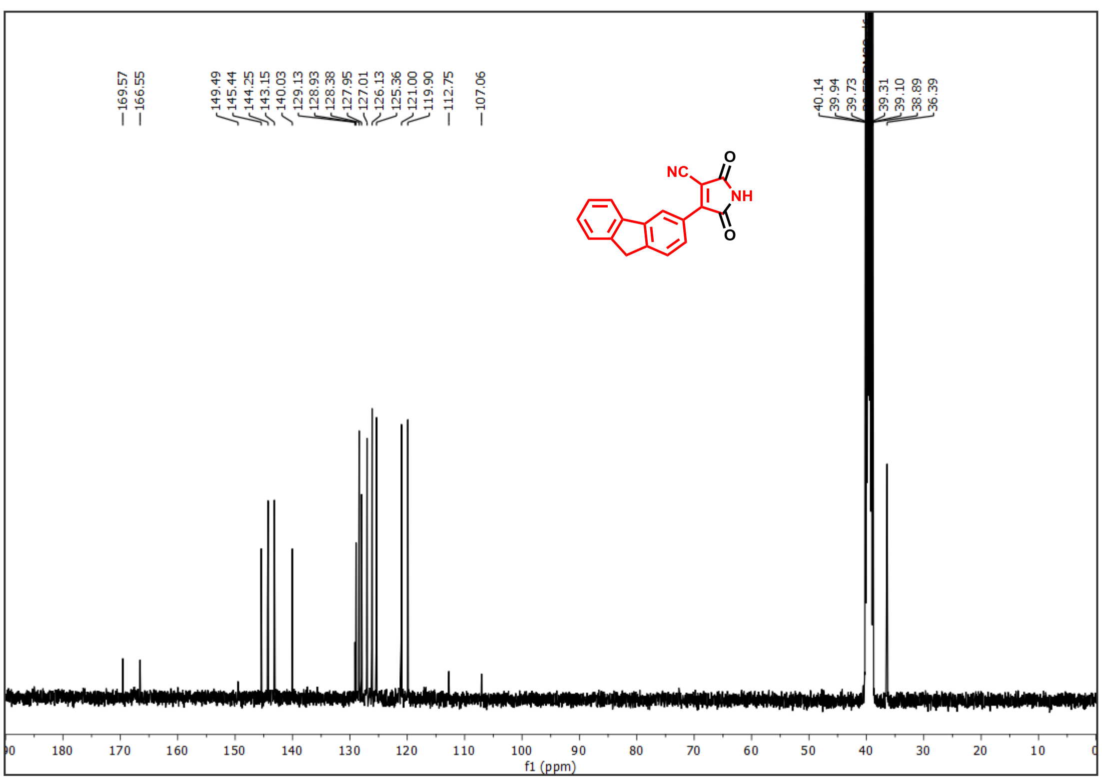

^{13}C NMR spectrum of compound **3n** (100 MHz, DMSO-d_6)

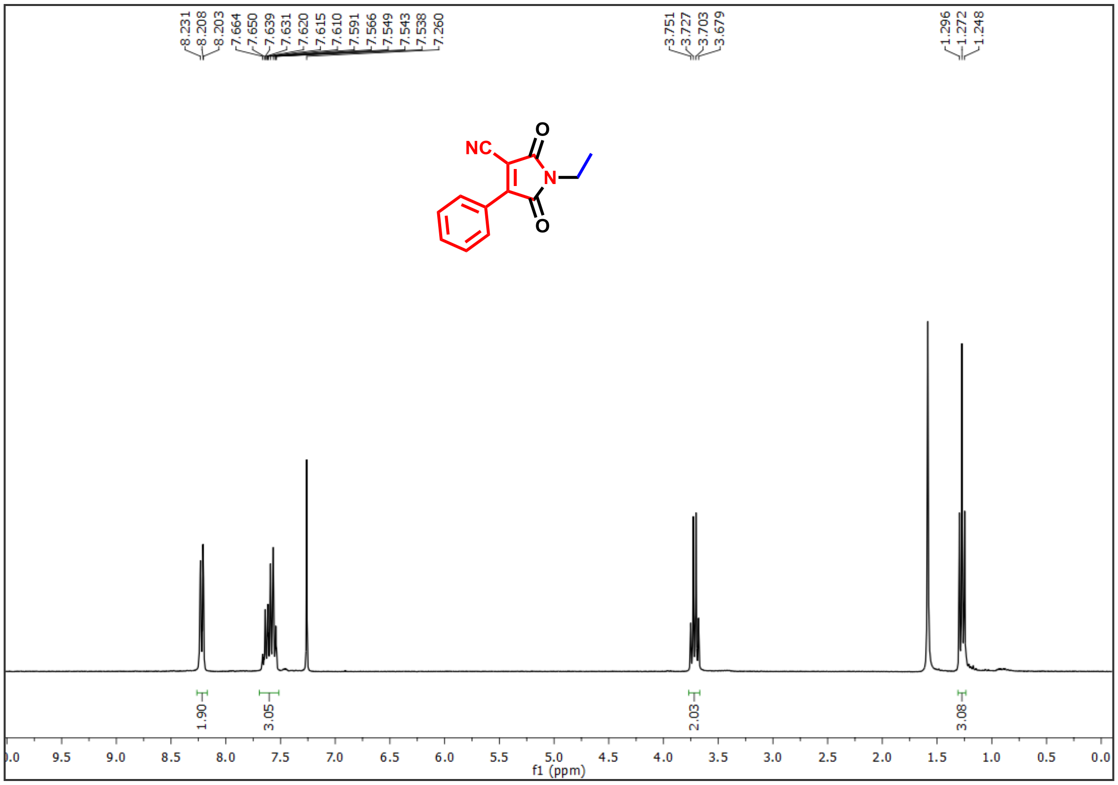

^{1}H NMR spectrum of compound **5a** (300 MHz, $CDCl_3$)

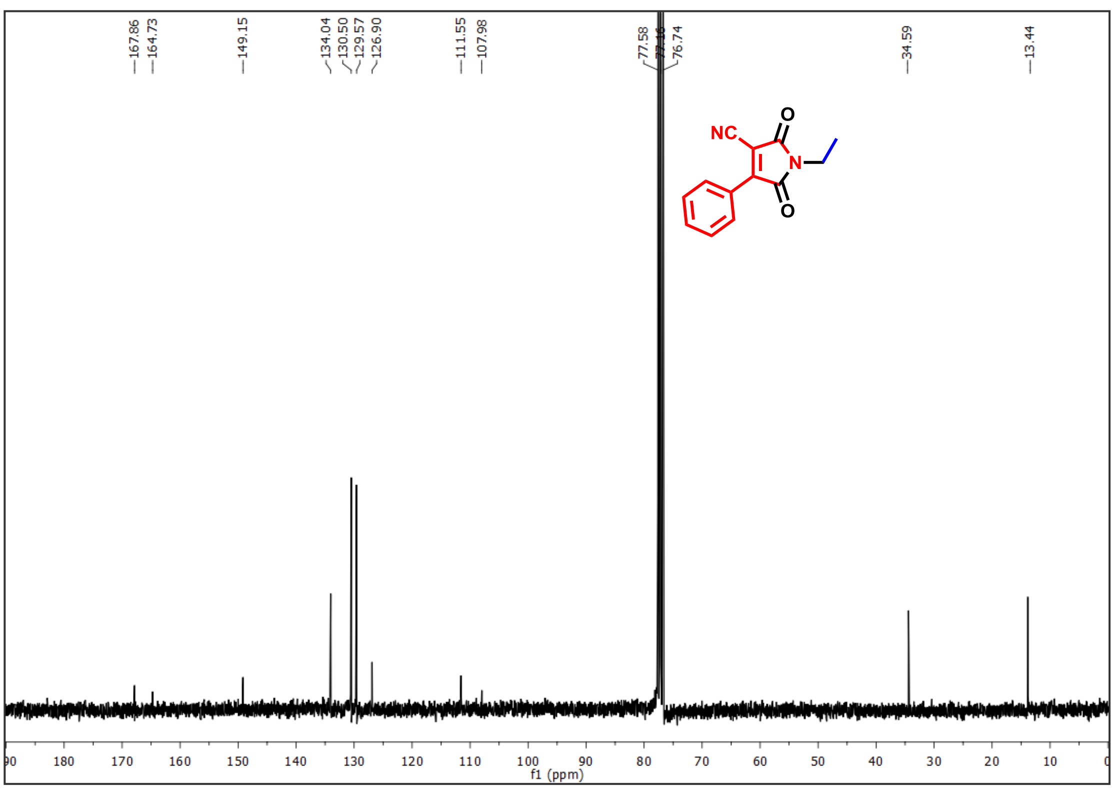

^{13}C NMR spectrum of compound **5a** (75 MHz, $CDCl_3$)

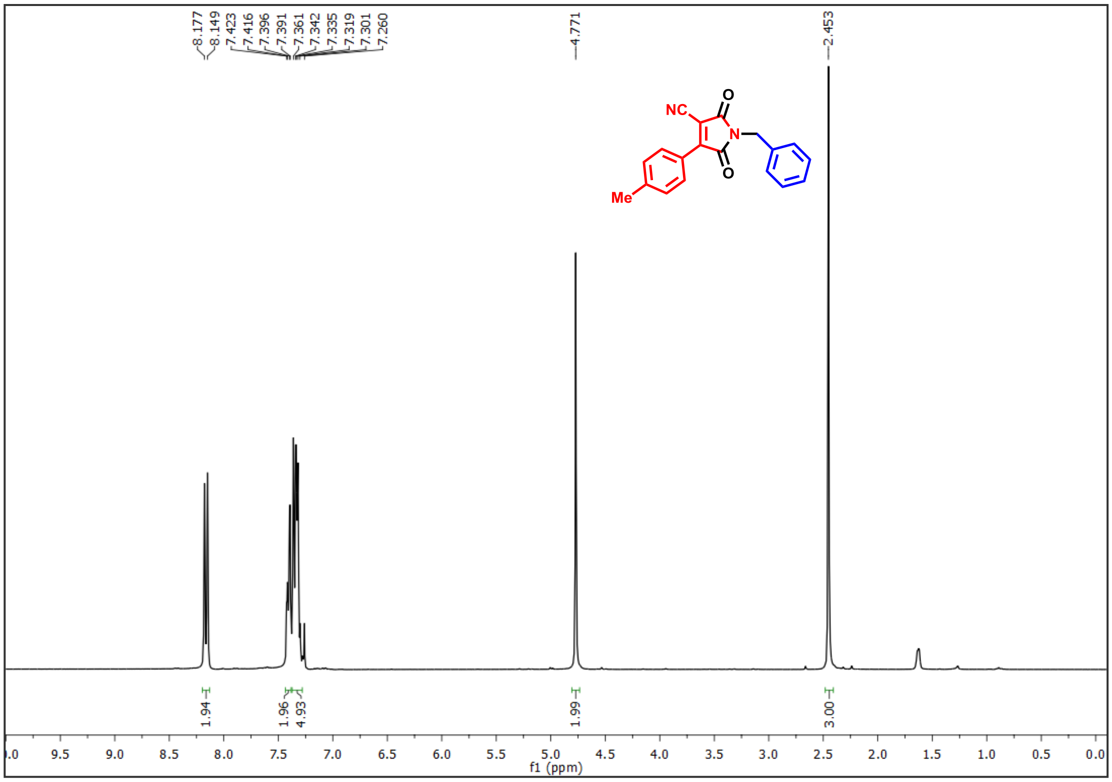

^{1}H NMR spectrum of compound **5b** (300 MHz, $CDCl_3$)

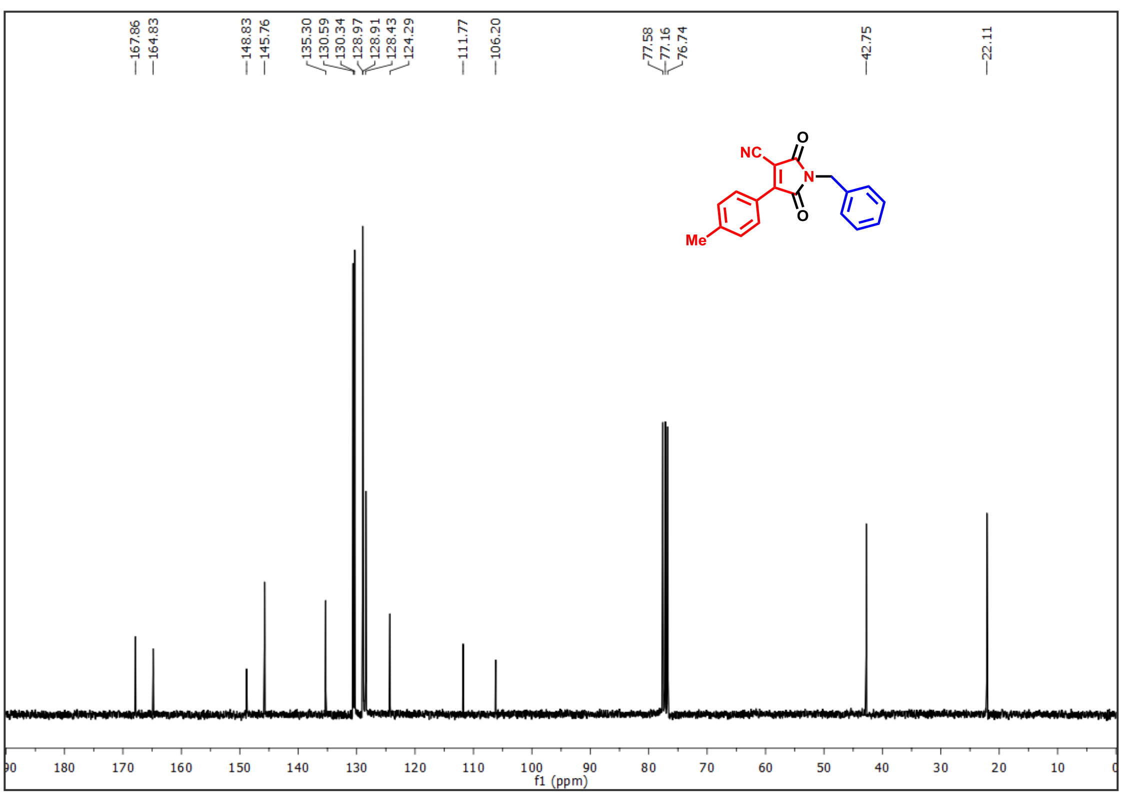

^{13}C NMR spectrum of compound **5b** (75 MHz, $CDCl_3$)

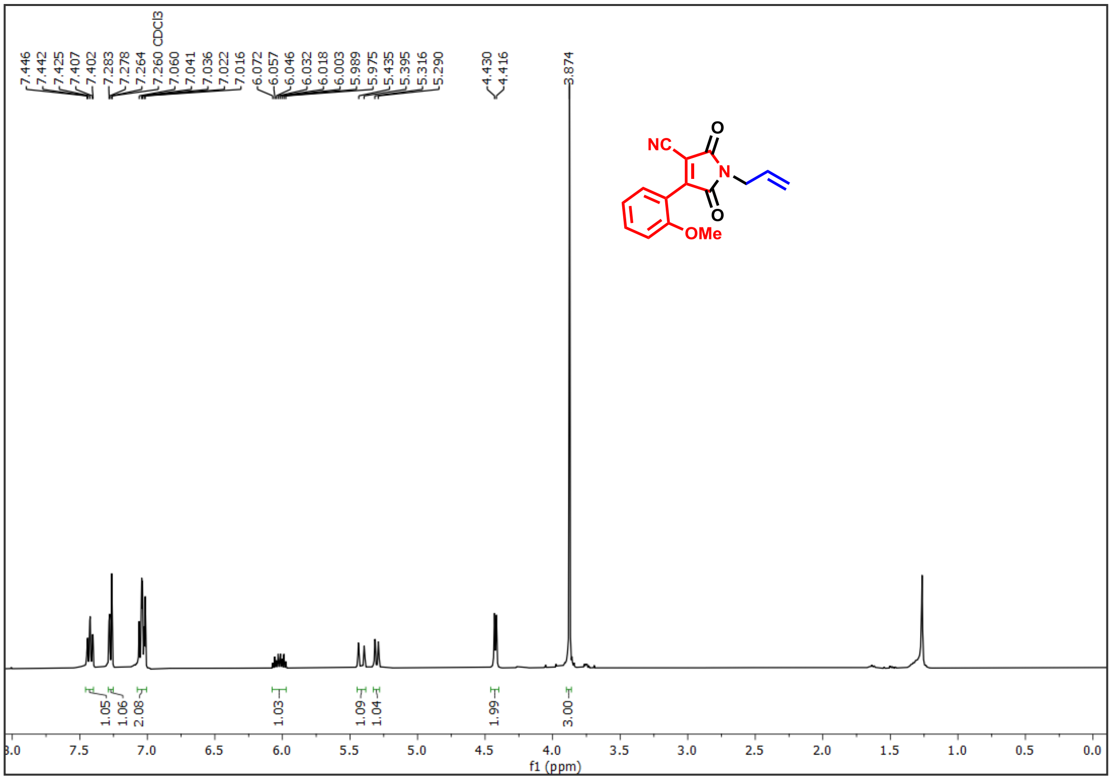

[1]H NMR spectrum of compound **5c** (400 MHz, $CDCl_3$)

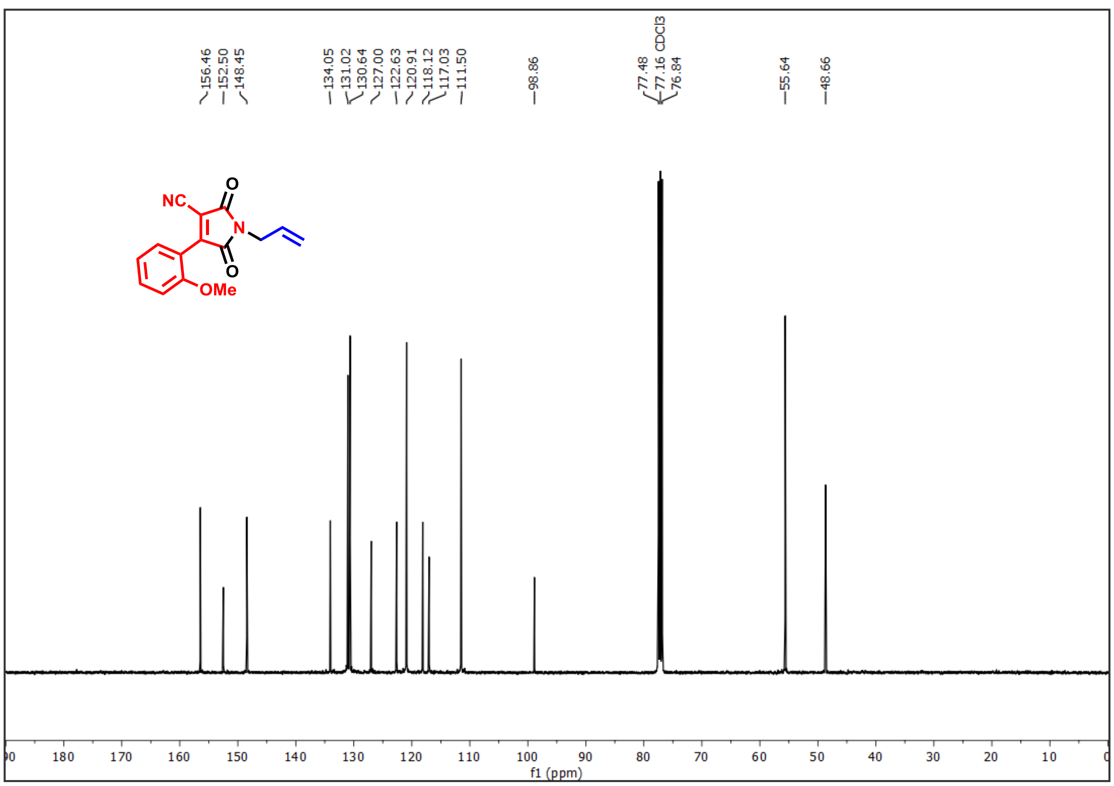

[13]C NMR spectrum of compound **5c** (100 MHz, $CDCl_3$)

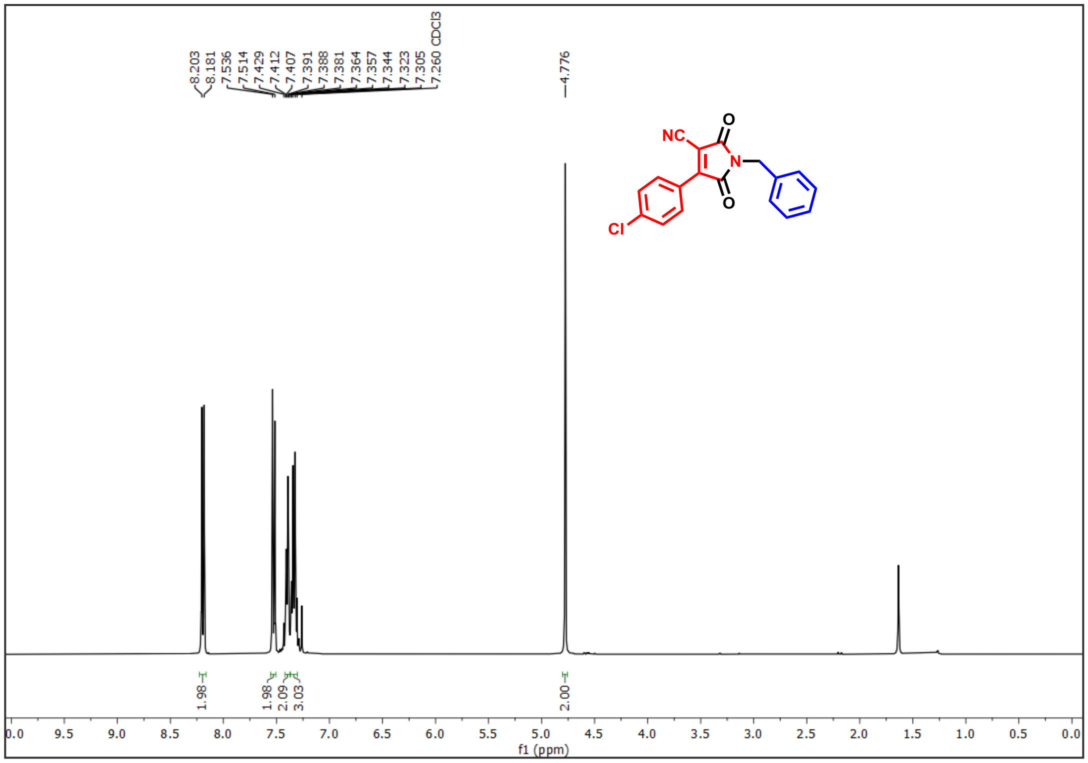

[1]H NMR spectrum of compound **5d** (400 MHz, $CDCl_3$)

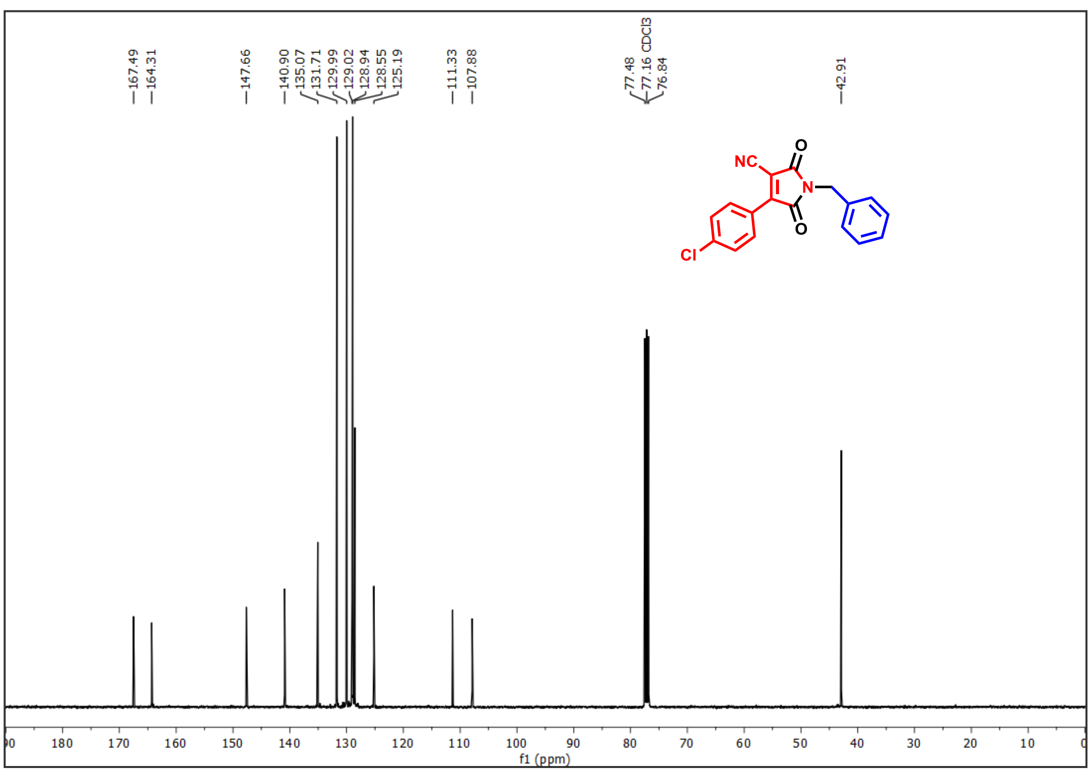

[13]C NMR spectrum of compound **5d** (100 MHz, $CDCl_3$)

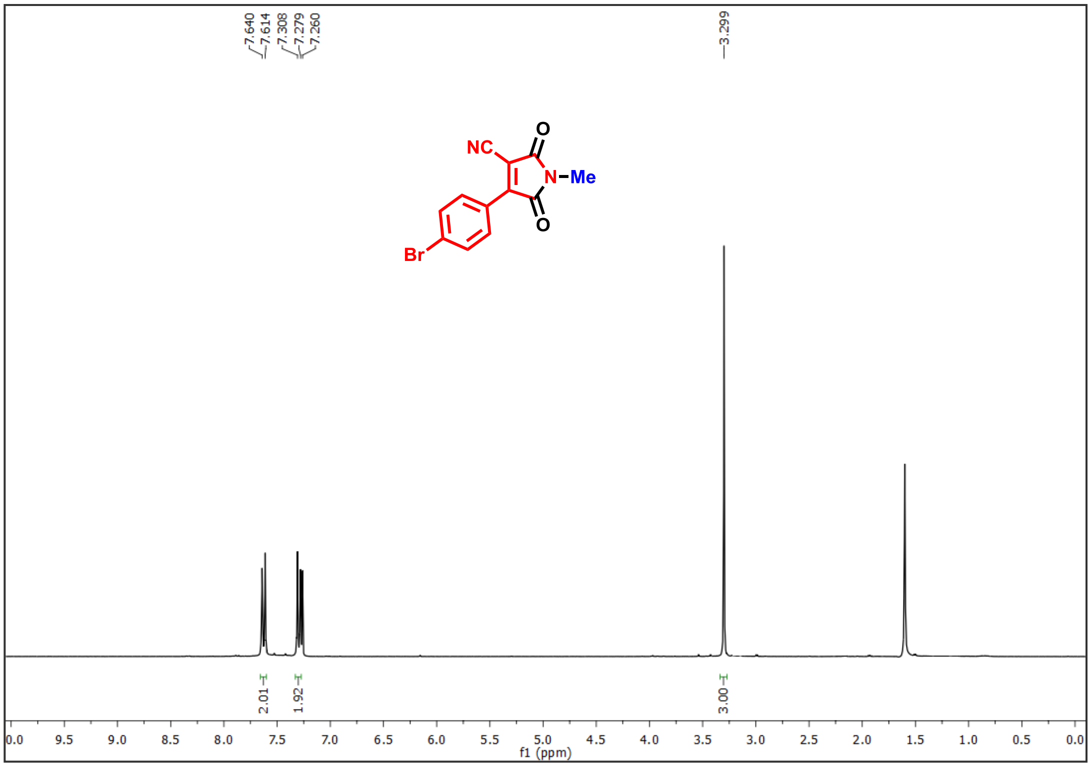

[1]H NMR spectrum of compound **5e** (300 MHz, $CDCl_3$)

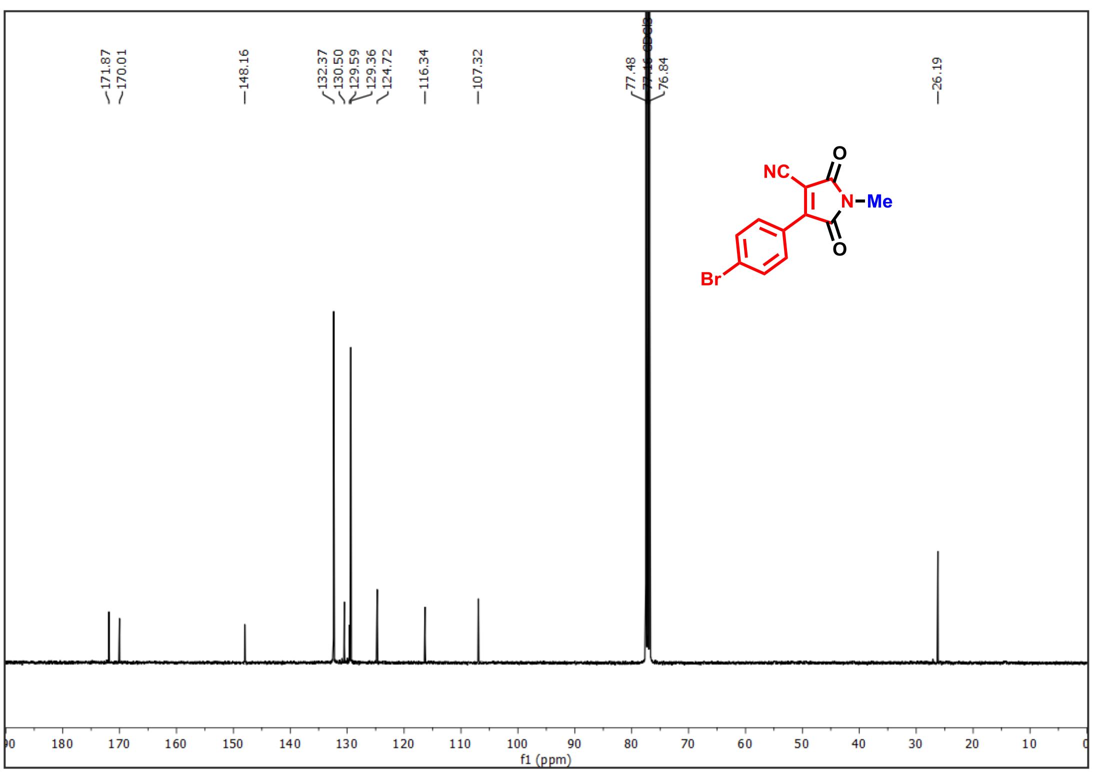

[13]C NMR spectrum of compound **5e** (100 MHz, $CDCl_3$)

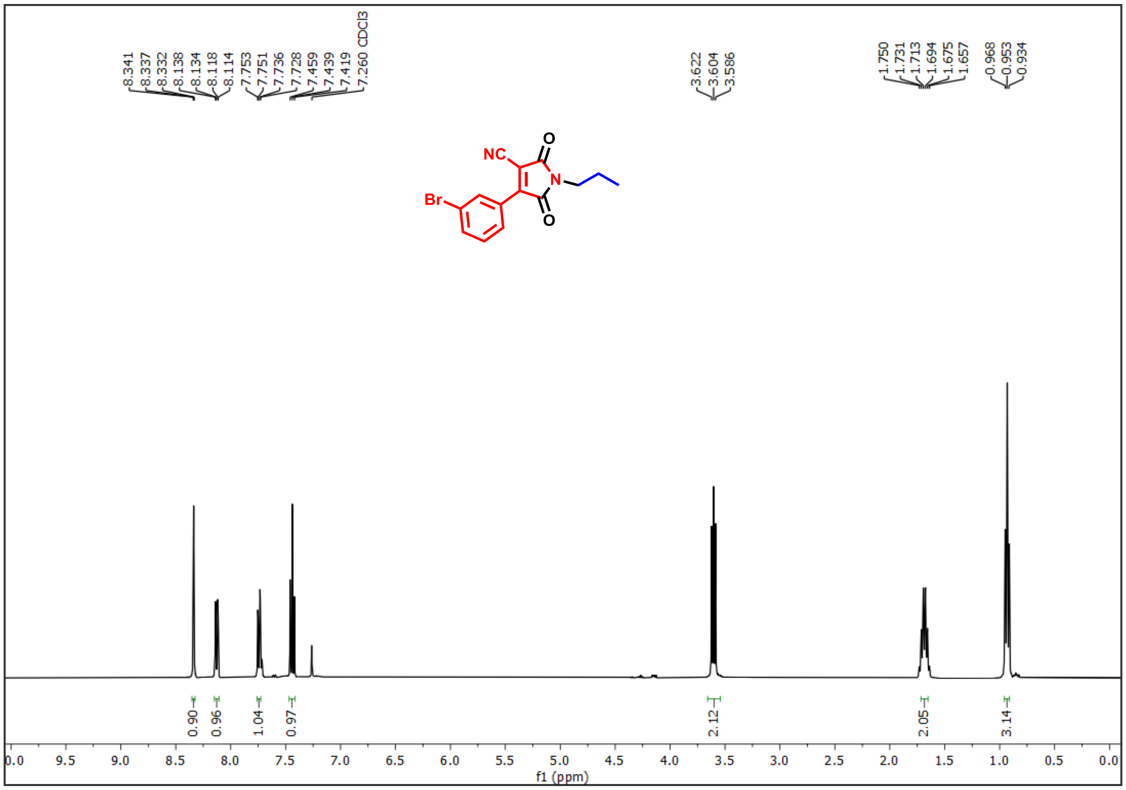

^{1}H NMR spectrum of compound **5f** (400 MHz, $CDCl_3$)

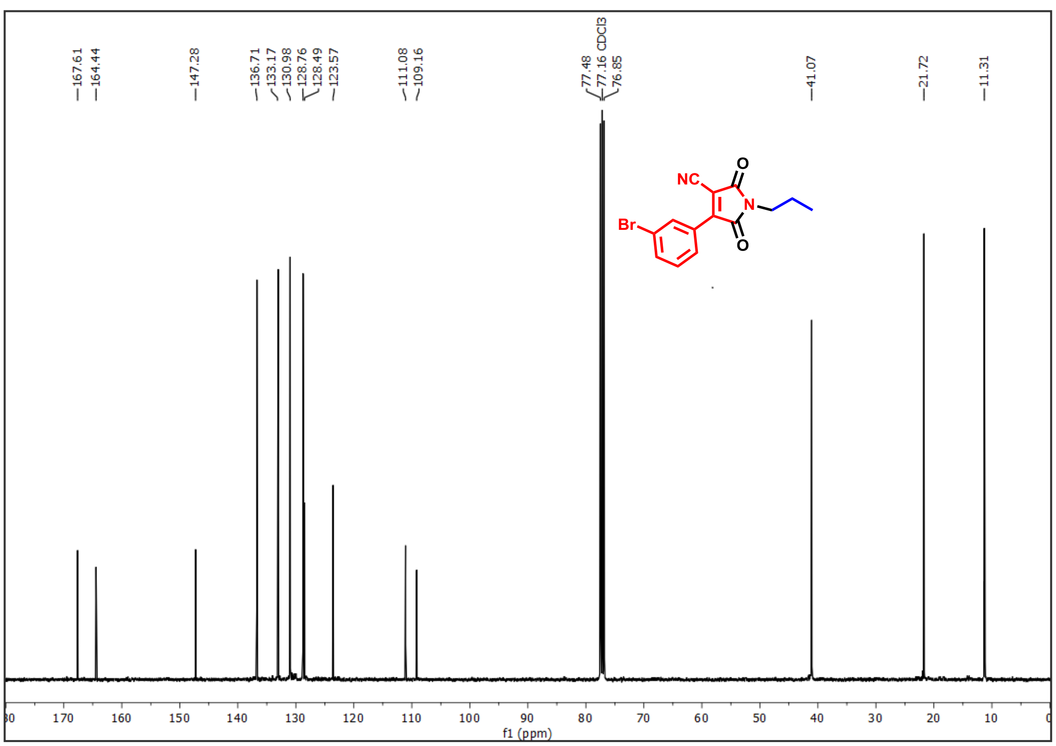

^{13}C NMR spectrum of compound **5f** (100 MHz, $CDCl_3$)

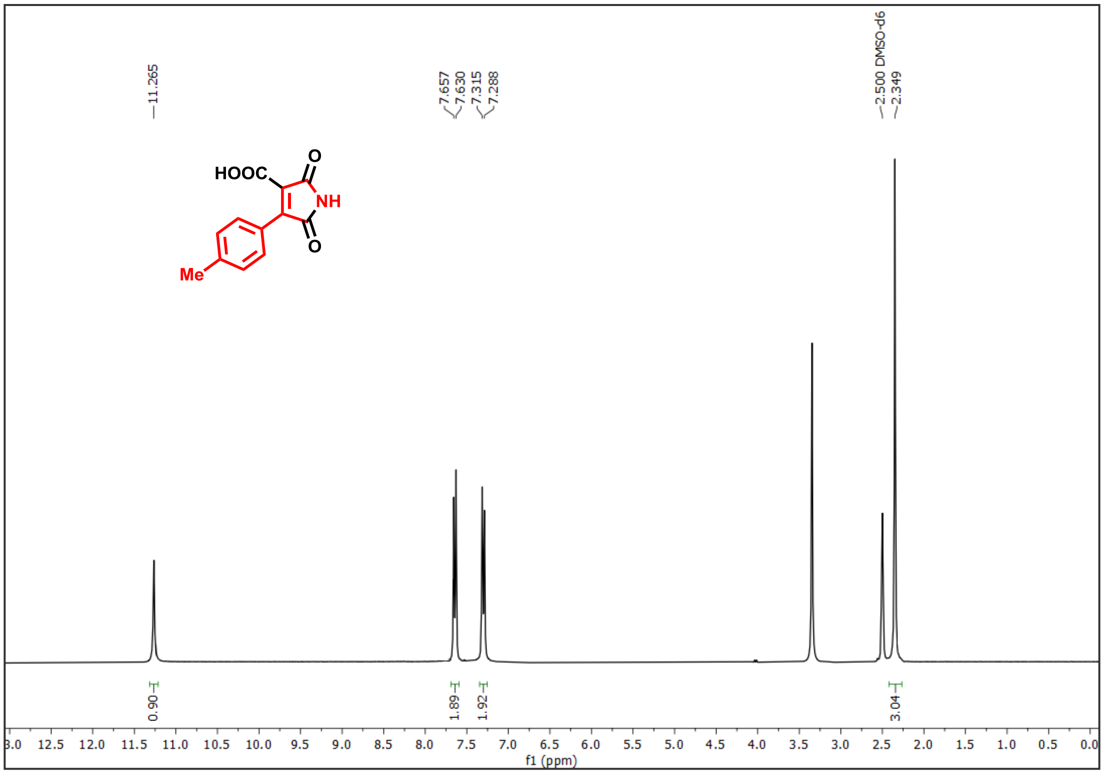

[1]H NMR spectrum of compound **6** (300 MHz, DMSO-d_6)

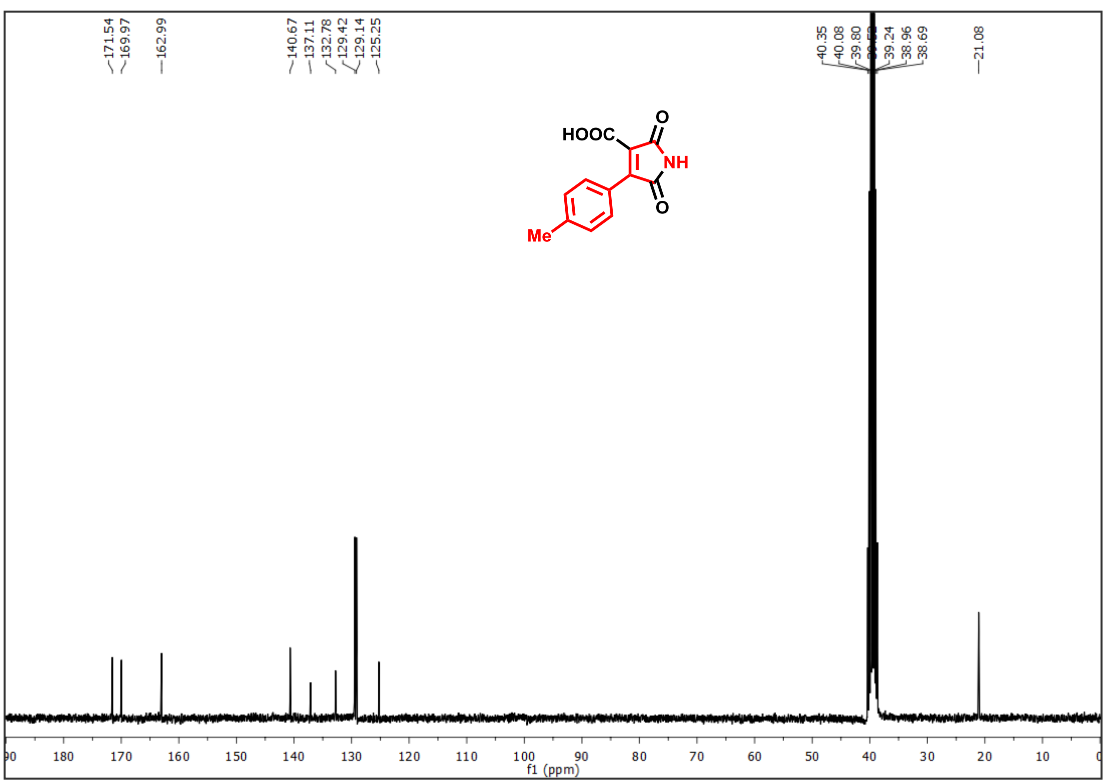

[13]C NMR spectrum of compound **6** (75 MHz, DMSO-d_6

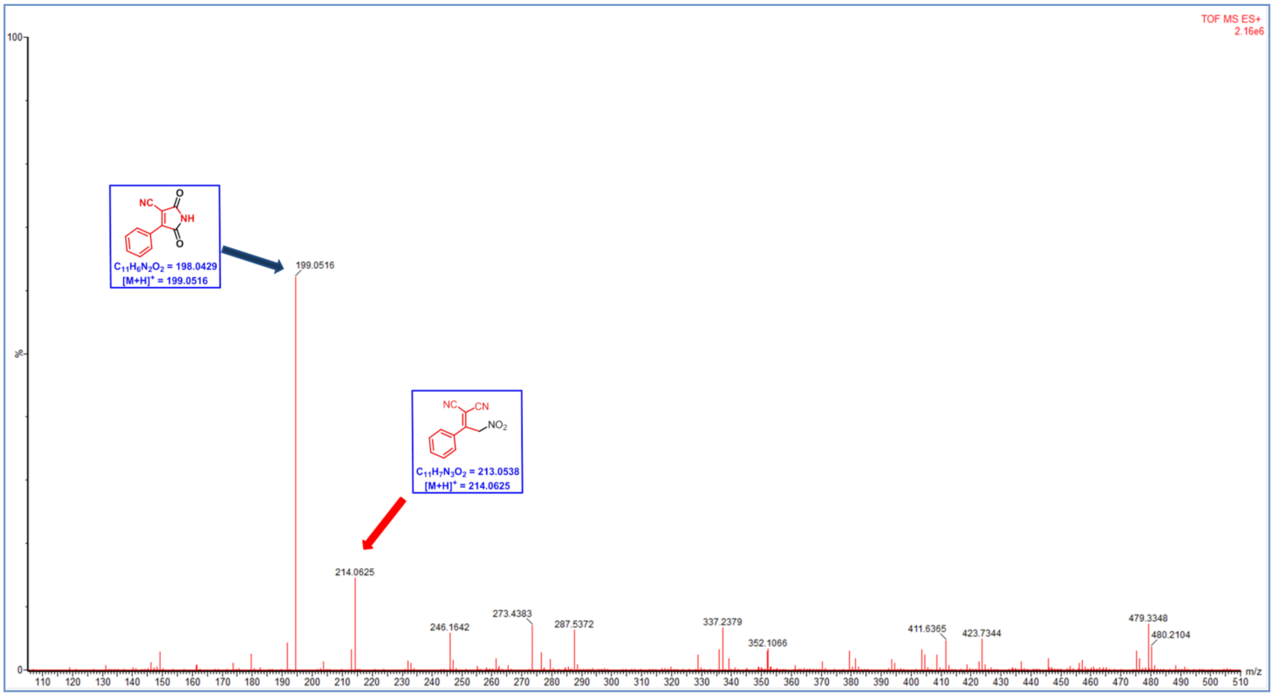

Figure 3. Crude mass data of intermediate **B** (after 4 h)

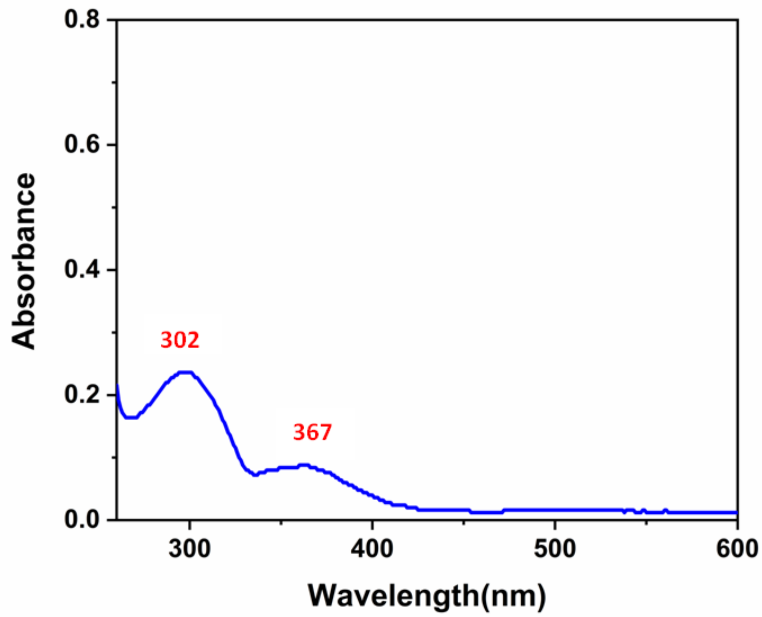

Figure 4. UV-Vis spectra of **3a** (5×10^{-5} M) in DMSO/H_2O (2:8 v/v) HEPES buffer solution

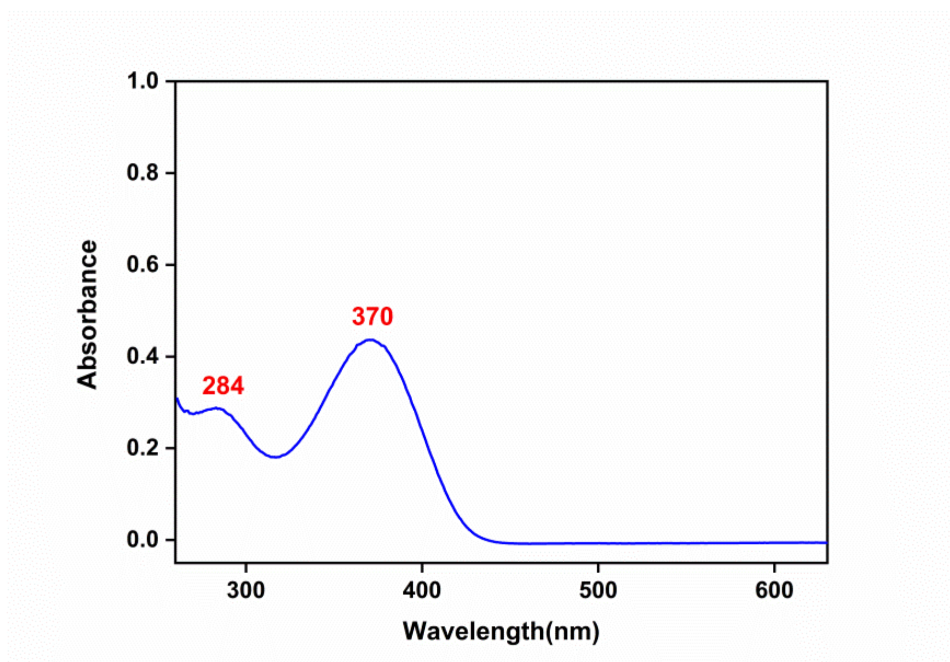

Figure 5. UV-Vis spectra of **3b** (5×10^{-5} M) in DMSO/H_2O (2:8 v/v) HEPES buffer solution.

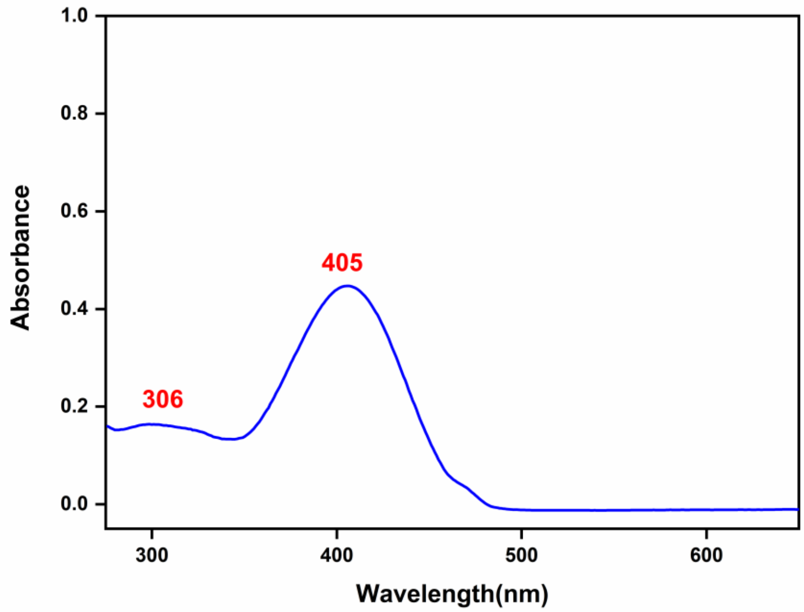

Figure 6. UV-Vis spectra of **3c** (5×10^{-5} M) in DMSO/H_2O (8:2 v/v) HEPES buffer solution.

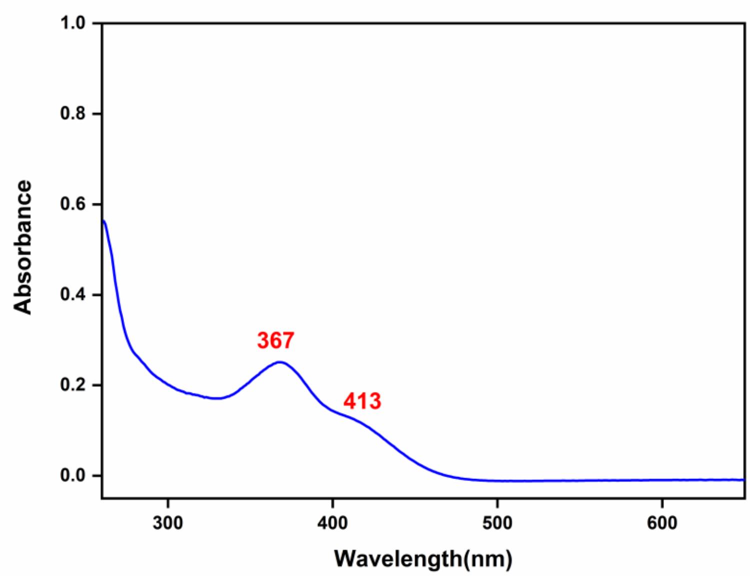

Figure 7. UV-Vis spectra of **3d** (5×10^{-5} M) in DMSO/H_2O (2:8 v/v) HEPES buffer solution.

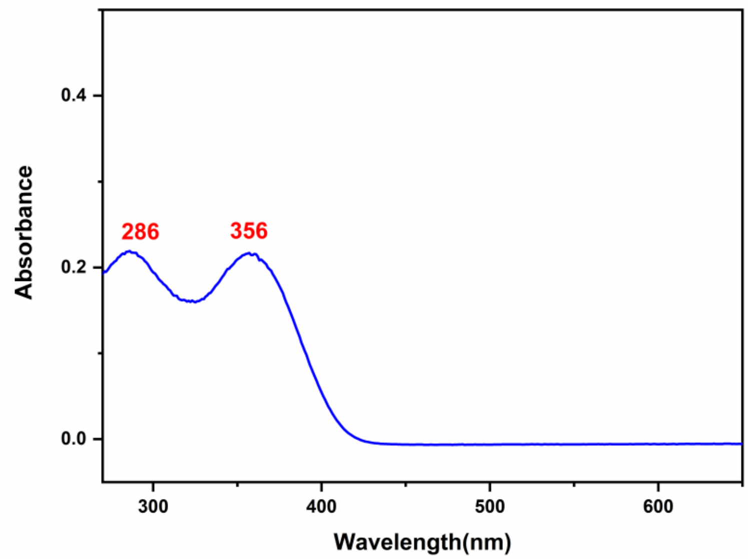

Figure 8. UV-Vis spectra of **3e** (5×10^{-5} M) in DMSO/H_2O (2:8 v/v) HEPES buffer solution.

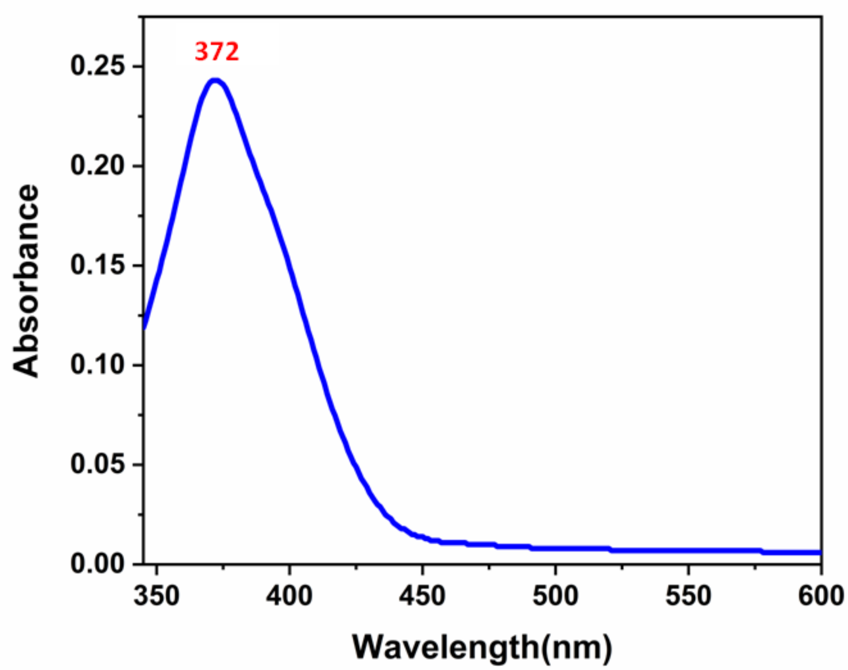

Figure 9. UV-Vis spectra of **3f** (5×10^{-5} M) in DMSO/H_2O (2:8 v/v) HEPES buffer solution

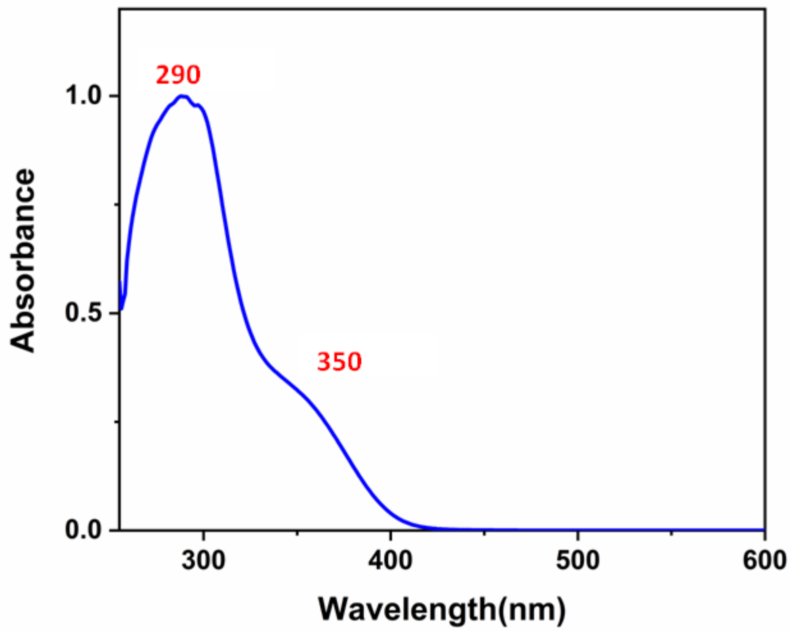

Figure 10. UV-Vis spectra of **3g** (5×10^{-5} M) in DMSO/H_2O (2:8 v/v) HEPES buffer solution

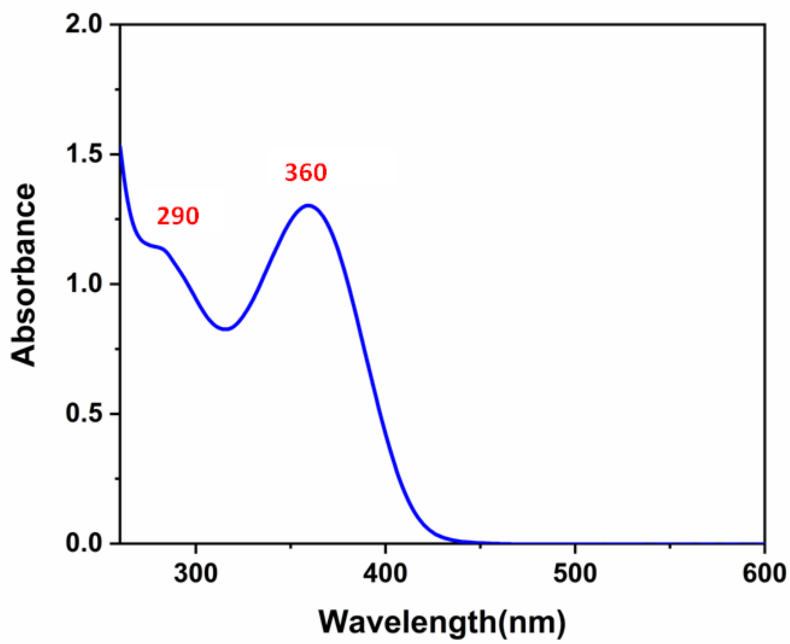

Figure 11. UV-Vis spectra of **3h** (5×10^{-5} M) in DMSO/H_2O (2:8 v/v) HEPES buffer solution

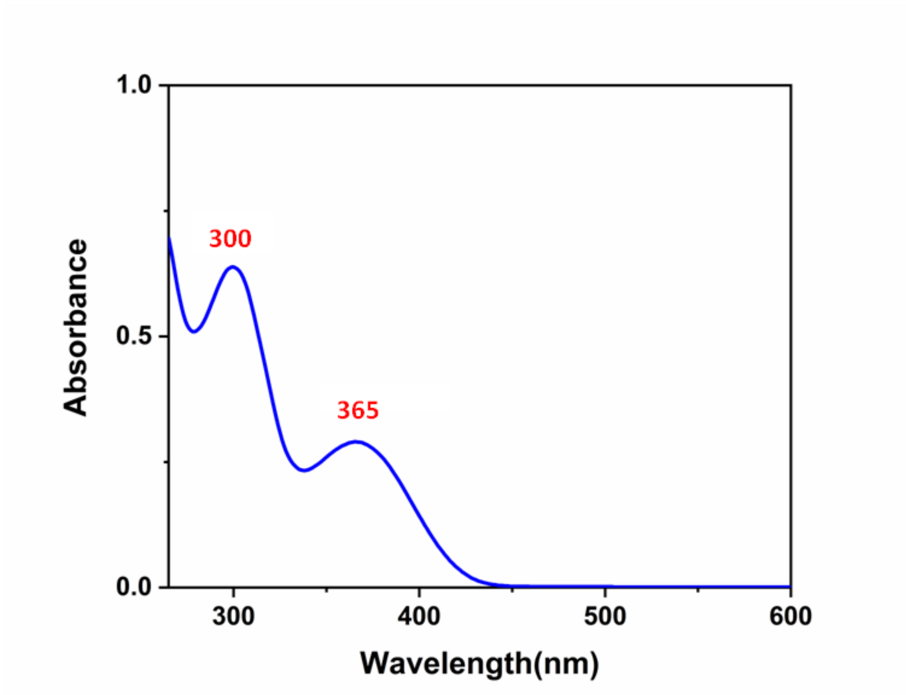

Figure 12. UV-Vis spectra of **3i** (5×10^{-5} M) in DMSO/H_2O (2:8 v/v) HEPES buffer solution

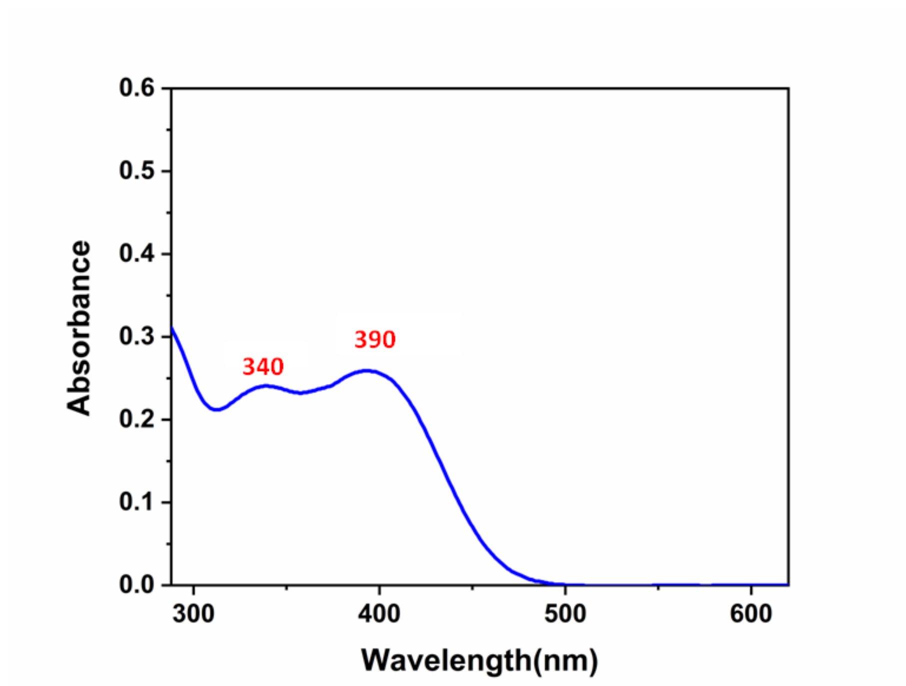

Figure 13. UV-Vis spectra of **3j** (5×10^{-5} M) in DMSO/H_2O (2:8 v/v) HEPES buffer solution

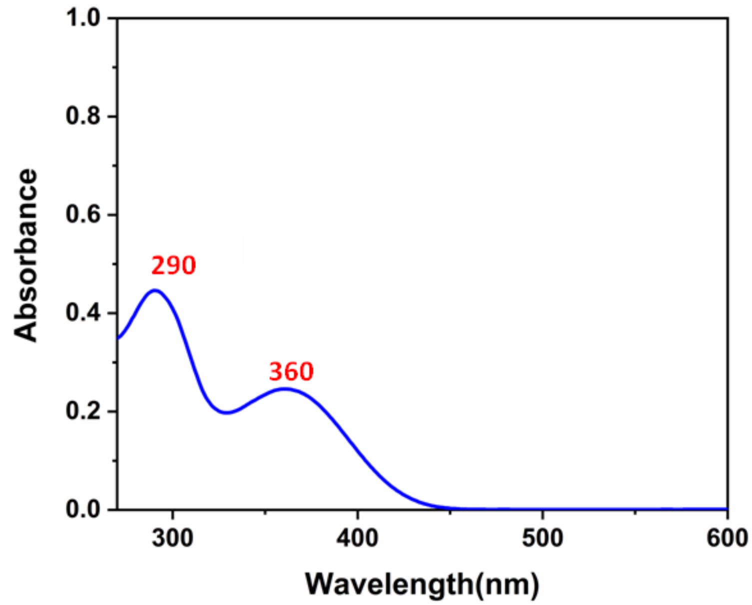

Figure 14. UV-Vis spectra of **3k** (5×10^{-5} M) in DMSO/H_2O (2:8 v/v) HEPES buffer solution

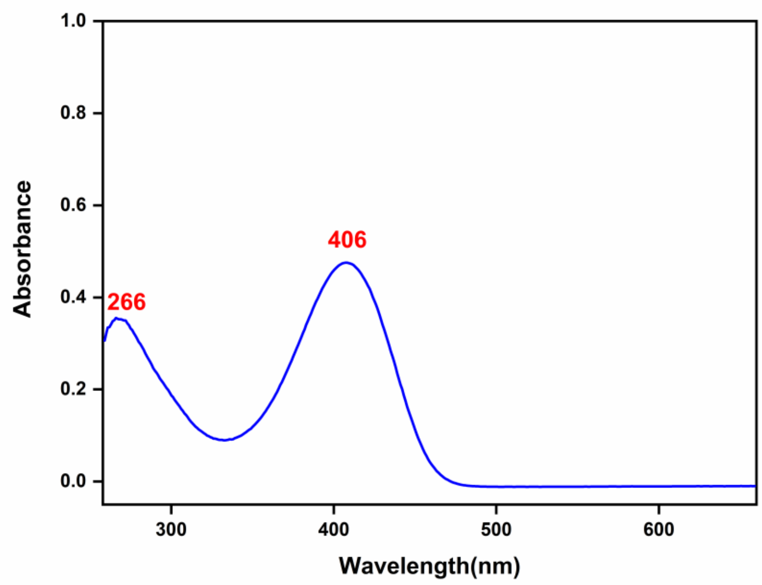

Figure 15. UV-Vis spectra of **3l** (5×10^{-5} M) in DMSO/H_2O (2:8 v/v) HEPES buffer solution.

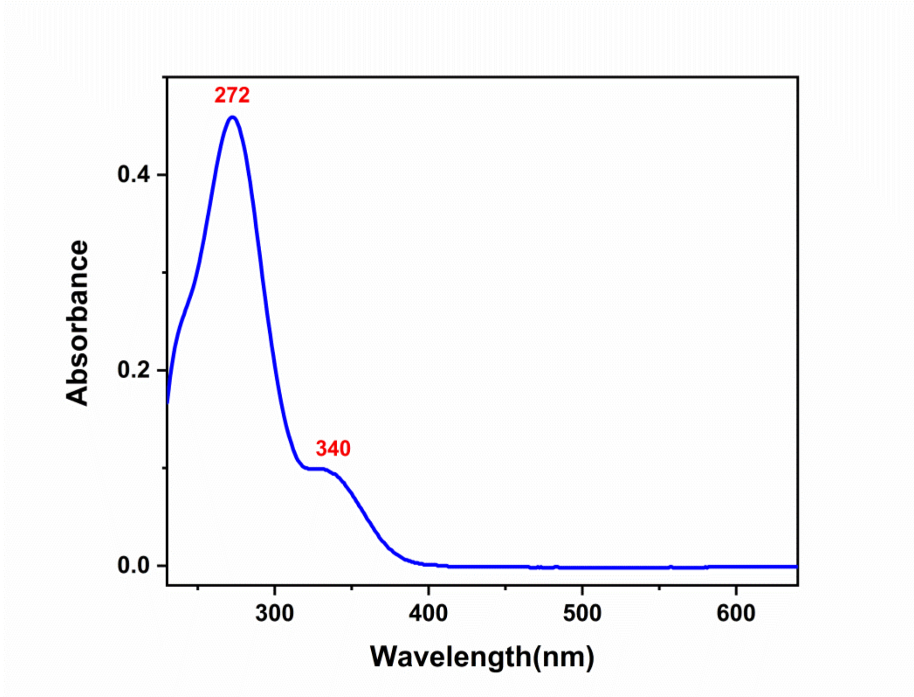

Figure 16. UV-Vis spectra of **3m** (5×10^{-5} M) in DMSO/H_2O (2:8 v/v) HEPES buffer solution

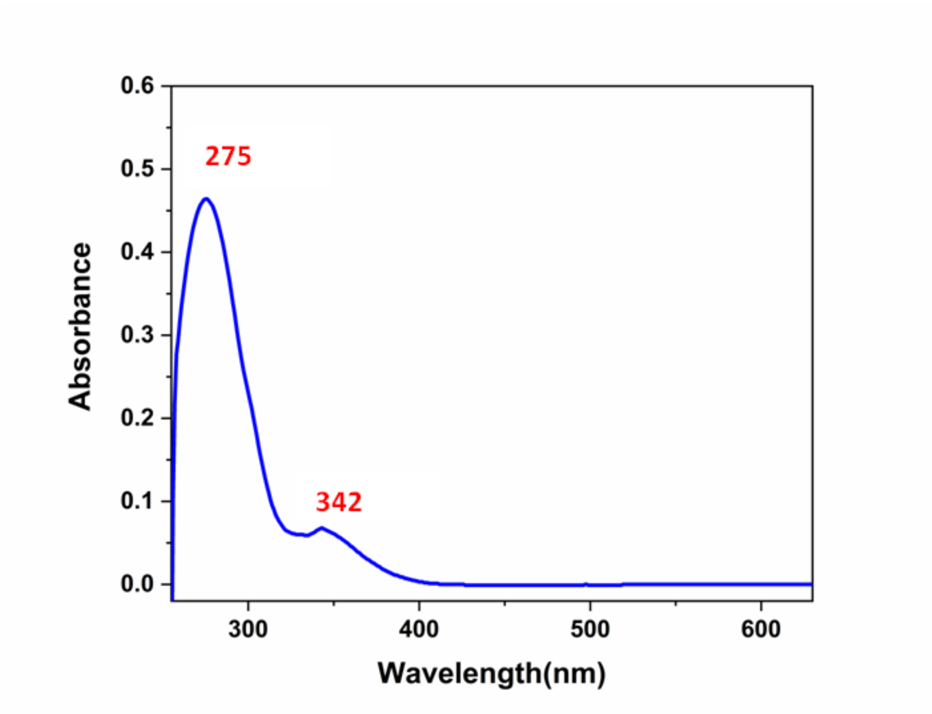

Figure 17. UV-Vis spectra of **3n** (5×10^{-5} M) in DMSO/H_2O (2:8 v/v) HEPES buffer solution

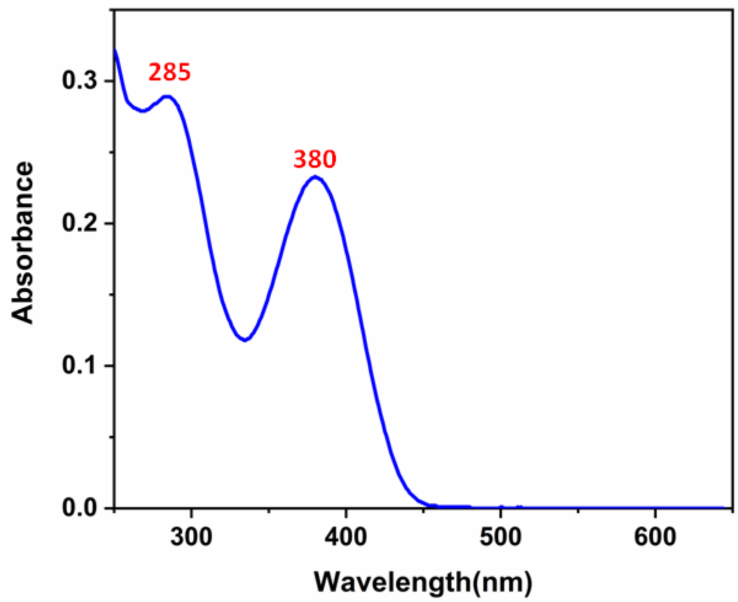

Figure 18. UV-Vis spectra of **5a** (5×10^{-5} M) in DMSO/H_2O (2:8 v/v) HEPES buffer solution

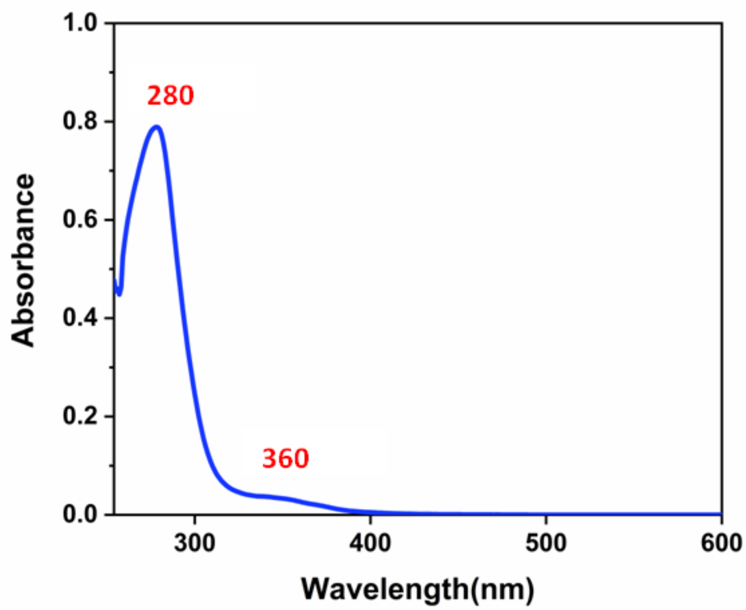

Figure 19. UV-Vis spectra of **5b** (5×10^{-5} M) in DMSO/H_2O (2:8 v/v) HEPES buffer solution

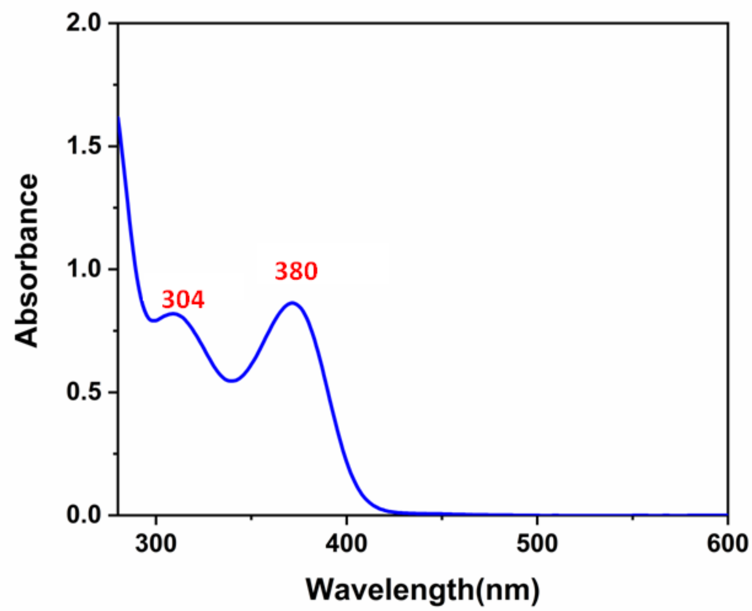

Figure 20. UV-Vis spectra of **5c** (5×10^{-5} M) in DMSO/H_2O (2:8 v/v) HEPES buffer solution

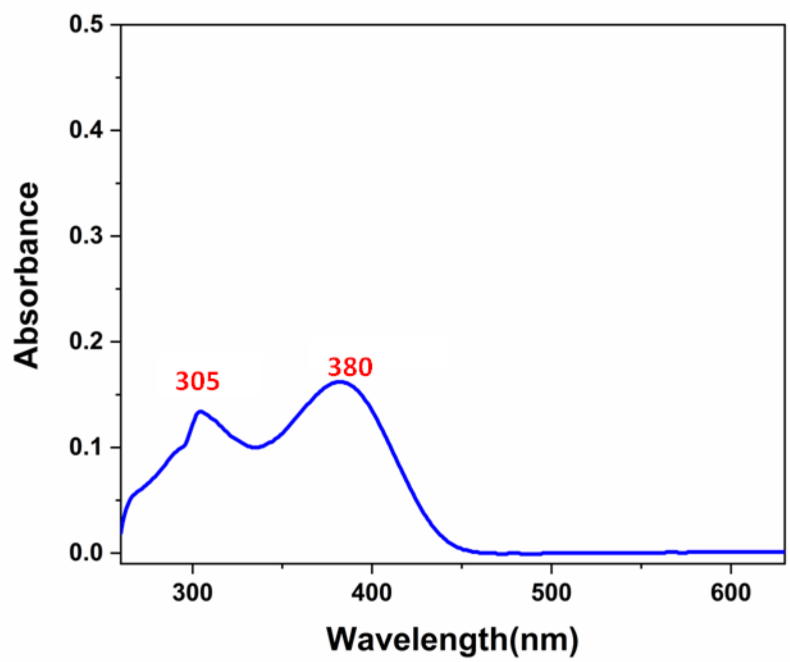

Figure 21. UV-Vis spectra of **5d** (5×10^{-5} M) in DMSO/H_2O (2:8 v/v) HEPES buffer solution

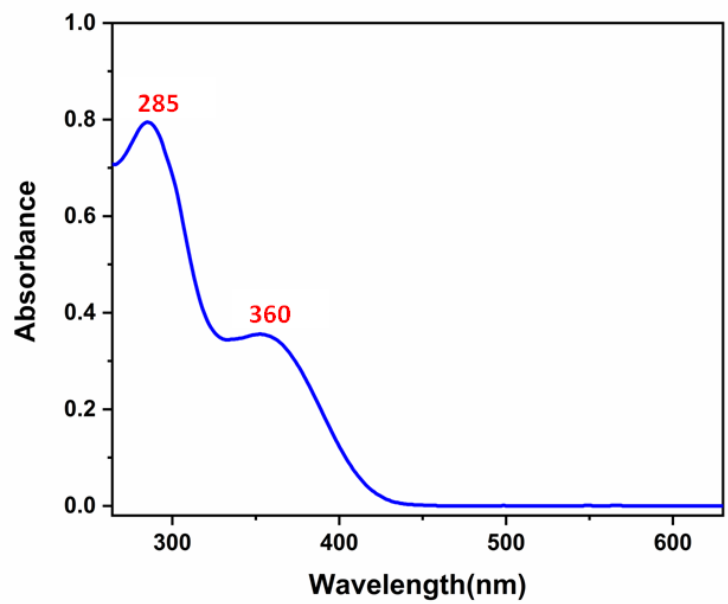

Figure 22. UV-Vis spectra of **5e** (5×10^{-5} M) in DMSO/H_2O (2:8 v/v) HEPES buffer solution

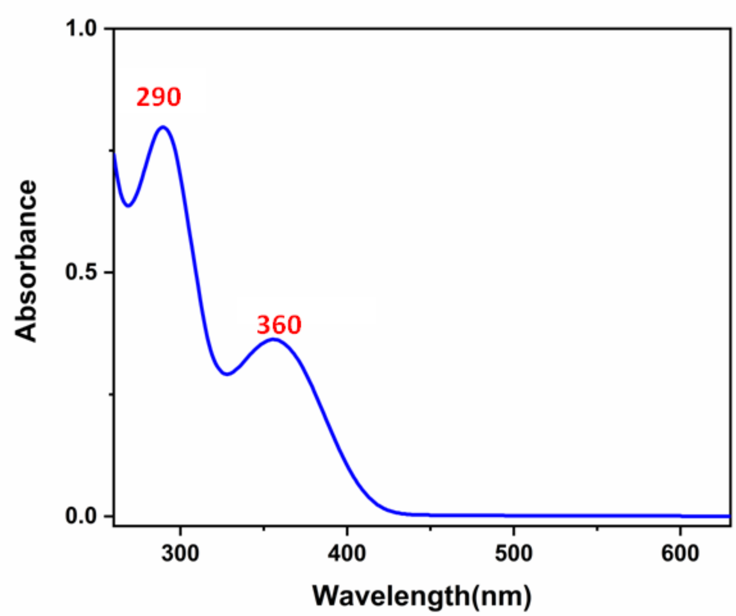

Figure 23. UV-Vis spectra of **5f** (5×10^{-5} M) in DMSO/H_2O (2:8 v/v) HEPES buffer solution

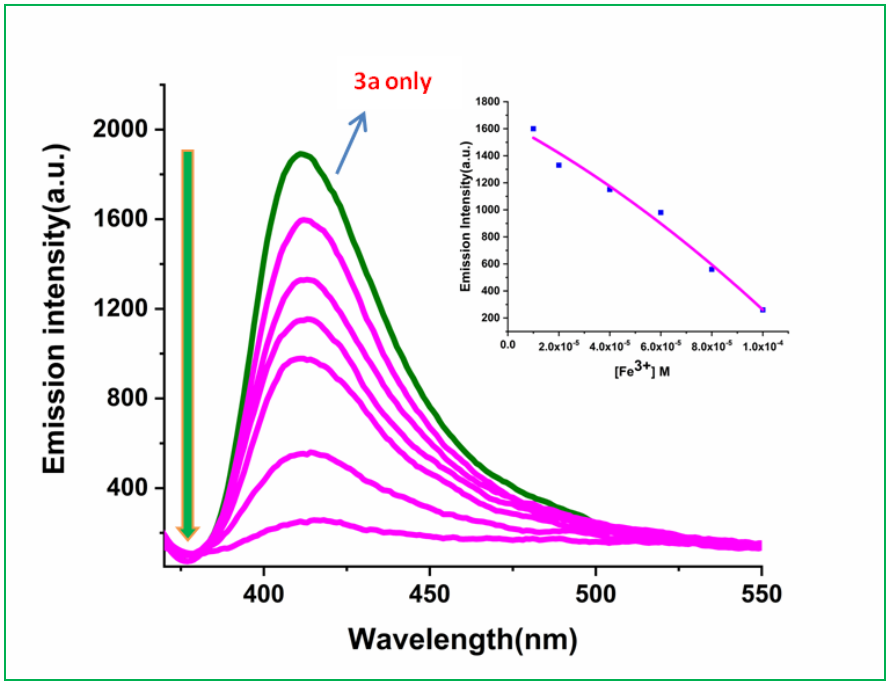

Figure 24. Fluorescence spectra of **3a** (50 µM) with incremental addition of Fe^{3+} (1, 2, 4, 6, 8, 10 ($\times 10^{-5}$ M) in DMSO/H_2O (2:8 v/v) HEPES buffer solution. **Inset:** Fluorescence emission intensity of **3a** as a function of [Fe^{3+}] (λ_{ex} = 367 nm, λ_{em} = 415 nm).

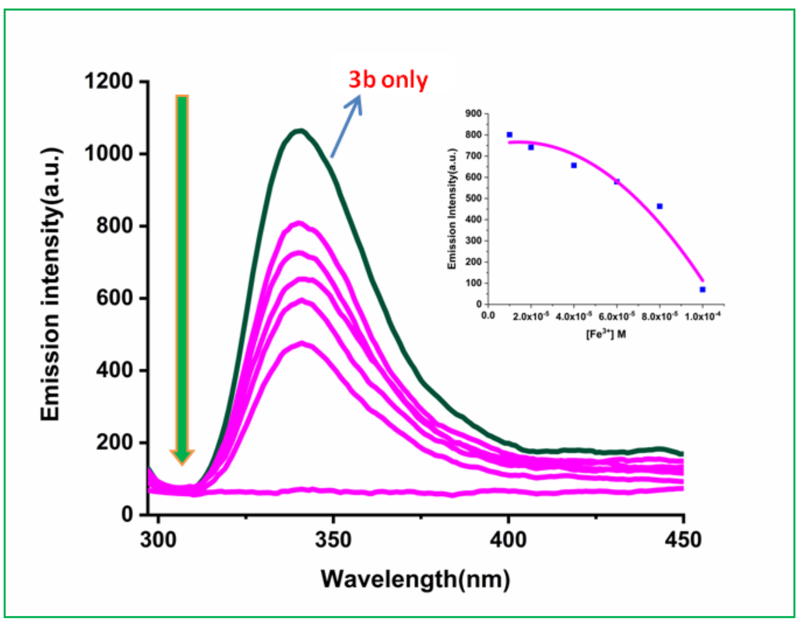

Figure 25. Fluorescence spectra of **3b** (50 µM) with incremental addition of Fe^{3+} (1, 2, 4, 6, 8, 10 ($\times 10^{-5}$ M) in DMSO/H_2O (2:8 v/v) HEPES buffer solution. **Inset:** Fluorescence emission intensity of **3b** as a function of [Fe^{3+}] (λ_{ex} = 284 nm, λ_{em} = 344 nm).

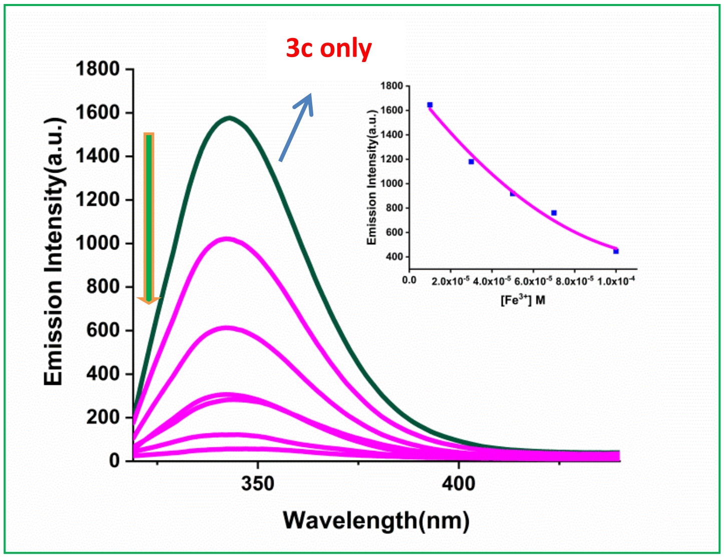

Figure 26. Fluorescence spectra of **3c** (5 μM) with incremental addition of Fe^{3+} (1, 3, 5, 7, 10 ($\times 10^{-5}$ M) in DMSO/H_2O (2:8 v/v) HEPES buffer Solution. **Inset:** Fluorescence emission intensity of **3c** as a function of [Fe^{3+}] (λ_{ex} = 306 nm, λ_{em} = 343 nm).

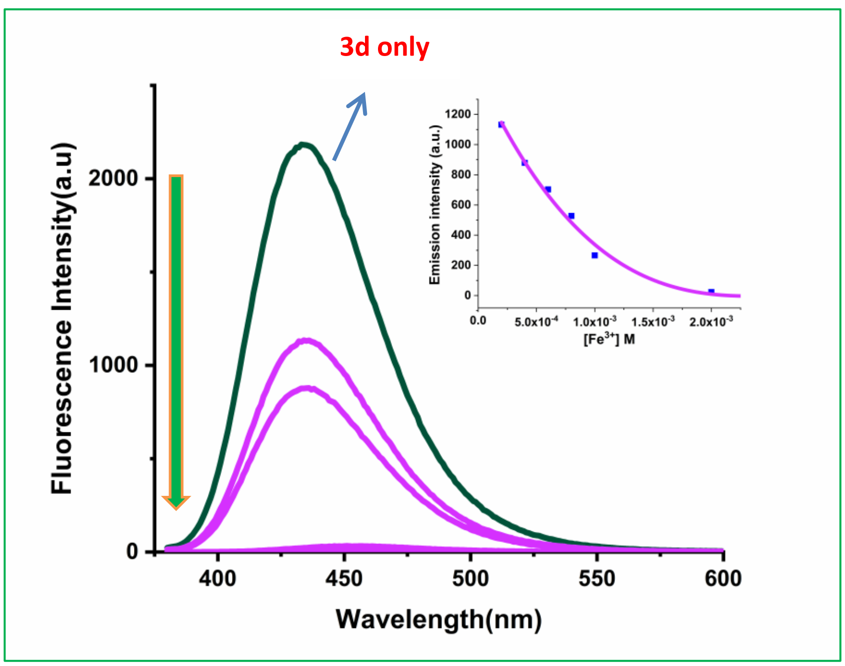

Figure 27. Fluorescence spectra of **3d** (5 $\times 10^{-4}$ M) with incremental addition of Fe^{3+} (2, 4, 6, 8, 10, 20 ($\times 10^{-4}$ M) in DMSO/H_2O (8:2 v/v) HEPES buffer Solution . **Inset:** Fluorescence emission intensity of **3d** as a function of [Fe^{3+}] (λ_{ex} = 367 nm, λ_{em} = 435 nm).

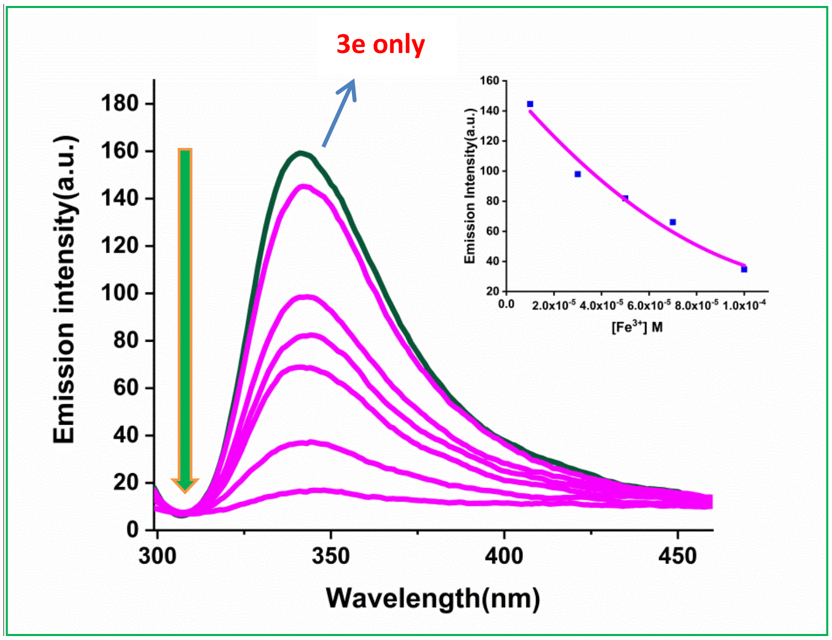

Figure 28. Fluorescence spectra of **3e** (5 ×10^{-5}M) with incremental addition of Fe^{3+} (0, 2, 4, 6, 8 and 10 (×10^{-5} M) in DMSO/H_2O (8:2 v/v) HEPES buffer solution. **Inset:** Fluorescence emission intensity of **3e** as a function of [Fe^{3+}] (λ_{ex} = 286 nm, λ_{em} = 343 nm).

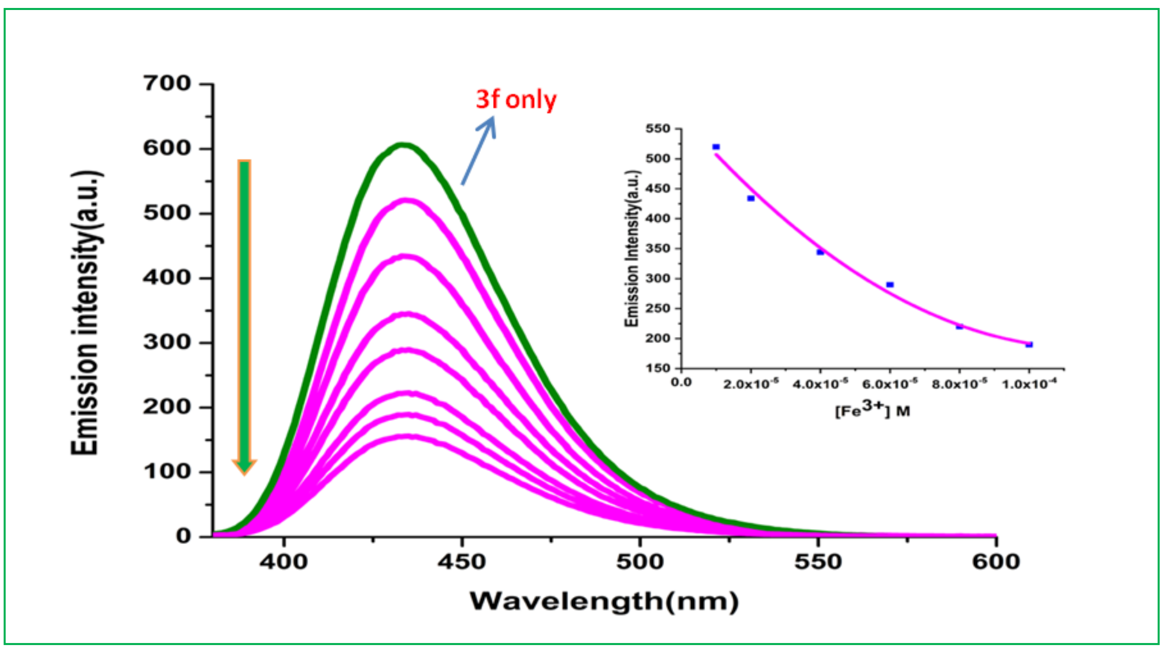

Figure 29. Fluorescence spectra of **3f** (5 ×10^{-5}M) with incremental addition of Fe^{3+} (0, 2, 4, 6, 8 and 10 (×10^{-5} M) in DMSO/H_2O (8:2 v/v) HEPES buffer solution. **Inset:** Fluorescence emission intensity of **3f** as a function of [Fe^{3+}] (λ_{ex} = 372 nm, λ_{em} = 434 nm).

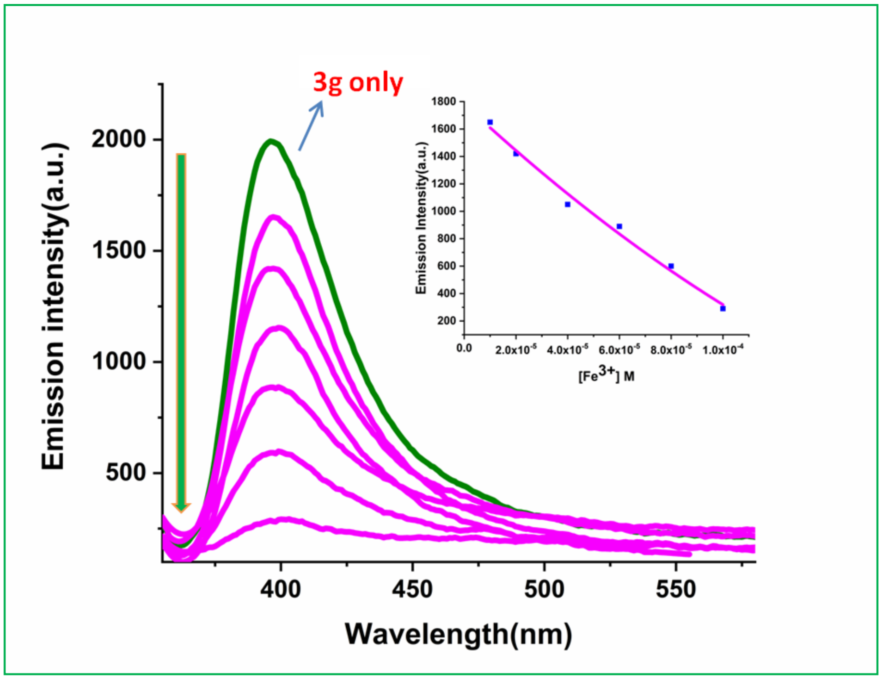

Figure 30. Fluorescence spectra of **3g** (50 µM) with incremental addition of Fe^{3+} (1, 2, 4, 6, 8 and 10 ($\times10^{-5}$ M) in DMSO/H_2O (2:8 v/v) HEPES buffer solution. **Inset:** Fluorescence emission intensity of **3g** as a function of [Fe^{3+}] (λ_{ex} = 350 nm, λ_{em} = 405 nm).

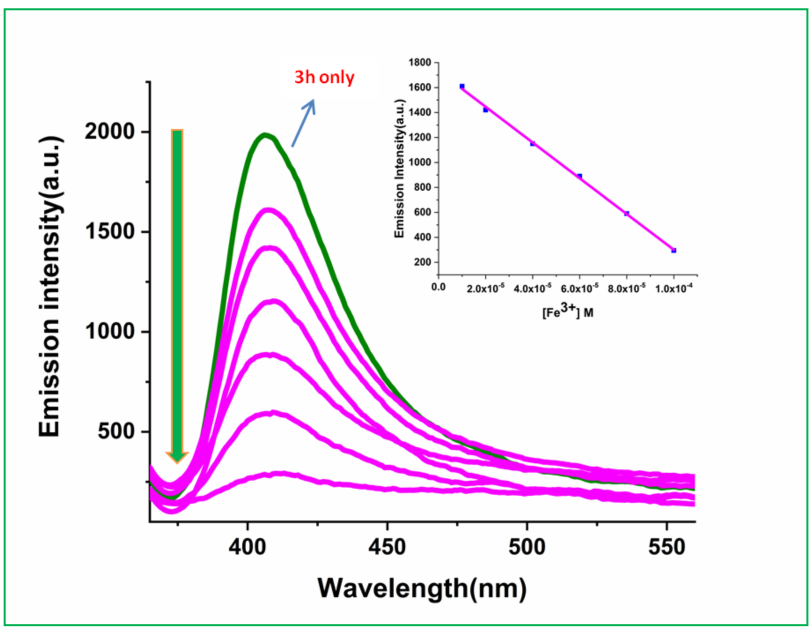

Figure 31. Fluorescence spectra of **3h** (50 µM) with incremental addition of Fe^{3+} (1, 2, 4, 6, 8 and 10 ($\times10^{-5}$ M) in DMSO/H_2O (2:8 v/v) HEPES buffer solution. **Inset:** Fluorescence emission intensity of **3h** as a function of [Fe^{3+}] (λ_{ex} = 360 nm, λ_{em} = 410 nm).

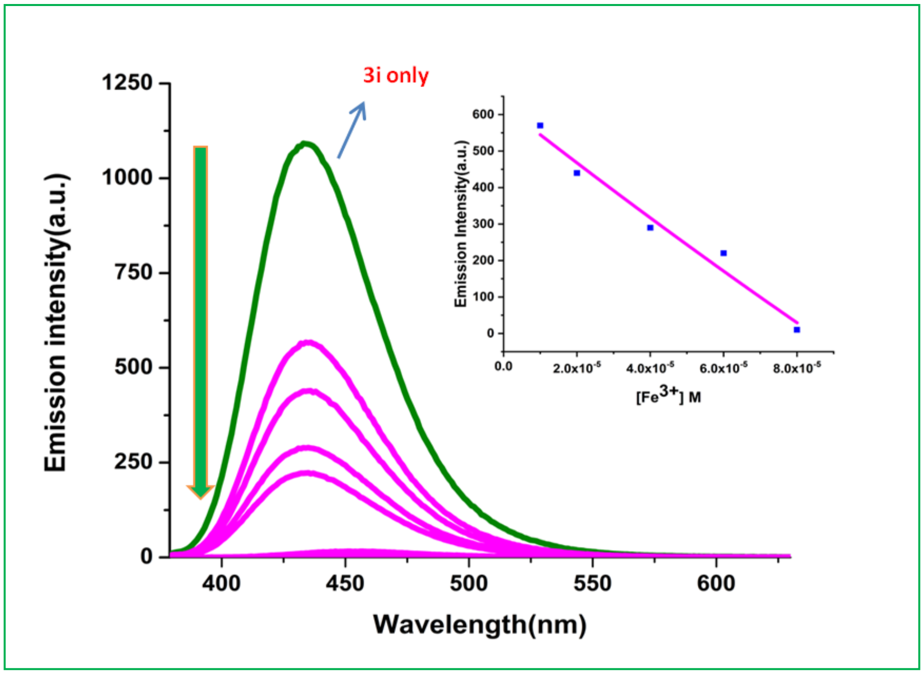

Figure 32. Fluorescence spectra of **3i** (50 µM) with incremental addition of Fe^{3+} (1, 2, 4, 6, 8 ($\times10^{-5}$ M) in DMSO/H_2O (2:8 v/v) HEPES buffer solution. **Inset:** Fluorescence emission intensity of **3i** as a function of [Fe^{3+}] (λ_{ex} = 365 nm, λ_{em} = 434 nm).

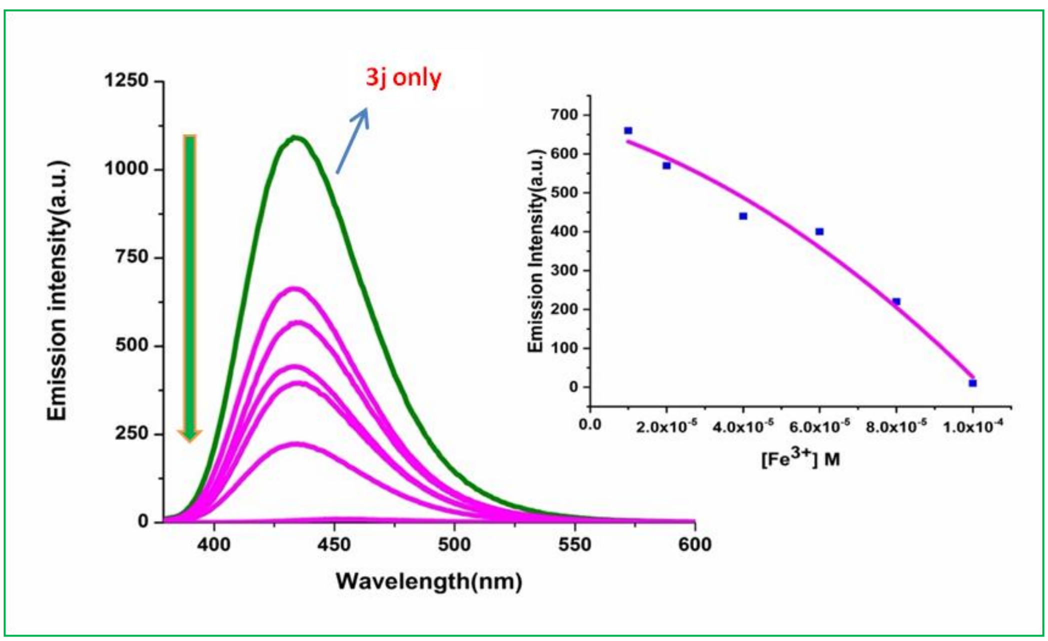

Figure 33. Fluorescence spectra of **3j** (50 µM) with incremental addition of Fe^{3+} (1, 2, 4, 6, 8 and 10 ($\times10^{-5}$ M) in DMSO/H_2O (2:8 v/v) HEPES buffer solution. **Inset:** Fluorescence emission intensity of **3j** as a function of [Fe^{3+}] (λ_{ex} = 390 nm, λ_{em} = 435 nm).

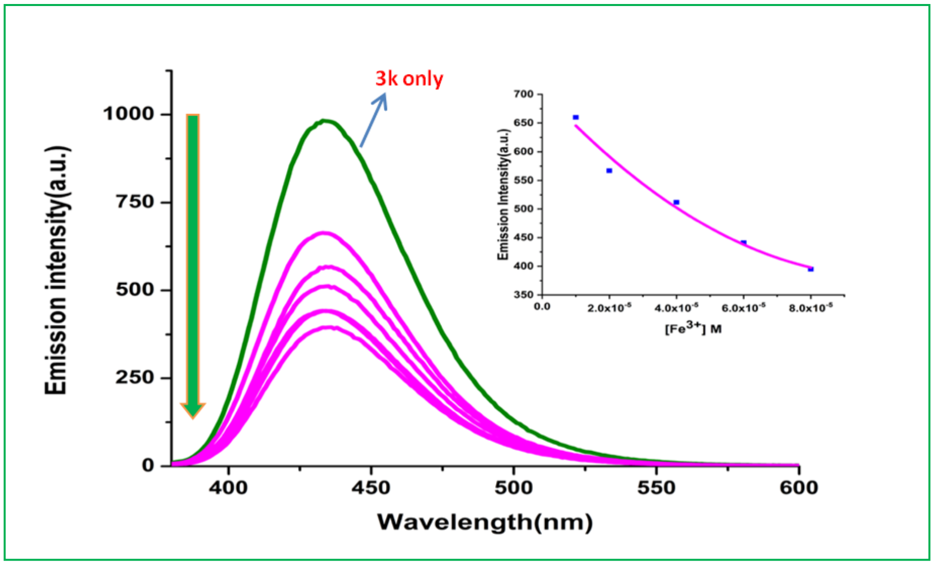

Figure 34. Fluorescence spectra of **3k** (50 µM) with incremental addition of Fe^{3+} (1, 2, 4, 6, 8 ($\times 10^{-5}$ M) in DMSO/H_2O (2:8 v/v) HEPES buffer solution. **Inset:** Fluorescence emission intensity of **3k** as a function of [Fe^{3+}] (λ_{ex} = 360 nm, λ_{em} = 430 nm).

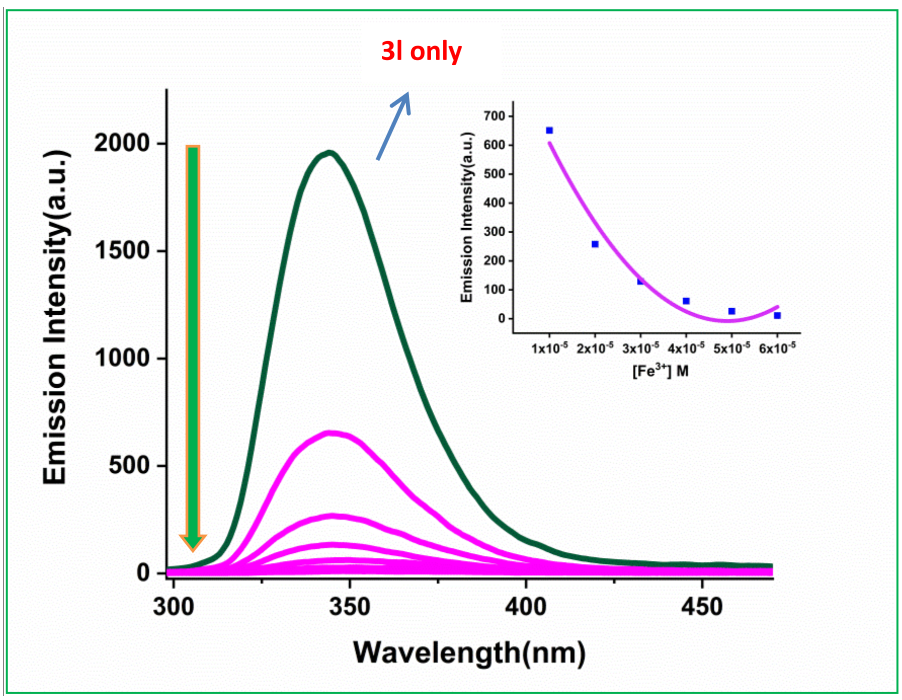

Figure 35. Fluorescence spectra of **3l** (5 $\times 10^{-5}$ M) with incremental addition of Fe^{3+} (0, 1, 2, 3, 4, 5 and 6 ($\times 10^{-5}$ M) in DMSO/H_2O (2:8 v/v) HEPES buffer solution. **Inset:** Fluorescence emission intensity of **3l** as a function of [Fe^{3+}] (λ_{ex} = 284 nm, λ_{em} = 345 nm).

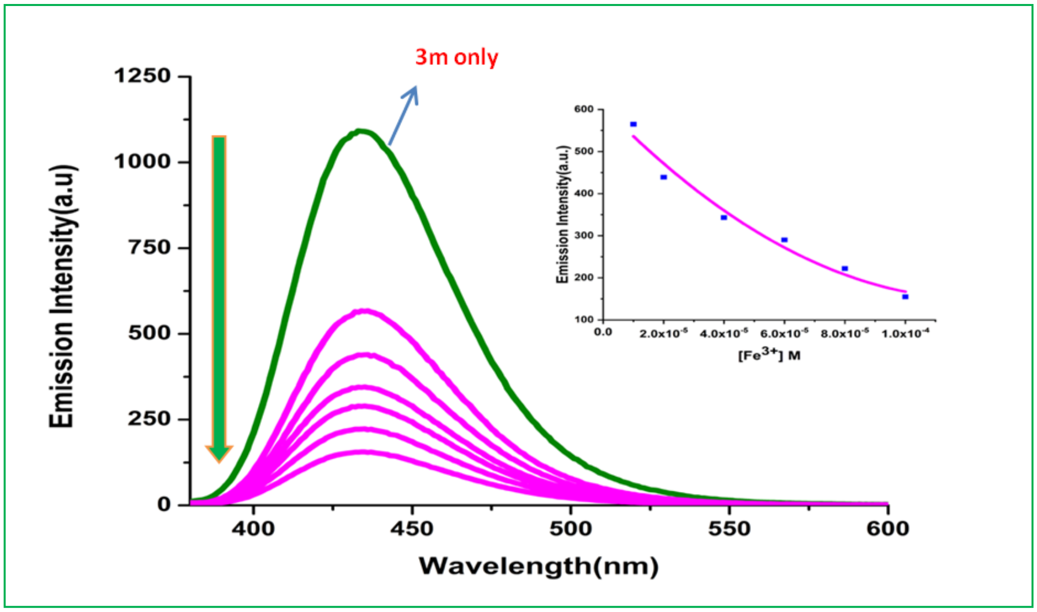

Figure 36. Fluorescence spectra of **3m** (50 µM) with incremental addition of Fe^{3+} (1, 2, 4, 6, 8 and 10 ($\times 10^{-5}$ M) in DMSO/H_2O (2:8 v/v) HEPES buffer solution. **Inset:** Fluorescence emission intensity of **3m** as a function of [Fe^{3+}] (λ_{ex} = 360 nm, λ_{em} = 435 nm).

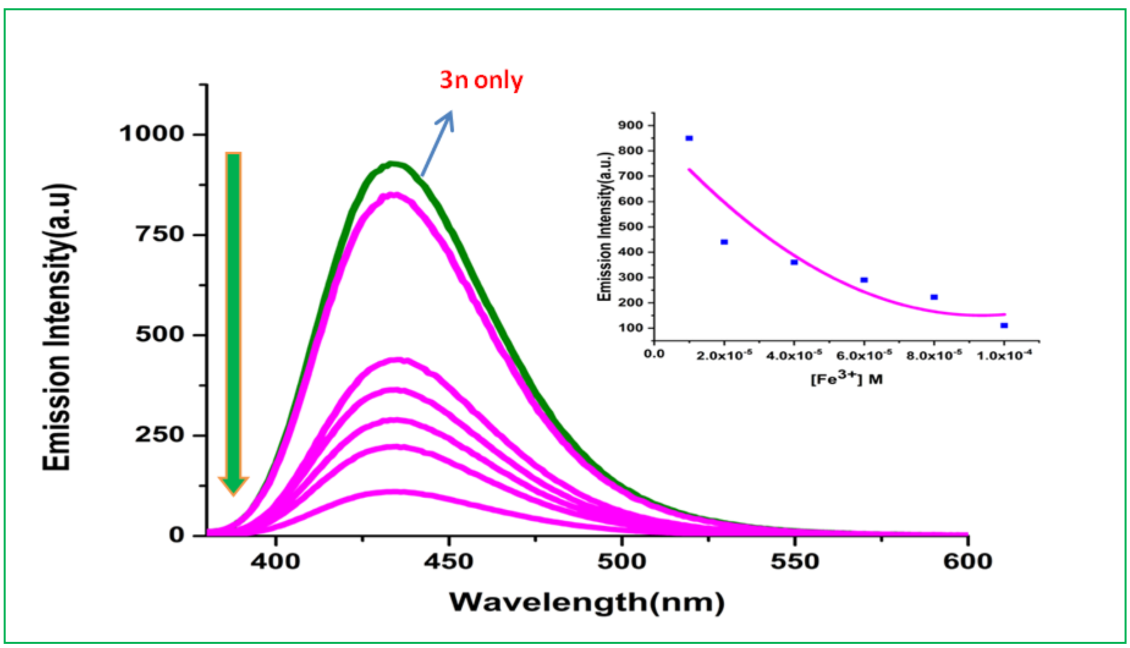

Figure 37. Fluorescence spectra of **3n** (50 µM) with incremental addition of Fe^{3+} (1, 2, 4, 6, 8 and 10 ($\times 10^{-5}$ M) in DMSO/H_2O (2:8 v/v) HEPES buffer solution. **Inset:** Fluorescence emission intensity of **3n** as a function of [Fe^{3+}] (λ_{ex} = 350 nm, λ_{em} = 434 nm).

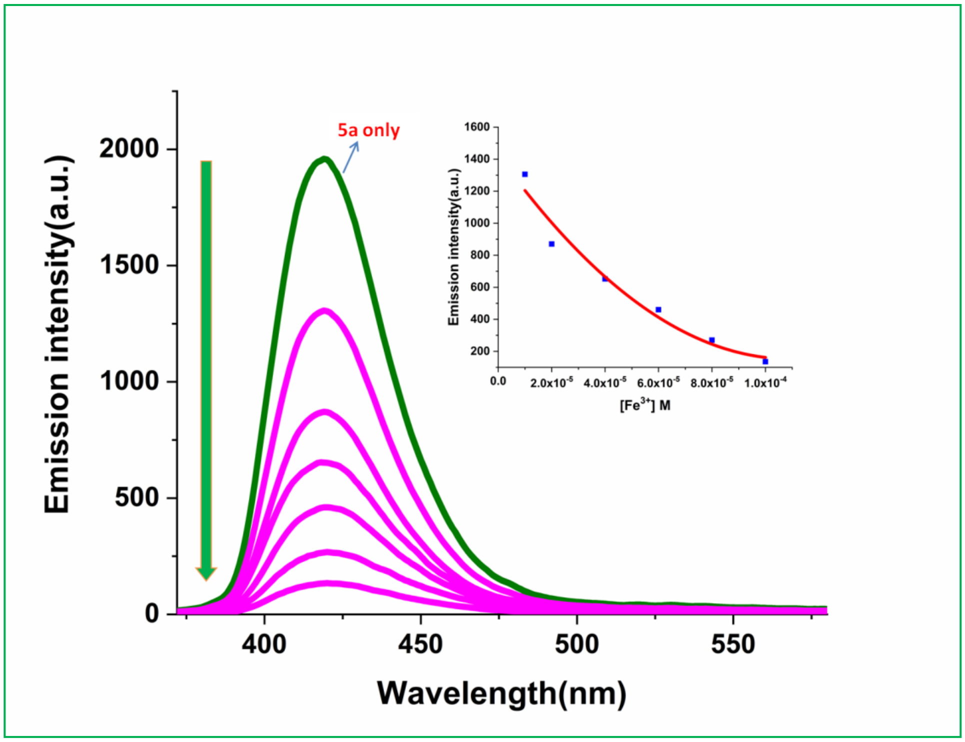

Figure 38. Fluorescence spectra of **5a** (50 µM) with incremental addition of Fe^{3+} (1, 2, 4, 6, 8 and 10 ($\times 10^{-5}$ M) in DMSO/H_2O (2:8 v/v) HEPES buffer solution. **Inset:** Fluorescence emission intensity of **5a** as a function of [Fe^{3+}] (λ_{ex} = 380 nm, λ_{em} = 420 nm).

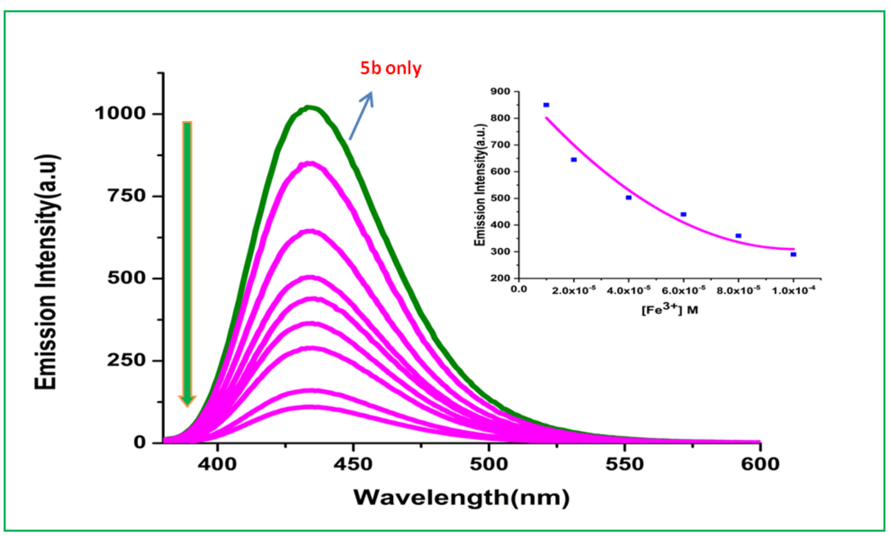

Figure 39. Fluorescence spectra of **5b** (50 µM) with incremental addition of Fe^{3+} (1, 2, 4, 6, 8 and 10 ($\times 10^{-5}$ M) in DMSO/H_2O (2:8 v/v) HEPES buffer solution. **Inset:** Fluorescence emission intensity of **5b** as a function of [Fe^{3+}] (λ_{ex} = 365 nm, λ_{em} = 435 nm).

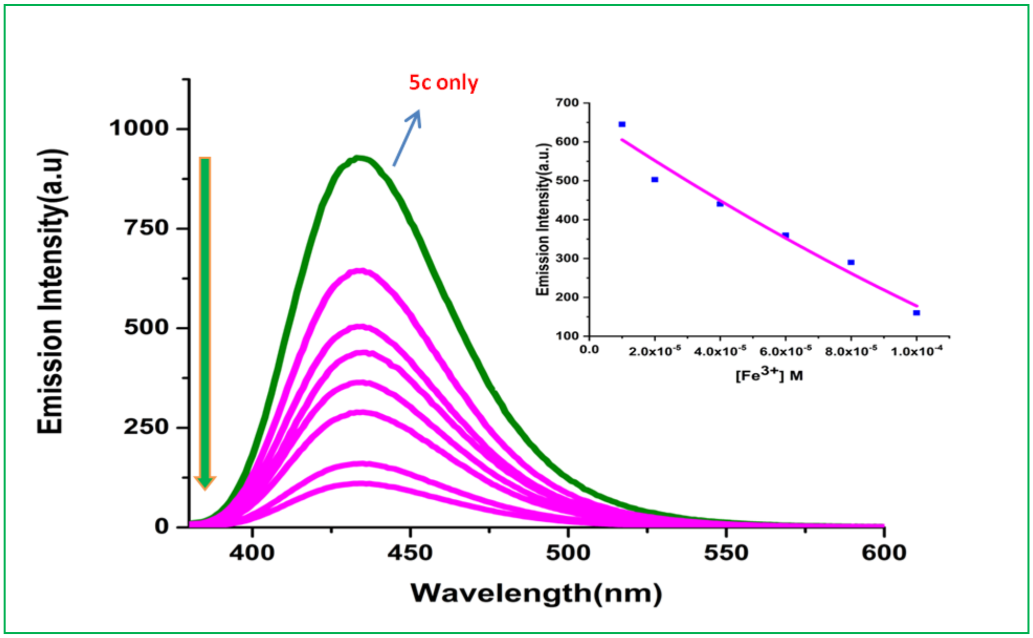

Figure 40. Fluorescence spectra of **5c** (50 µM) with incremental addition of Fe^{3+} (1, 2, 4, 6, 8 and 10 ($\times10^{-5}$ M) in DMSO/H_2O (2:8 v/v) HEPES buffer solution. **Inset:** Fluorescence emission intensity of **5c** as a function of [Fe^{3+}] (λ_{ex} = 380 nm, λ_{em} = 436 nm).

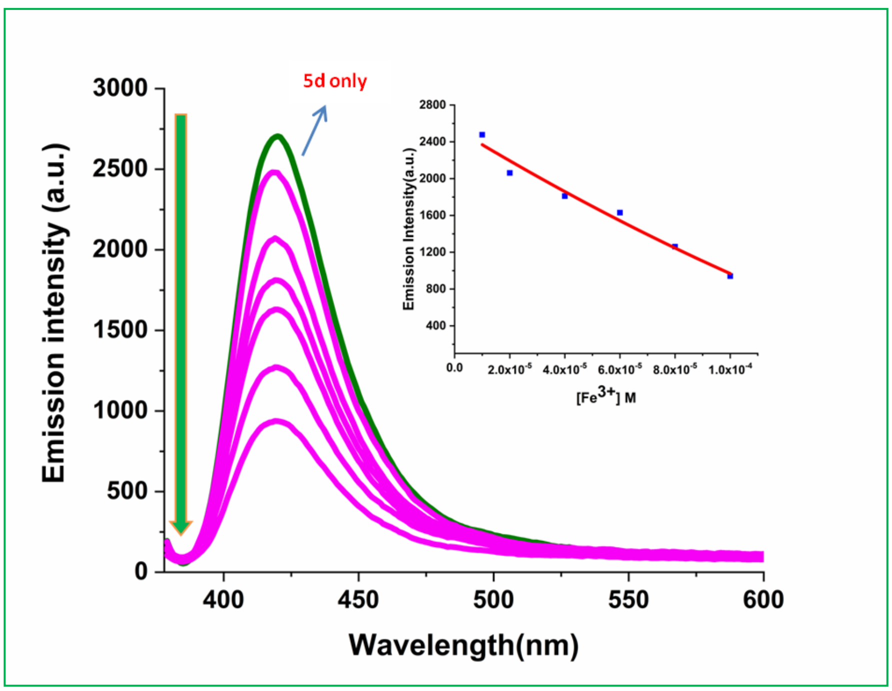

Figure 41. Fluorescence spectra of **5d** (50 µM) with incremental addition of Fe^{3+} (1, 2, 4, 6, 8 and 10 ($\times10^{-5}$ M) in DMSO/H_2O (2:8 v/v) HEPES buffer solution. **Inset:** Fluorescence emission intensity of **5d** as a function of [Fe^{3+}] (λ_{ex} = 380 nm, λ_{em} = 425 nm).

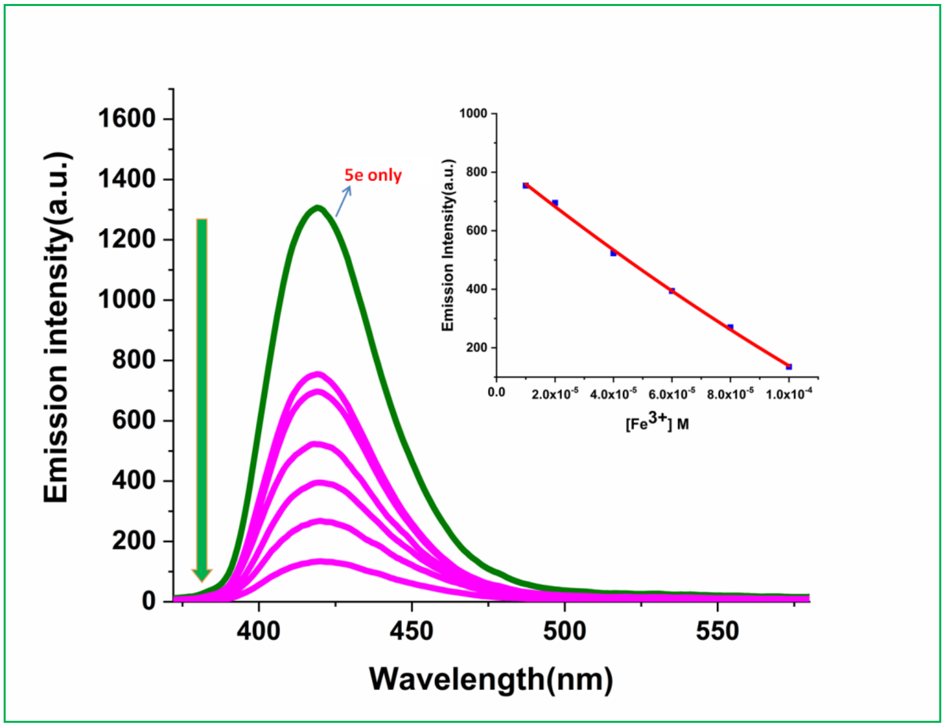

Figure 42. Fluorescence spectra of **5e** (50 µM) with incremental addition of Fe^{3+} (1, 2, 4, 6, 8 and 10 (×10^{-5} M) in DMSO/H_2O (2:8 v/v) HEPES buffer solution. **Inset:** Fluorescence emission intensity of **5e** as a function of [Fe^{3+}] (λ_{ex} = 380 nm, λ_{em} = 425 nm).

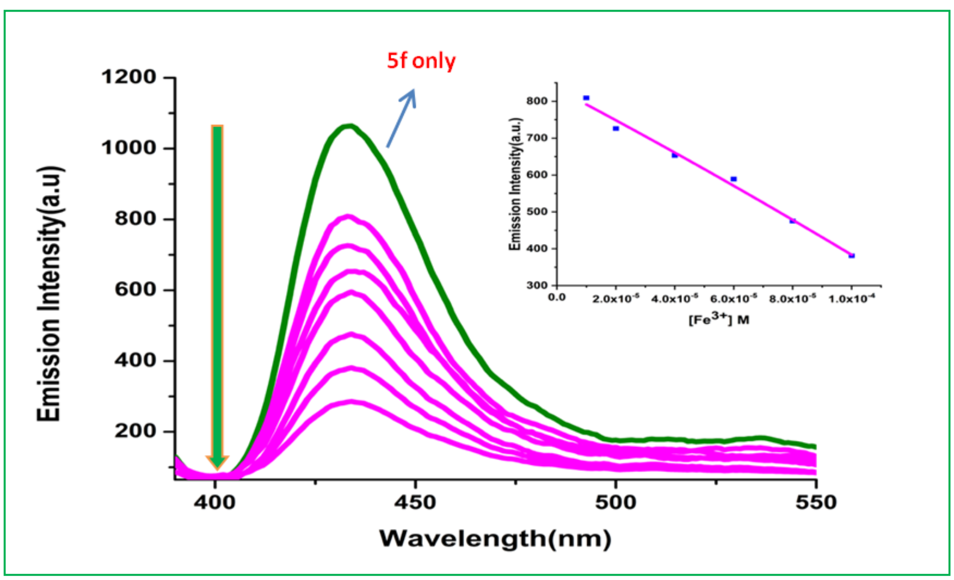

Figure 43. Fluorescence spectra of **5f** (50 µM) with incremental addition of Fe^{3+} (1, 2, 4, 6, 8 and 10 (×10^{-5} M) in DMSO/H_2O (2:8 v/v) HEPES buffer solution. **Inset:** Fluorescence emission intensity of **5f** as a function of [Fe^{3+}] (λ_{ex} = 380 nm, λ_{em} = 435 nm).

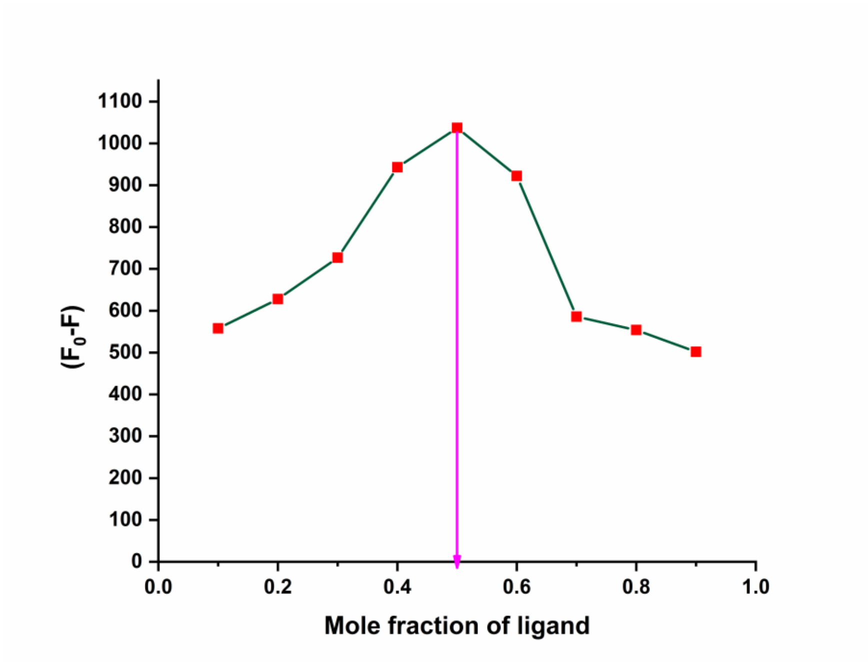

Figure 44. Job's plot to determine the stoichiometry of Fe^{3+}: **3a** in solution.

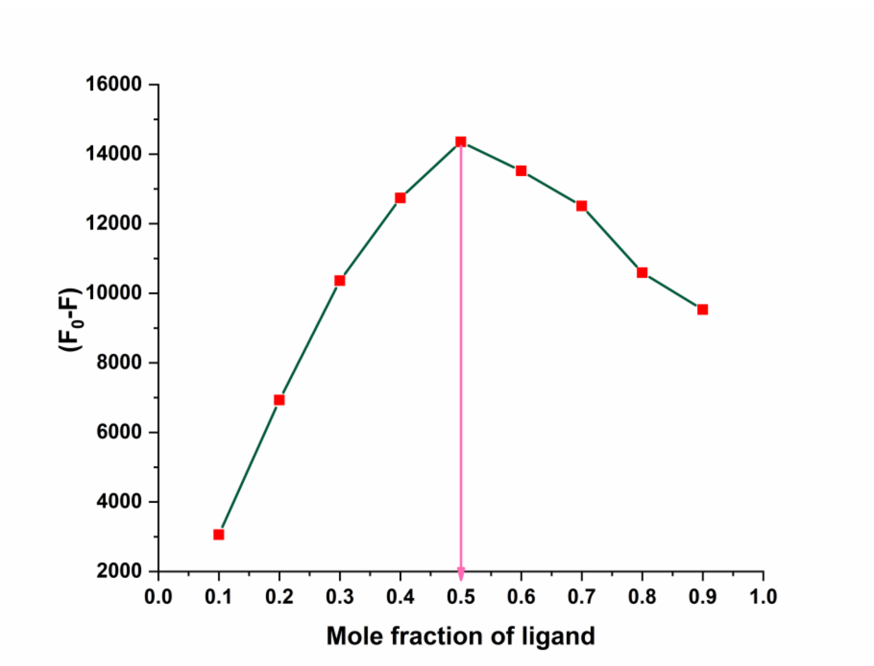

Figure 45. Job's plot to determine the stoichiometry of Fe^{3+}: **3b** in solution.

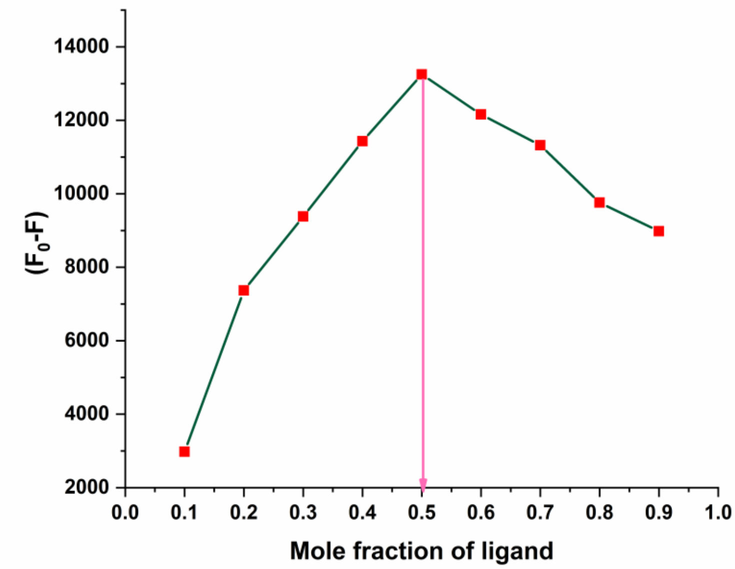

Figure 46. Job's plot to determine the stoichiometry of Fe^{3+}: **3c** in solution.

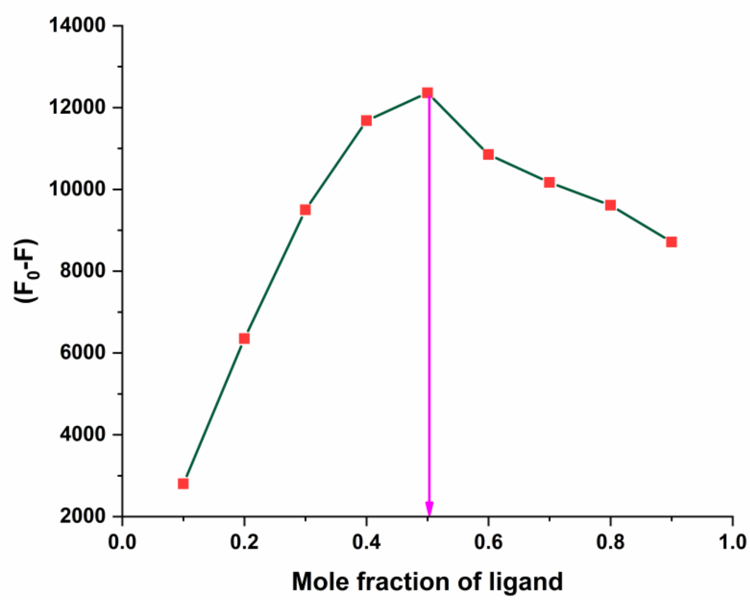

Figure 47. Job's plot to determine the stoichiometry of Fe^{3+}: **3d** in solution.

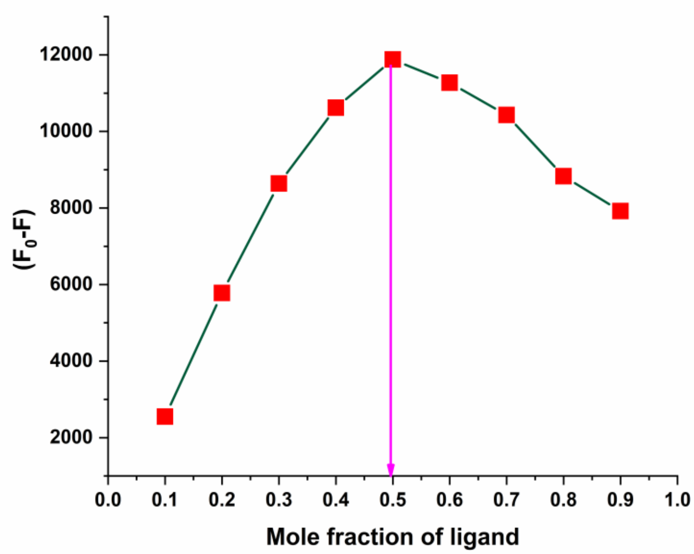

Figure 48. Job’s plot to determine the stoichiometry of Fe^{3+}: **3e** in solution.

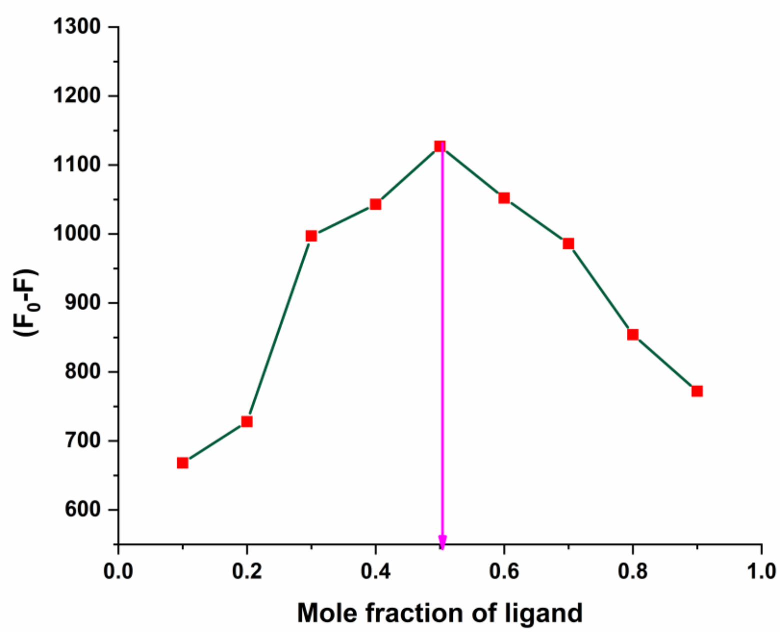

Figure 49. Job’s plot to determine the stoichiometry of Fe^{3+}: **3g** in solution.

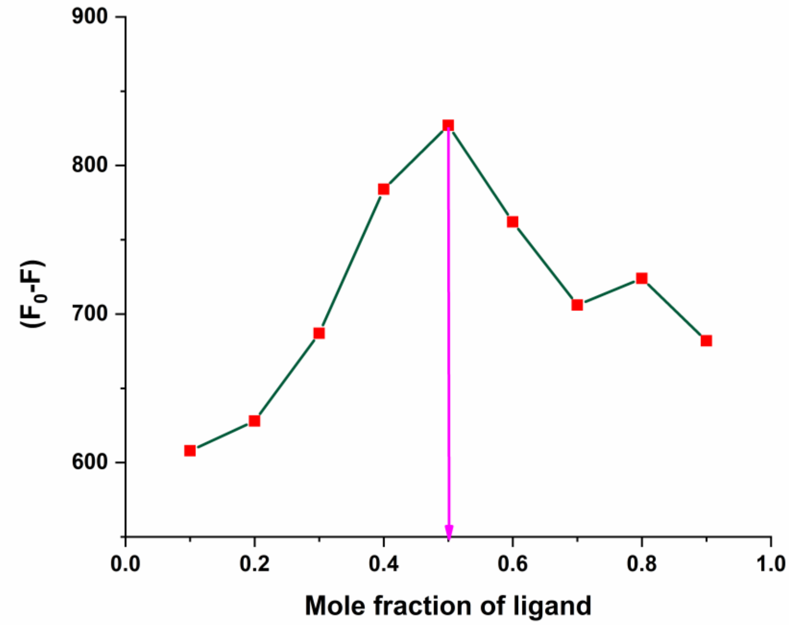

Figure 50. Job's plot to determine the stoichiometry of Fe^{3+}: **3h** in solution

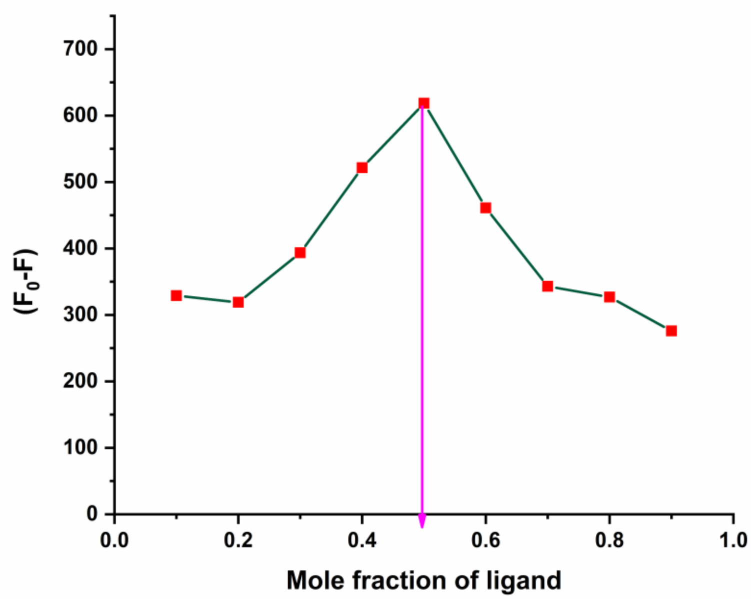

Figure 51. Job's plot to determine the stoichiometry of Fe^{3+}: **3i** in solution.

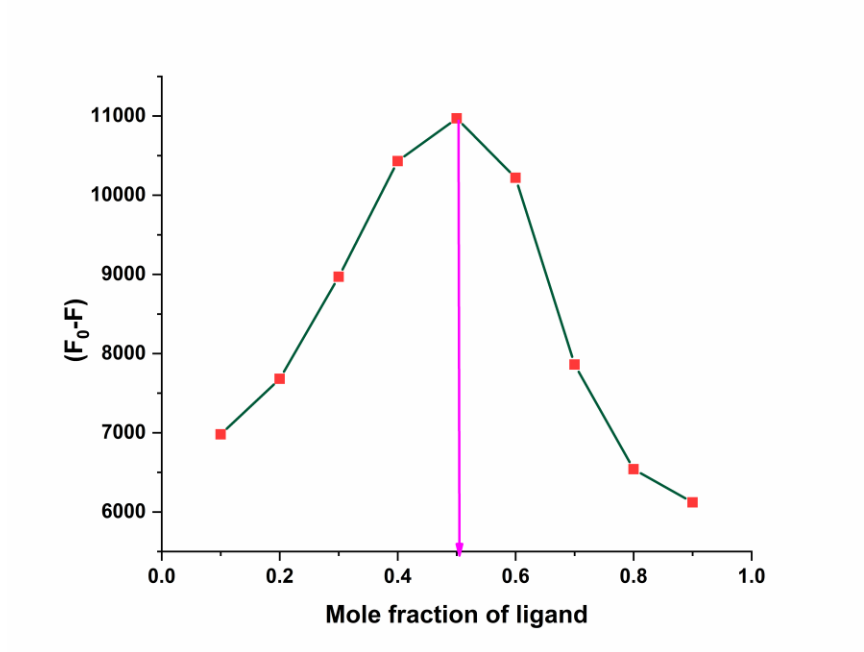

Figure 52. Job's plot to determine the stoichiometry of Fe^{3+}: **3l** in Solution.

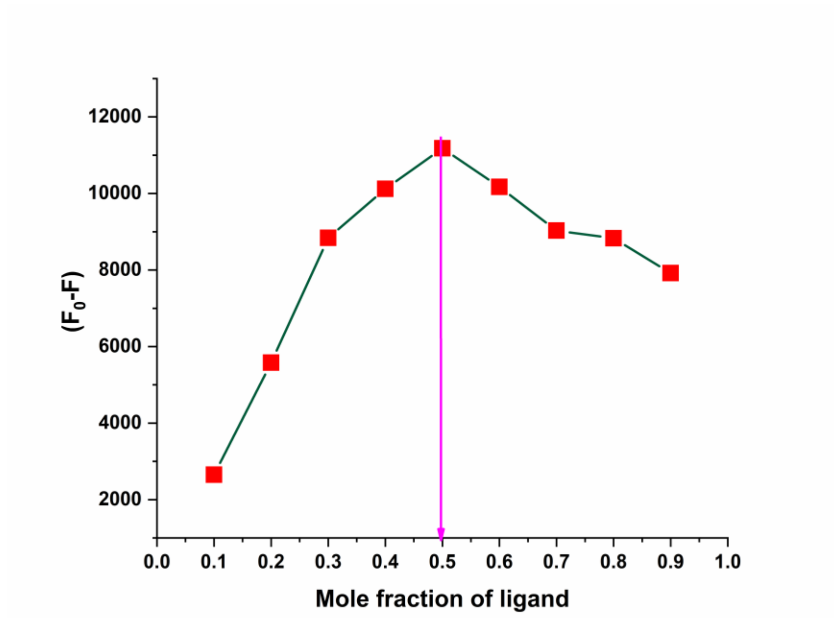

Figure 53. Job's plot to determine the stoichiometry of Fe^{3+}: **5a** in solution.

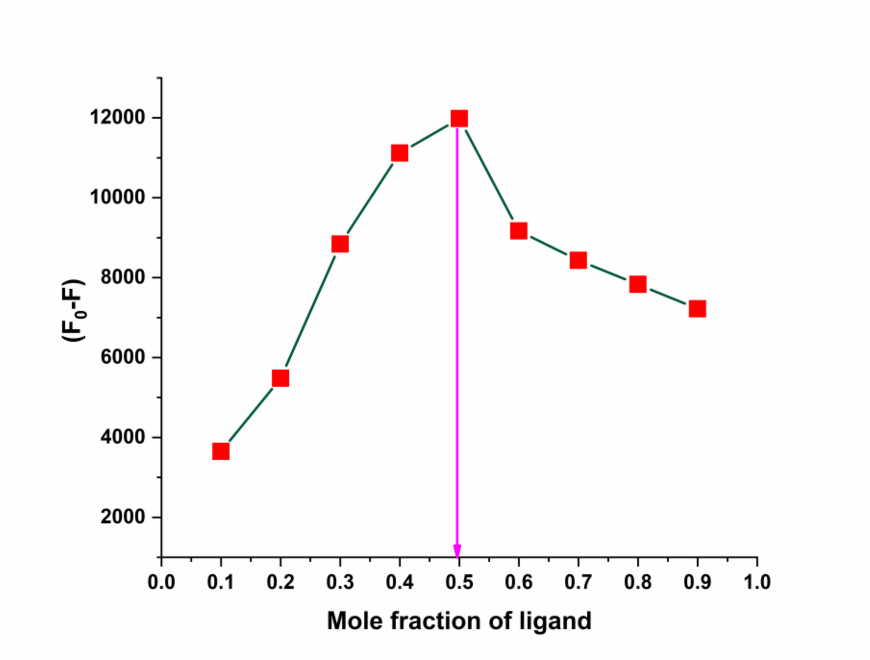

Figure 54. Job's plot to determine the stoichiometry of Fe^{3+}: **5b** in solution.

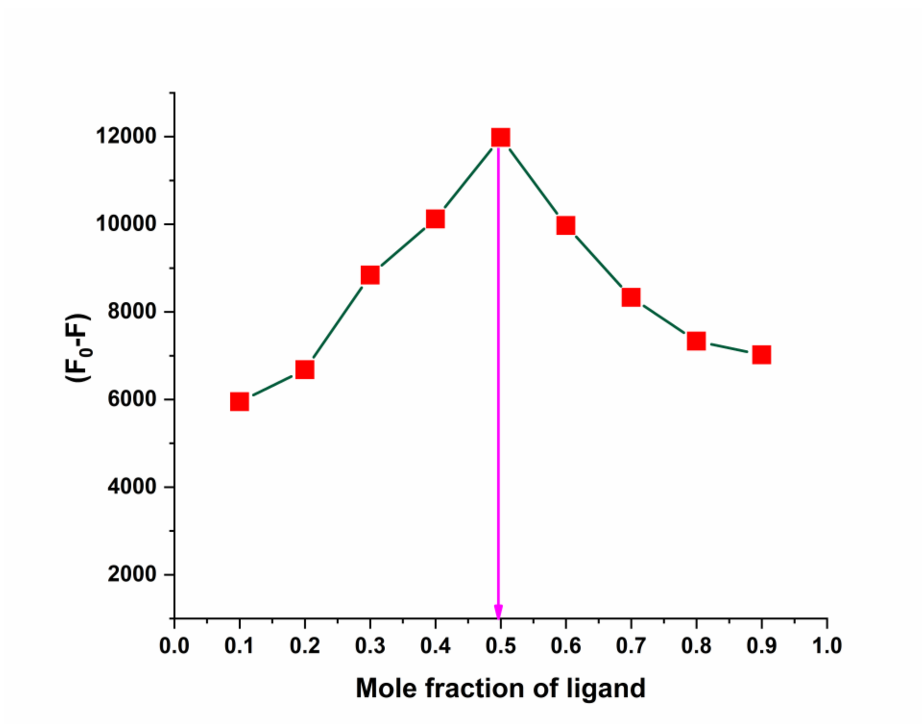

Figure 55. Job's plot to determine the stoichiometry of Fe^{3+}: **5c** in solution.

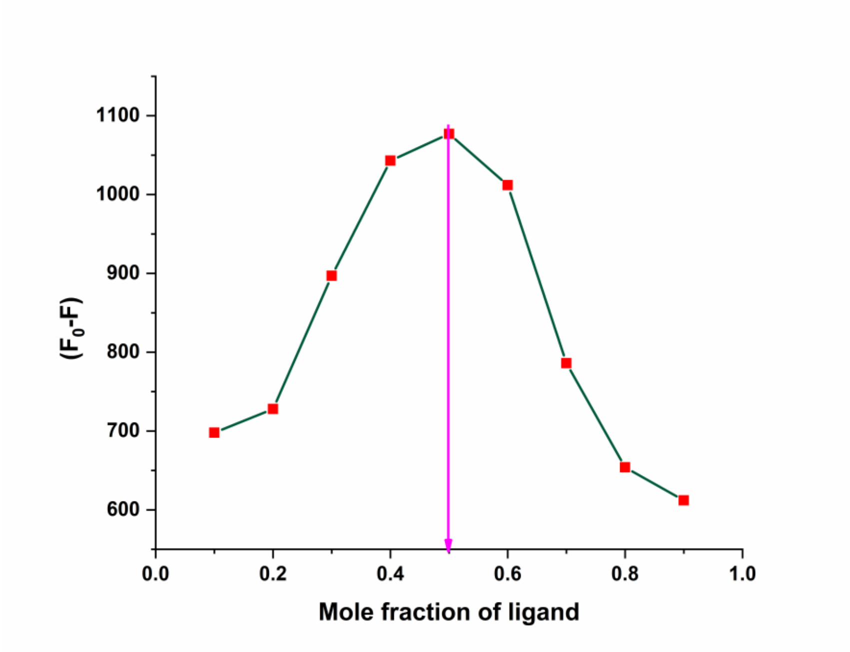

Figure 56. Job's plot to determine the stoichiometry of Fe^{3+}: **5d** in solution.

According to the linear Benesi–Hildebrand expression[1], the measured fluorescence intensity 1 / (F_0-F) varied as a function of $1/[Fe^{3+}]$ in a linear relationship, which indicates the formation of 1 : 1 stoichiometry between Fe^{3+} and chemosensors in the complex.

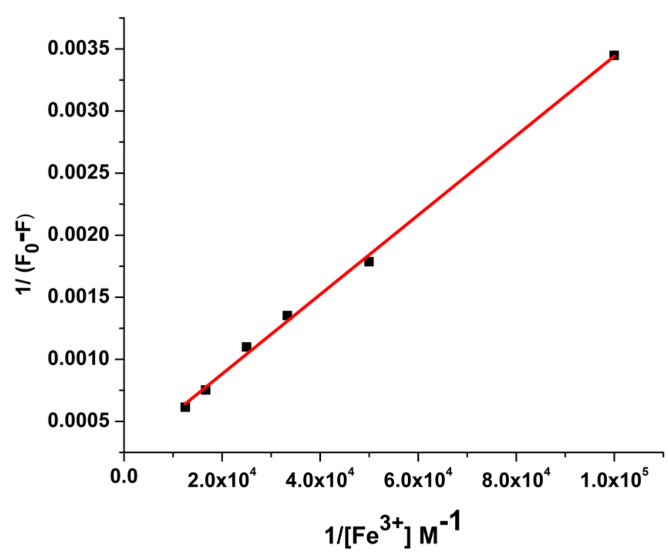

Figure 57. Benesi – Hindebrand plot of $1/(F_0\text{-}F)$ vs $1/[Fe^{3+}]$ for determination of stoichiometry and binding constant between **3a** and Fe^{3+} derived from emission titration curve.

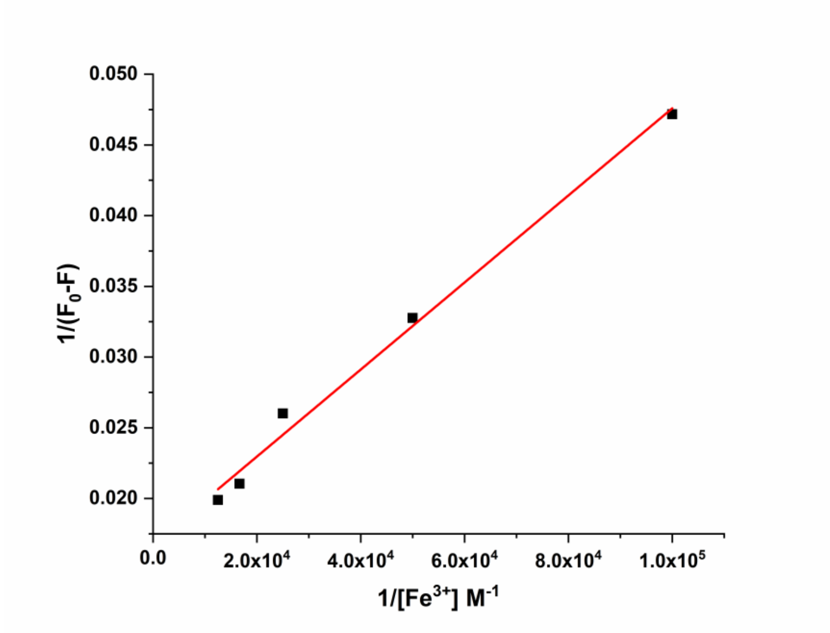

Figure 58. Benesi – Hindebrand plot of $1/(F_0\text{-}F)$ vs $1/[Fe^{3+}]$ for determination of stoichiometry and binding constant between **3b** and Fe^{3+} derived from emission titration curve.

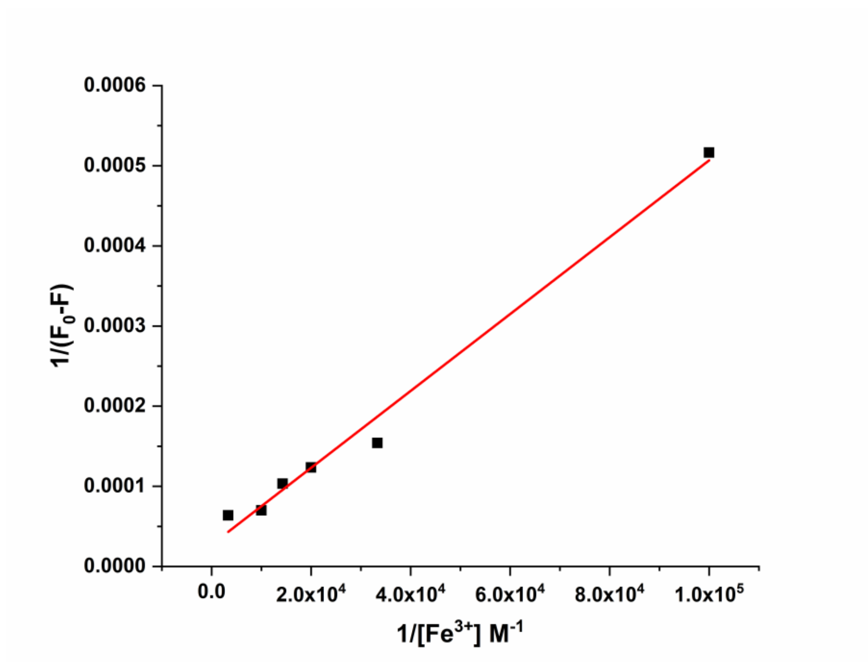

Figure 59. Benesi – Hindebrand plot of $1/(F_0\text{-}F)$ vs $1/[Fe^{3+}]$ for determination of stoichiometry and binding constant between **3c** and Fe^{3+} derived from emission titration curve.

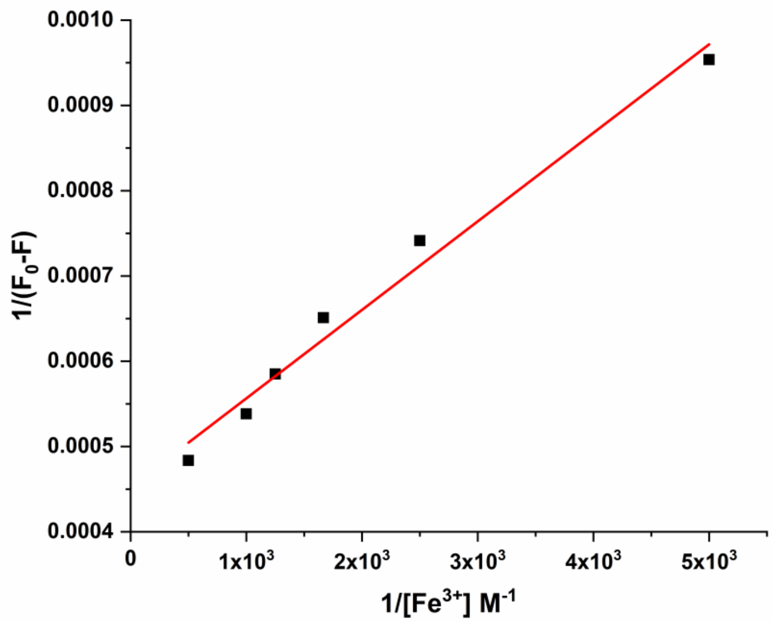

Figure 60. Benesi – Hindebrand plot of $1/(F_0\text{-}F)$ vs $1/[Fe^{3+}]$ for determination of stoichiometry and binding constant between **3d** and Fe^{3+} derived from emission titration curve .

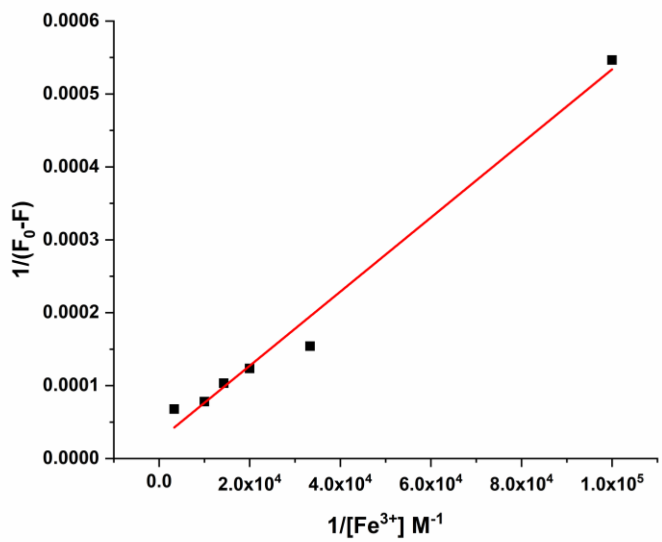

Figure 61. Benesi – Hindebrand plot of $1/(F_0\text{-}F)$ vs $1/[Fe^{3+}]$ for determination of stoichiometry and binding constant between **3e** and Fe^{3+} derived from emission titration curve.

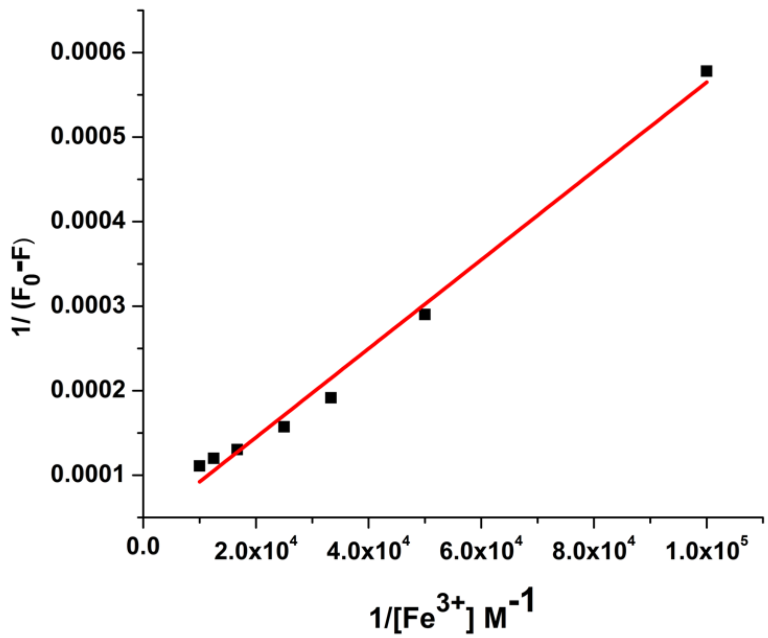

Figure 62. Benesi – Hindebrand plot of $1/(F_0\text{-}F)$ vs $1/[Fe^{3+}]$ for determination of stoichiometry and binding constant between **3f** and Fe^{3+} derived from emission titration curve.

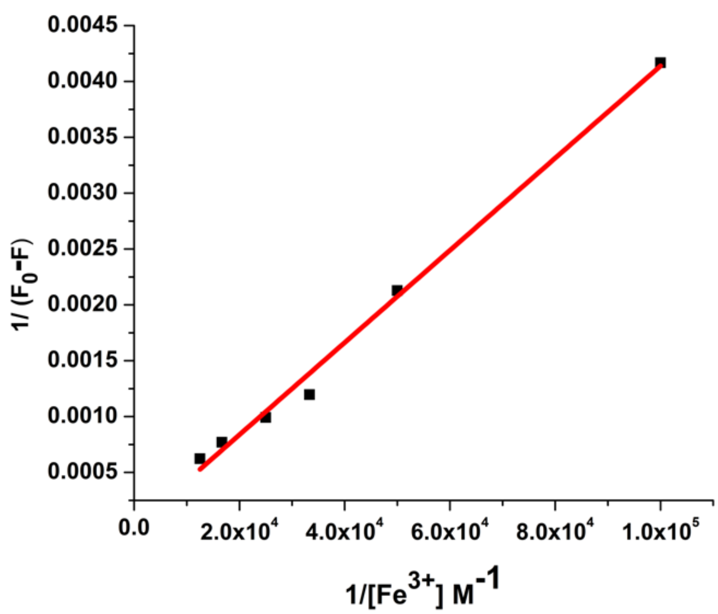

Figure 63. Benesi – Hindebrand plot of $1/(F_0\text{-}F)$ vs $1/[Fe^{3+}]$ for determination of stoichiometry and binding constant between **3g** and Fe^{3+} derived from emission titration curve.

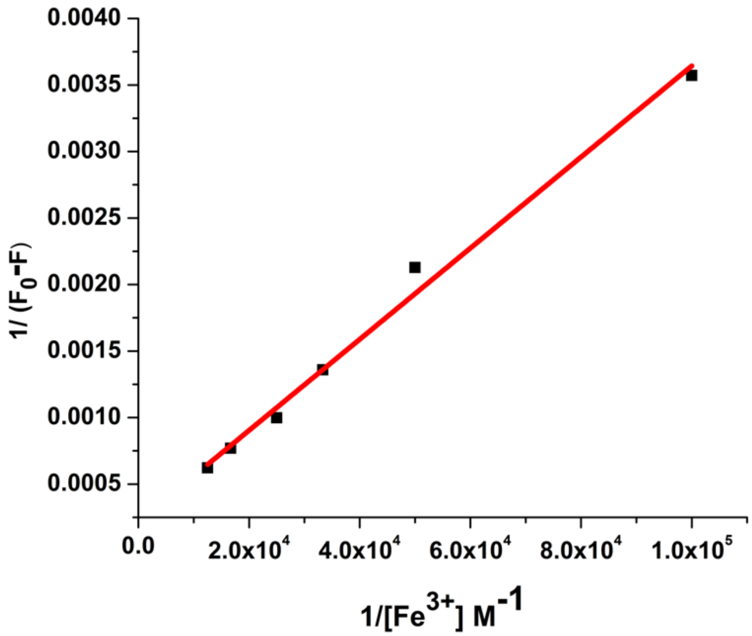

Figure 64. Benesi – Hindebrand plot of $1/(F_0\text{-}F)$ vs $1/[Fe^{3+}]$ for determination of stoichiometry and binding constant between **3h** and Fe^{3+} derived from emission titration curve.

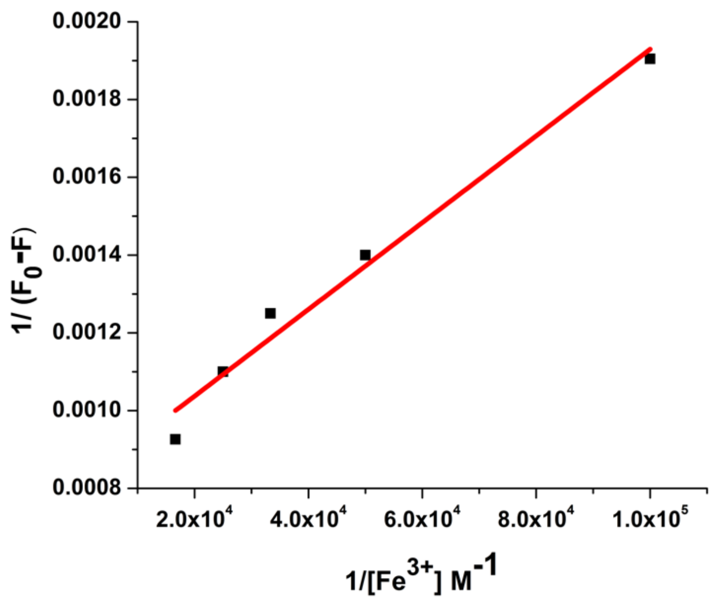

Figure 65. Benesi – Hindebrand plot of $1/(F_0\text{-}F)$ vs $1/[Fe^{3+}]$ for determination of stoichiometry and binding constant between **3i** and Fe^{3+} derived from emission titration curve.

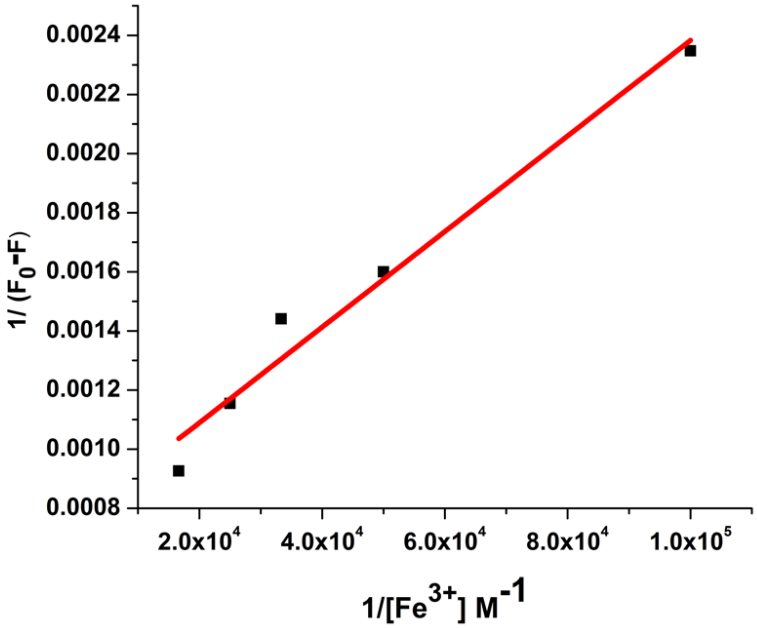

Figure 66. Benesi – Hindebrand plot of 1/(F_0-F) vs 1/[Fe^{3+}] for determination of stoichiometry and binding constant between **3j** and Fe^{3+} derived from emission titration curve.

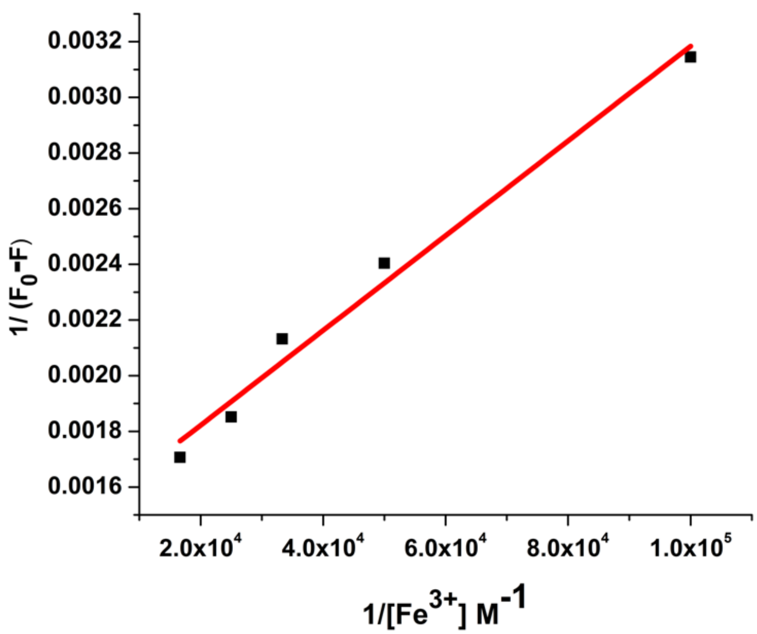

Figure 67. Benesi – Hindebrand plot of 1/(F_0-F) vs 1/[Fe^{3+}] for determination of stoichiometry and binding constant between **3k** and Fe^{3+} derived from emission titration curve.

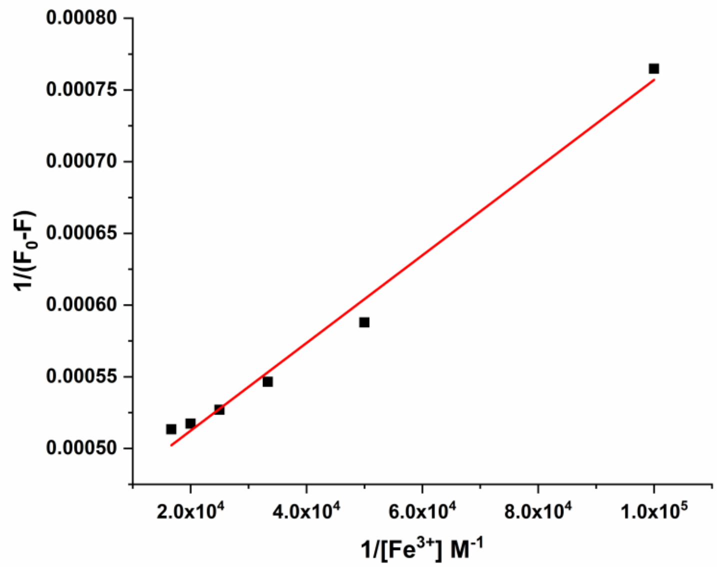

Figure 68. Benesi – Hindebrand plot of $1/(F_0\text{-}F)$ vs $1/[Fe^{3+}]$ for determination of stoichiometry and binding constant between **3l** and Fe^{3+} derived from emission titration curve.

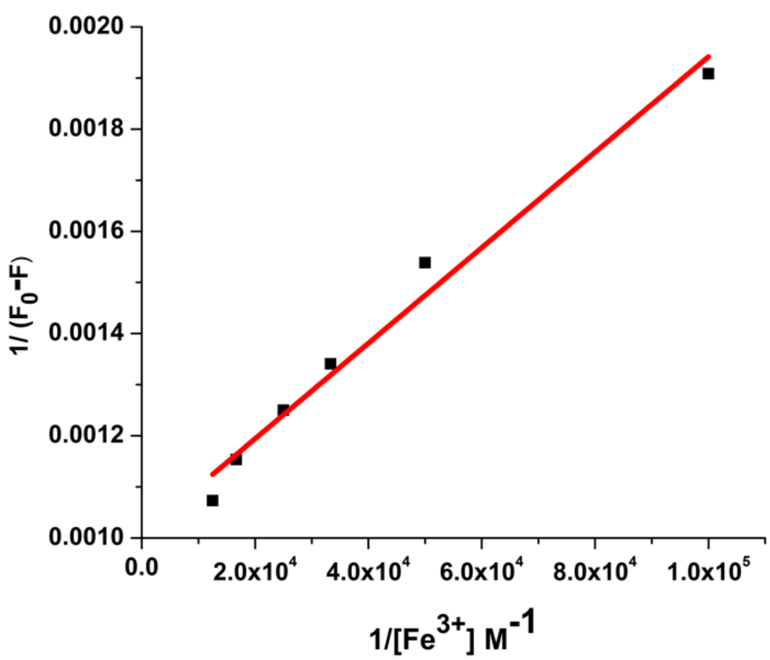

Figure 69. Benesi – Hindebrand plot of $1/(F_0\text{-}F)$ vs $1/[Fe^{3+}]$ for determination of stoichiometry and binding constant between **3m** and Fe^{3+} derived from emission titration curve

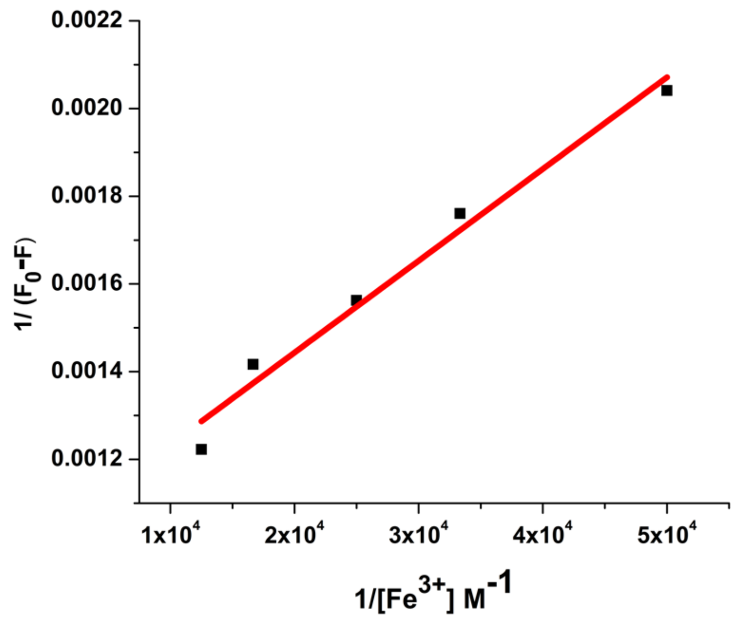

Figure 70. Benesi – Hindebrand plot of $1/(F_0\text{-}F)$ vs $1/[Fe^{3+}]$ for determination of stoichiometry and binding constant between **3n** and Fe^{3+} derived from emission titration curve.

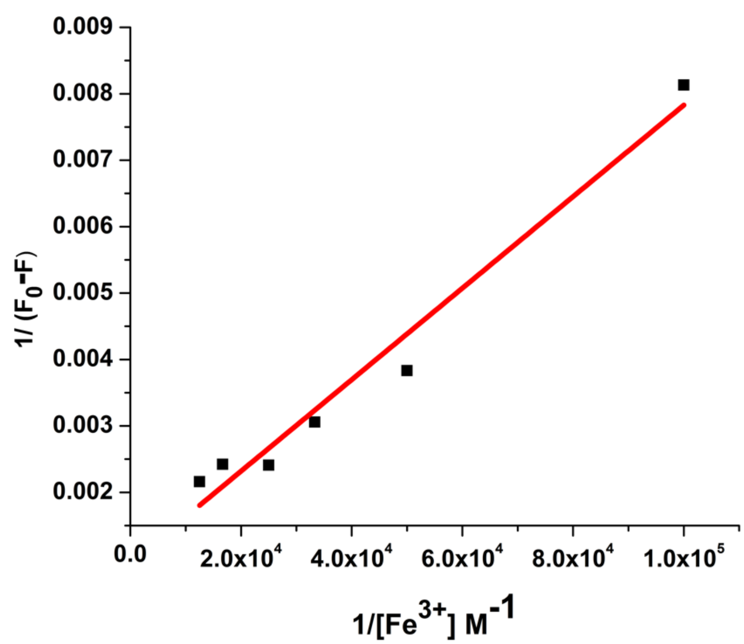

Figure 71. Benesi – Hindebrand plot of $1/(F_0\text{-}F)$ vs $1/[Fe^{3+}]$ for determination of stoichiometry and binding constant between **5a** and Fe^{3+} derived from emission titration curve.

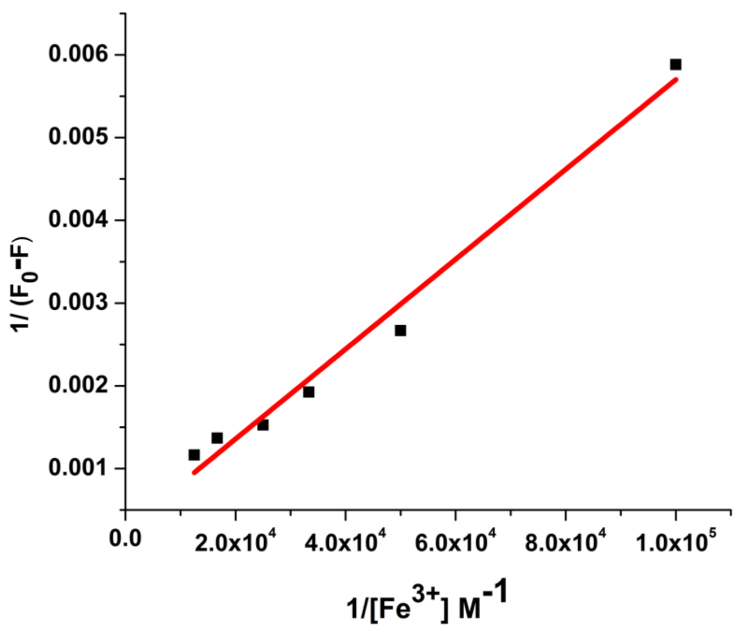

Figure 72. Benesi – Hindebrand plot of $1/(F_0\text{-}F)$ vs $1/[Fe^{3+}]$ for determination of stoichiometry and binding constant between **5b** and Fe^{3+} derived from emission titration curve.

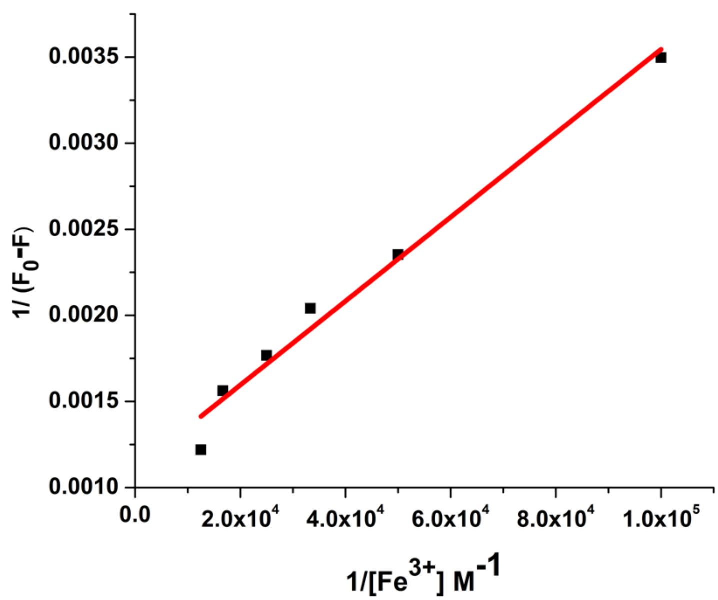

Figure 73. Benesi – Hindebrand plot of $1/(F_0\text{-}F)$ vs $1/[Fe^{3+}]$ for determination of stoichiometry and binding constant between **5c** and Fe^{3+} derived from emission titration curve.

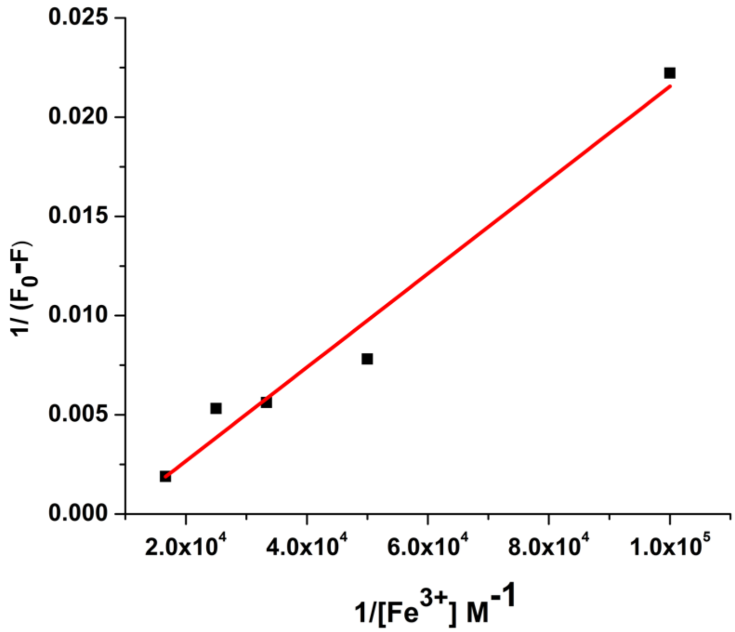

Figure 74. Benesi – Hindebrand plot of $1/(F_0\text{-}F)$ vs $1/[Fe^{3+}]$ for determination of stoichiometry and binding constant between **5d** and Fe^{3+} derived from emission titration curve.

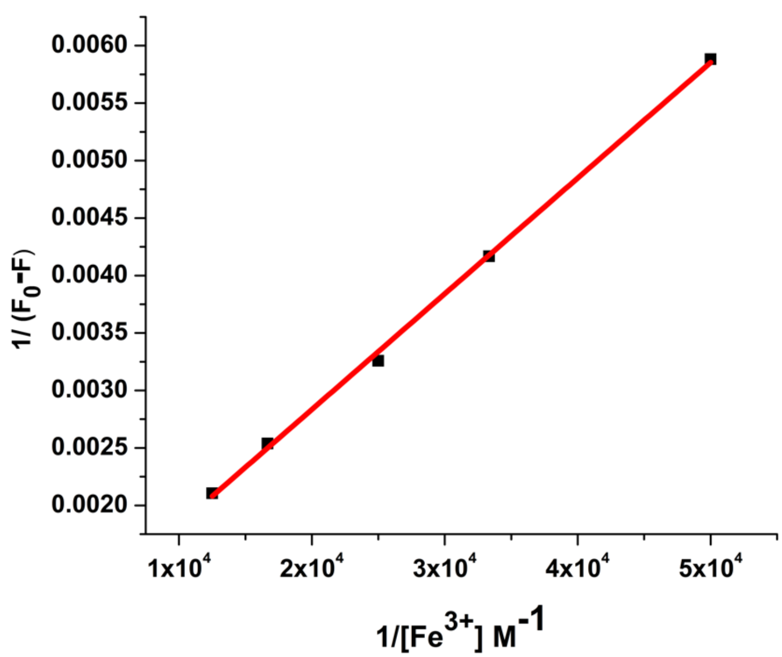

Figure 75. Benesi – Hindebrand plot of $1/(F_0\text{-}F)$ vs $1/[Fe^{3+}]$ for determination of stoichiometry and binding constant between **5e** and Fe^{3+} derived from emission titration curve.

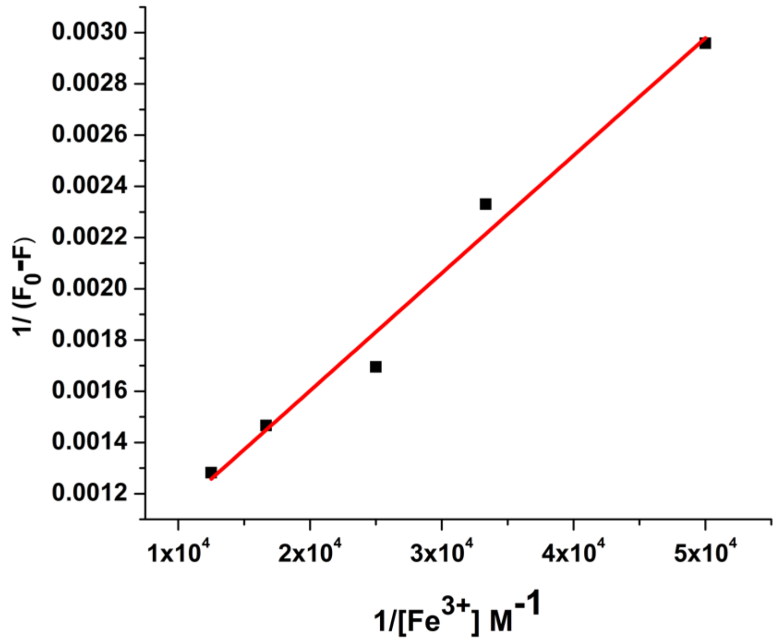

Figure 76. Benesi – Hindebrand plot of 1/(F_0-F) vs 1/[Fe^{3+}] for determination of stoichiometry and binding constant between **5f** and Fe^{3+} derived from emission titration curve.

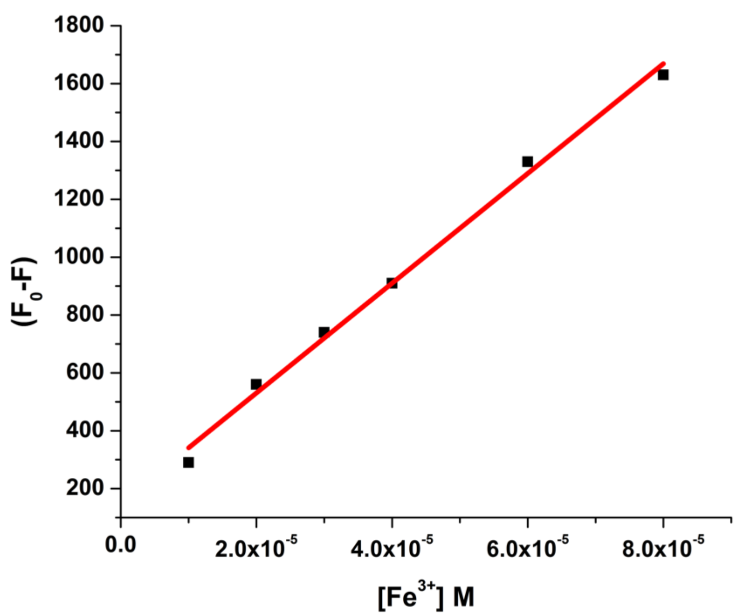

Figure 77. The limit of detection (LOD) of **3a** and [Fe^{3+}] derived from emission titration curve.

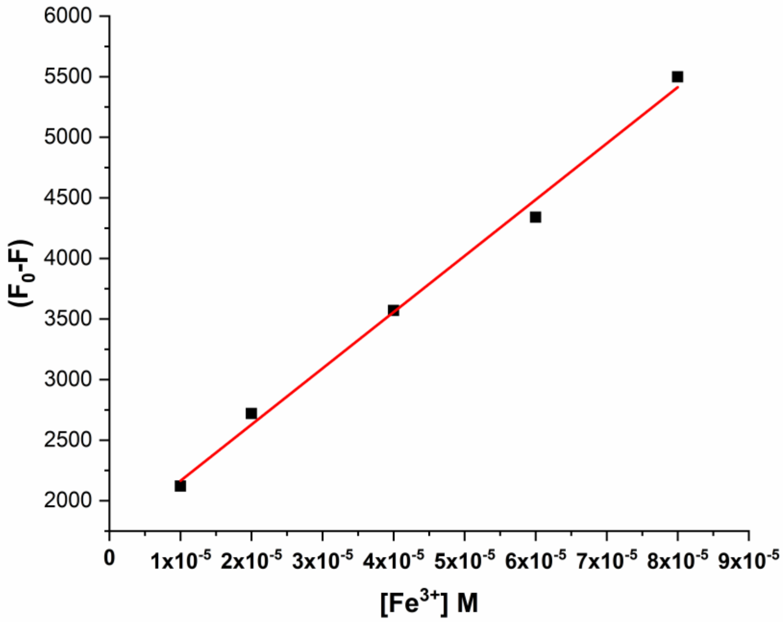

Figure 78. The limit of detection (LOD) of **3b** and [Fe^{3+}] derived from emission titration curve.

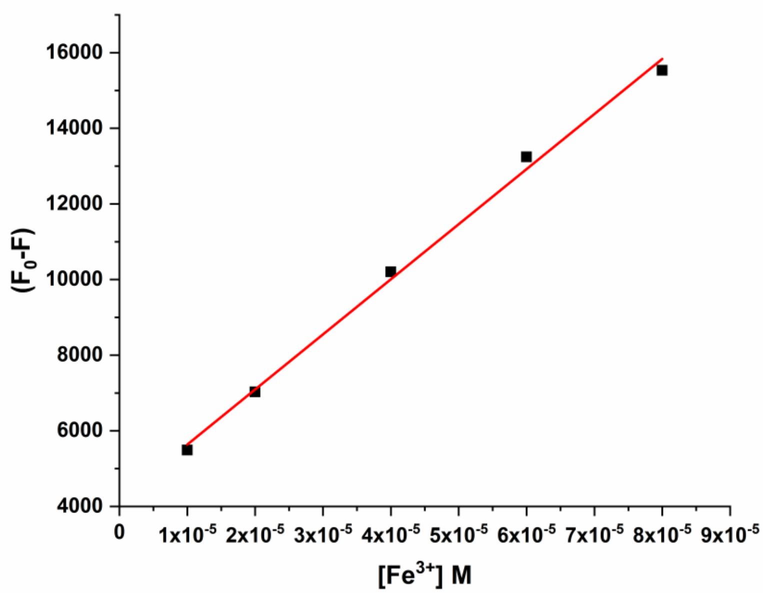

Figure 79. The limit of detection (LOD) of **3c** and [Fe^{3+}] derived from emission titration curve.

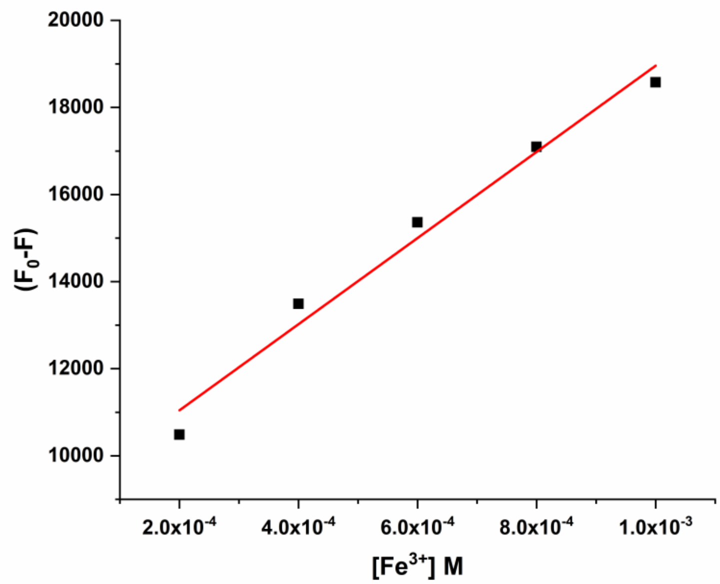

Figure 80. The limit of detection (LOD) of **3d** and [Fe^{3+}] derived from emission titration curve.

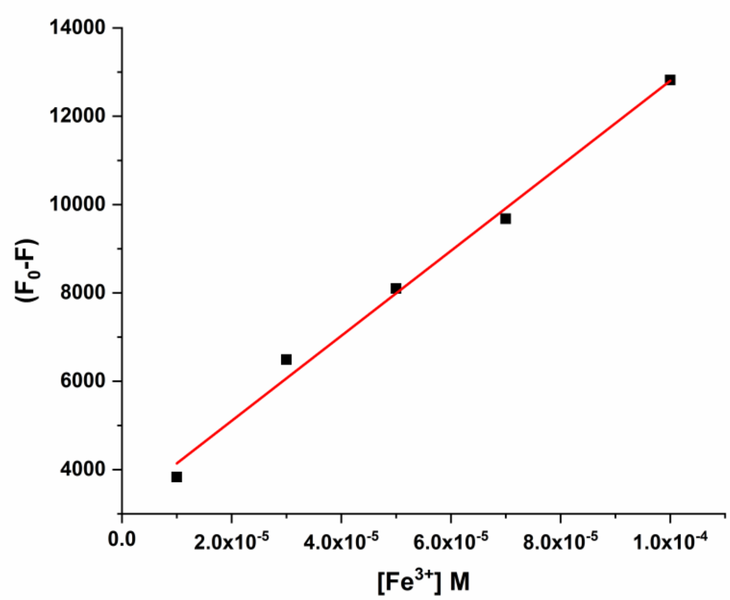

Figure 81. The limit of detection (LOD) of **3e** and [Fe^{3+}] derived from emission titration curve.

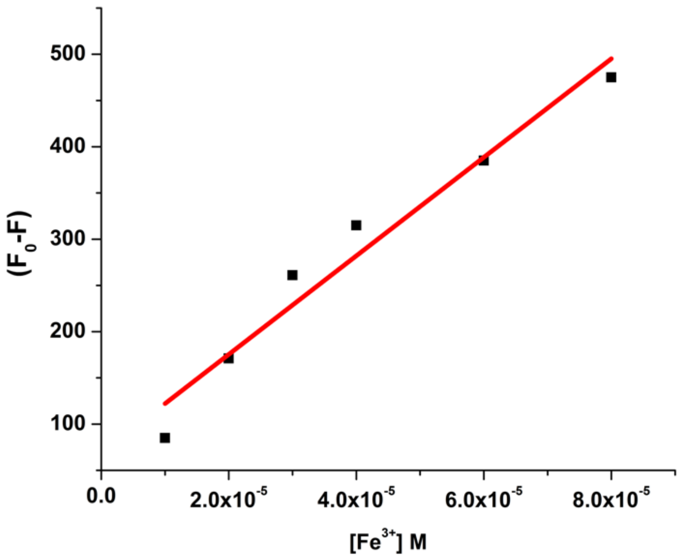

Figure 82. The limit of detection (LOD) of **3f** and [Fe^{3+}] derived from emission titration curve.

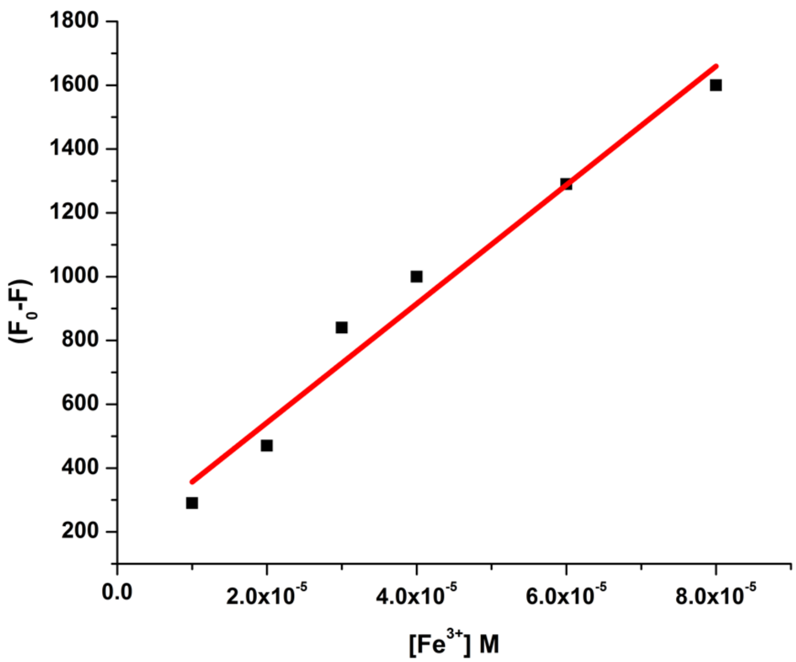

Figure 83. The limit of detection (LOD) of **3g** and [Fe^{3+}] derived from emission titration curve.

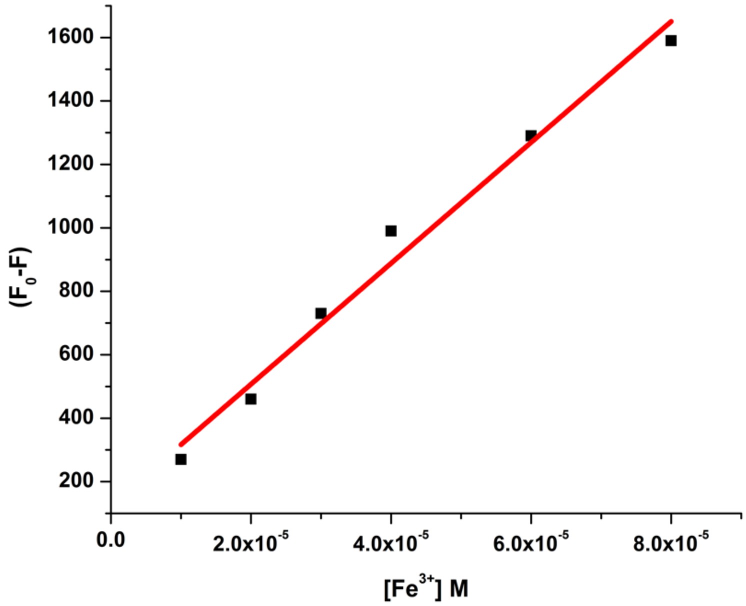

Figure 84. The limit of detection (LOD) of **3h** and $[Fe^{3+}]$ derived from emission titration curve

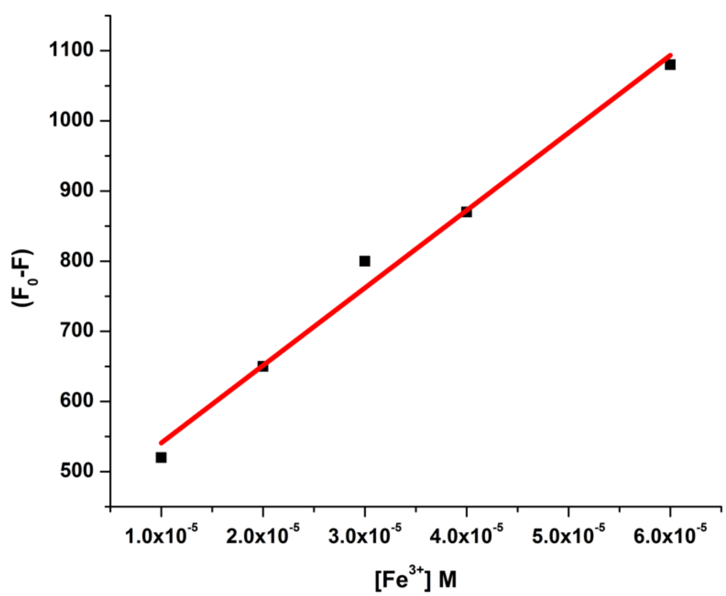

Figure 85. The limit of detection (LOD) of **3i** and $[Fe^{3+}]$ derived from emission titration curve.

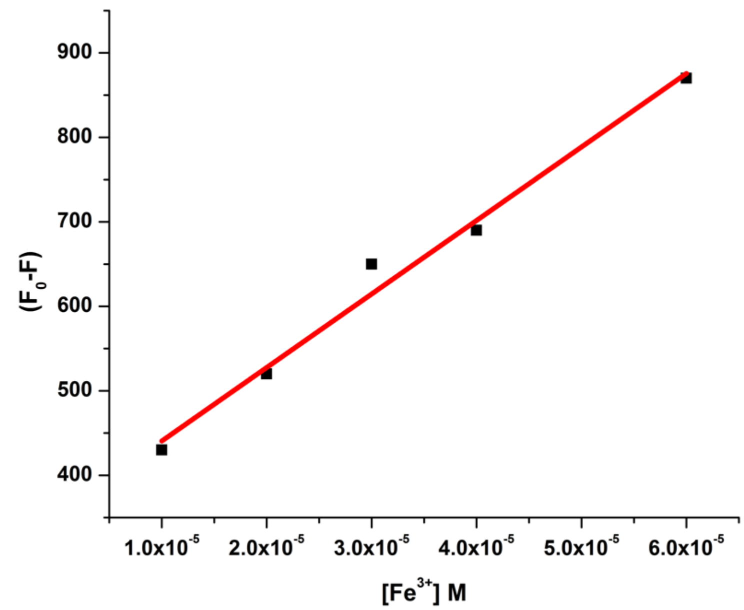

Figure 86. The limit of detection (LOD) of **3j** and [Fe^{3+}] derived from emission titration curve.

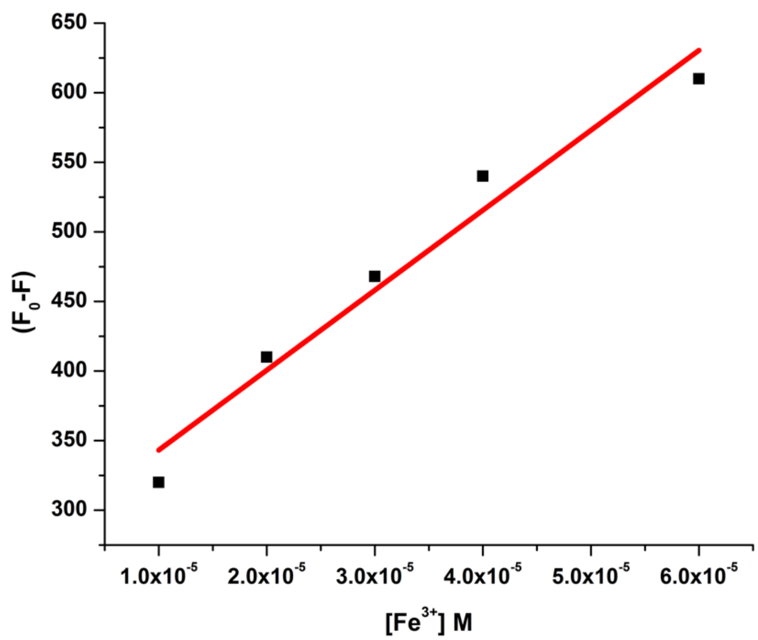

Figure 87. The limit of detection (LOD) of **3k** and [Fe^{3+}] derived from emission titration curve.

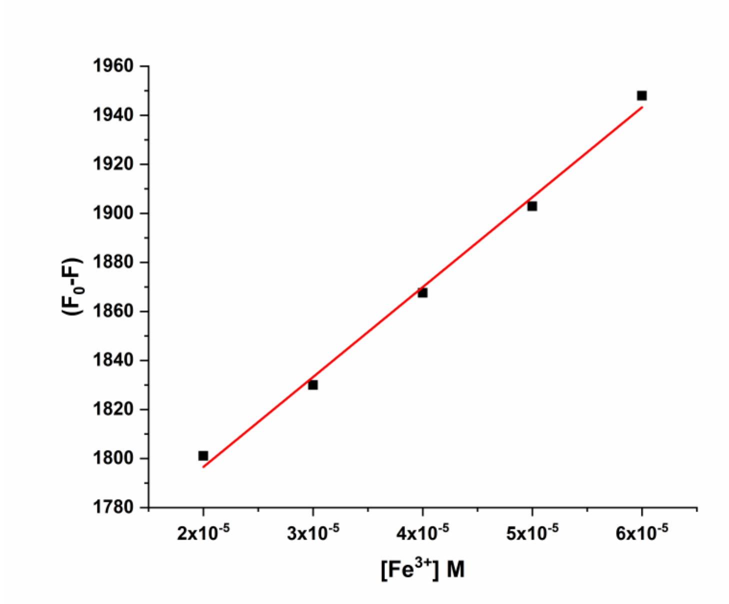

Figure 88. The limit of detection (LOD) of **3l** and [Fe^{3+}] derived from emission titration curve.

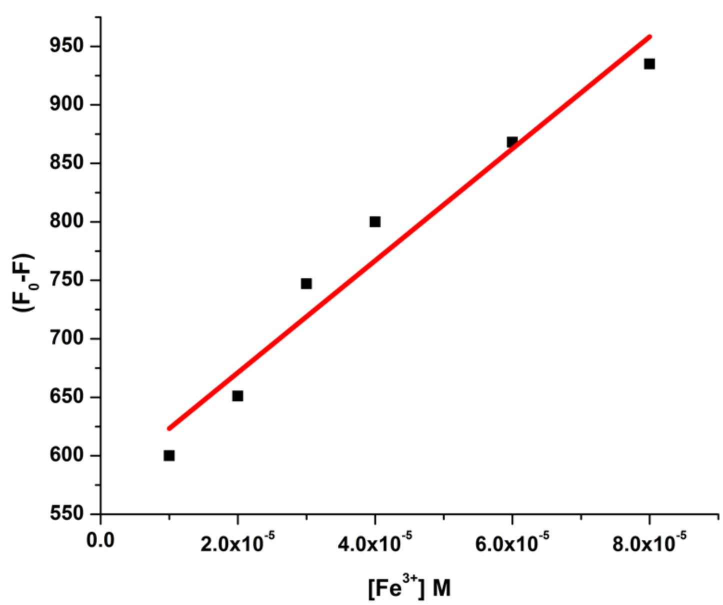

Figure 89. The limit of detection (LOD) of **3m** and [Fe^{3+}] derived from emission titration curve.

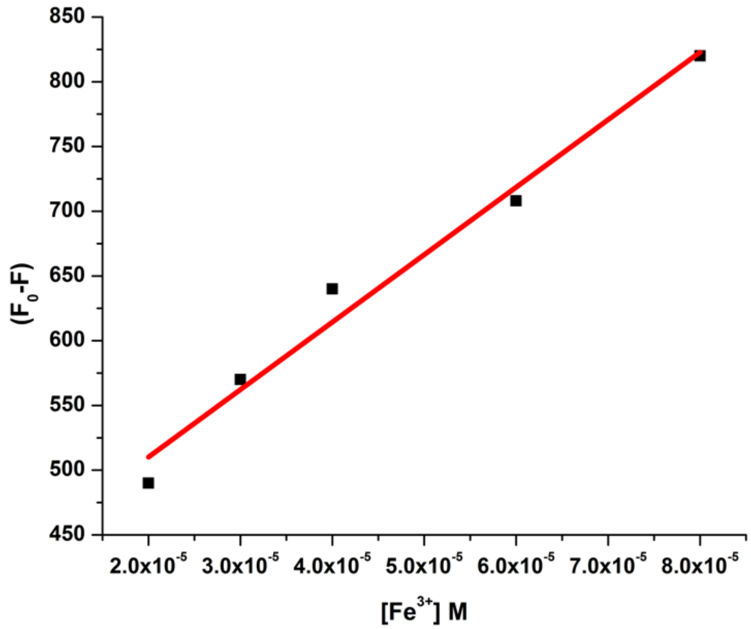

Figure 90. The limit of detection (LOD) of **3n** and [Fe^{3+}] derived from emission titration curve.

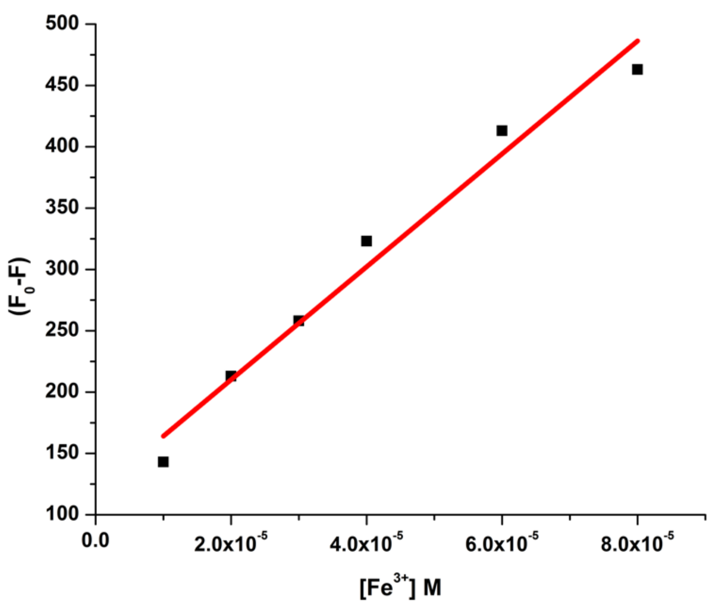

Figure 91. The limit of detection (LOD) of **5a** and [Fe^{3+}] derived from emission titration curve.

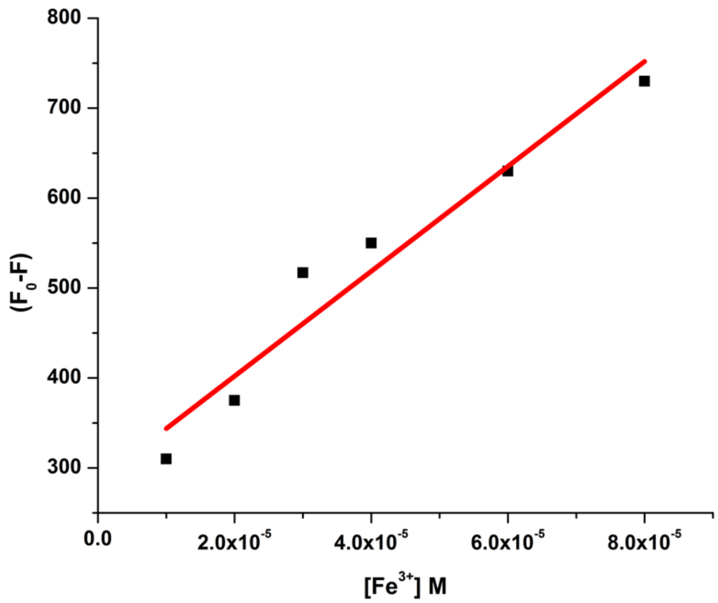

Figure 92. The limit of detection (LOD) of **5b** and [Fe^{3+}] derived from emission titration curve.

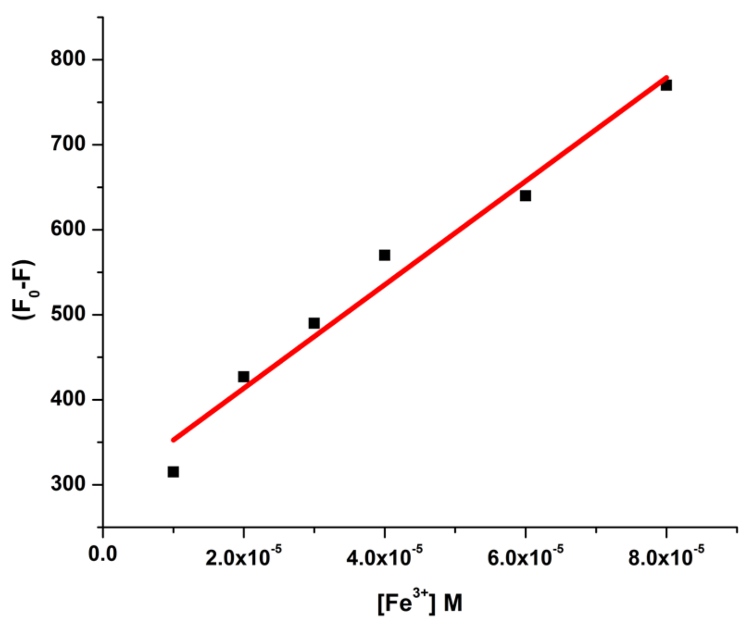

Figure 93. The limit of detection (LOD) of **5c** and [Fe^{3+}] derived from emission titration curve.

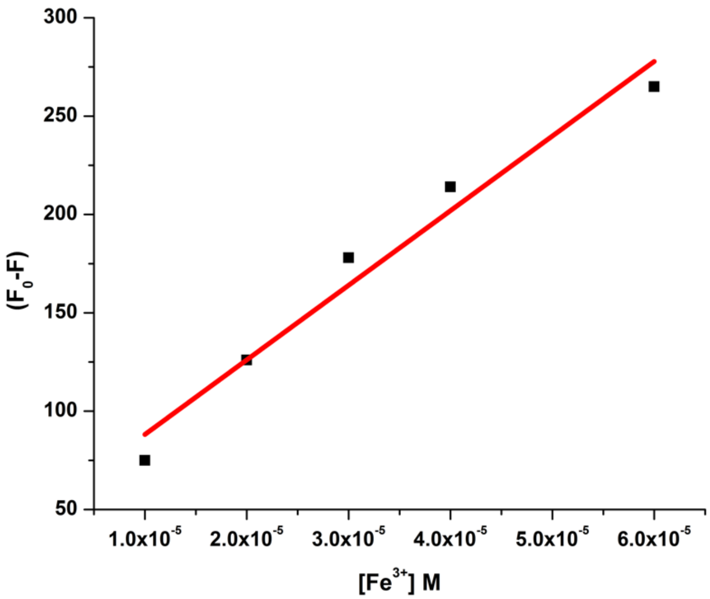

Figure 94. The limit of detection (LOD) of **5d** and $[Fe^{3+}]$ derived from emission titration curve.

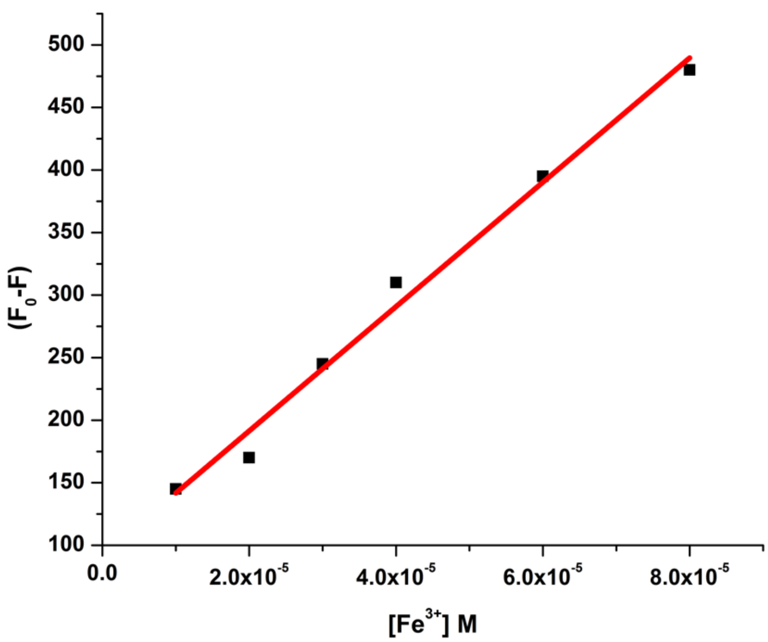

Figure 95. The limit of detection (LOD) of **5e** and $[Fe^{3+}]$ derived from emission titration curve.

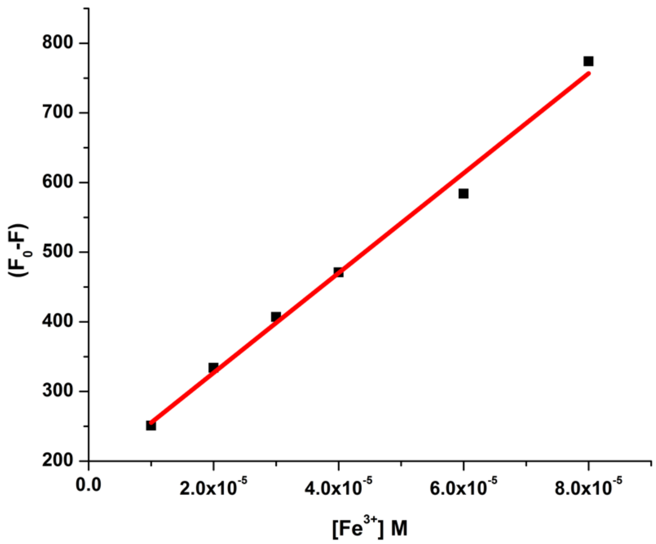

Figure 96. The limit of detection (LOD) of **5f** and $[Fe^{3+}]$ derived from emission titration curve.

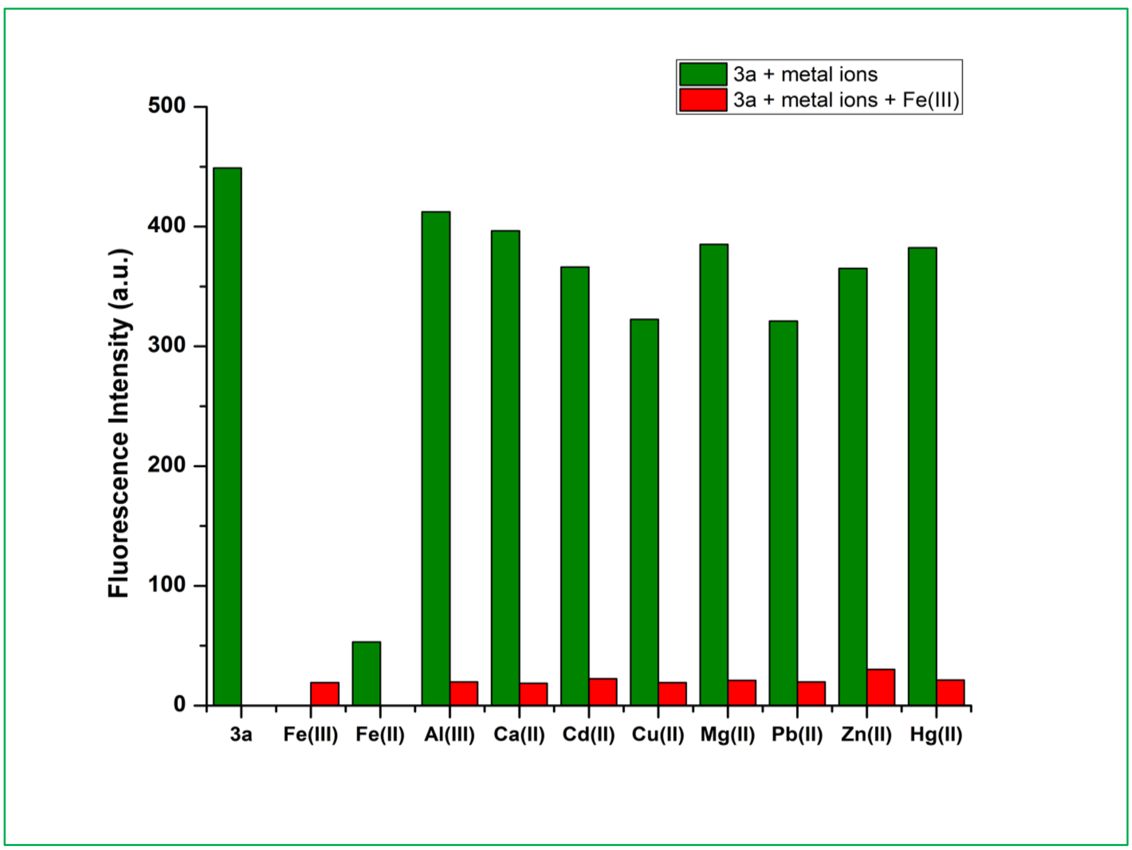

Figure 97. Selective quenching of fluorescence emission of **3a** (50 μM) and Fe^{3+} (2 equiv.) in the presence of 5 equiv. of different cations (red bar); **3a** and other metal ions only (5 equiv.) (green bar) in DMSO/H_2O (2:8, v/v) HEPES buffer solution (pH = 7.4) (λ_{ex} = 367 nm , λ_{em} = 415 nm).

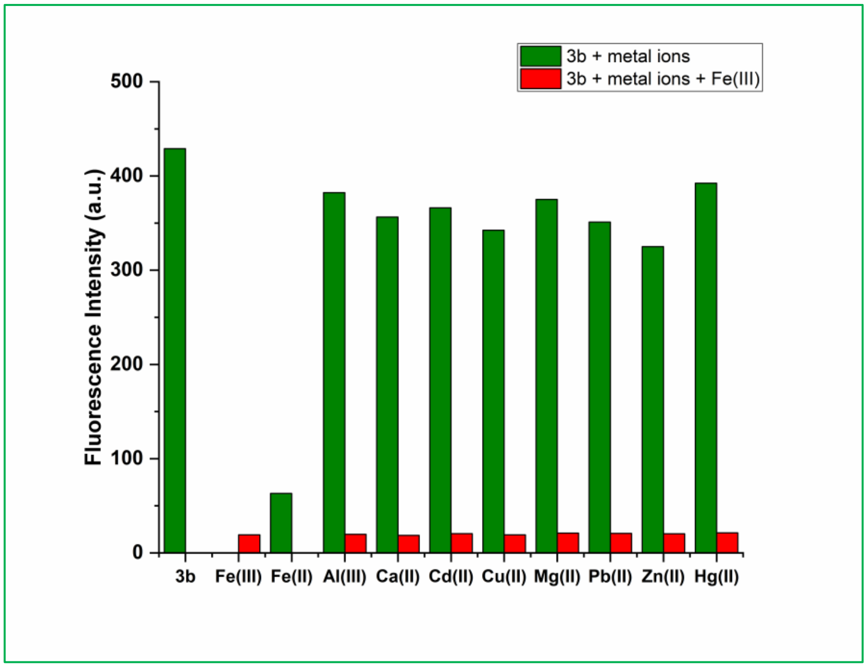

Figure 98. Selective quenching of fluorescence emission of **3b** (50 μM) and Fe^{3+} (2 equiv.) in the presence of 5 equiv. of different cations (red bar); **3b** and other metal ions only (5 equiv.) (green bar) in DMSO/H_2O (2:8, v/v) HEPES buffer solution (pH = 7.4) (λ_{ex} = 284 nm , λ_{em} = 344nm)

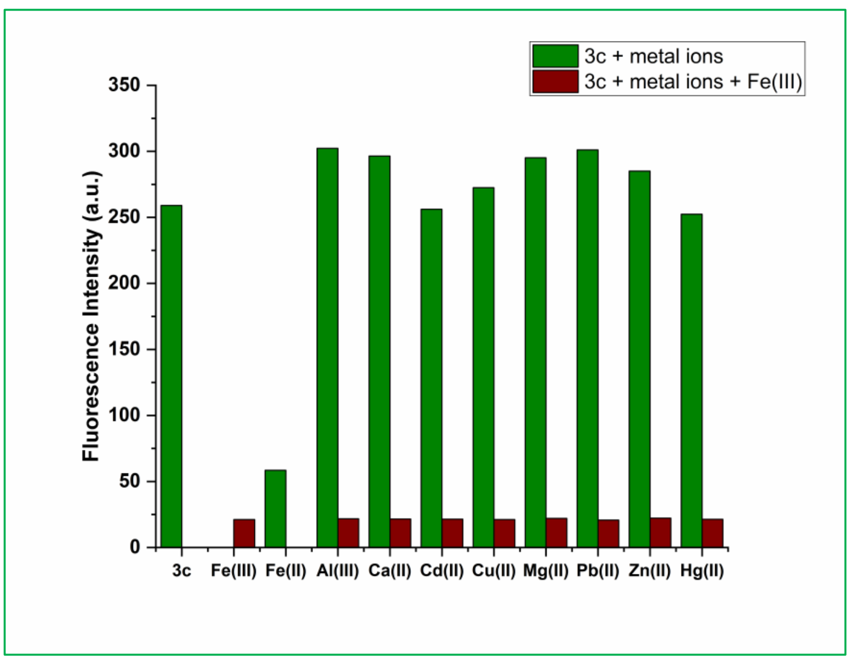

Figure 99. Selective quenching of fluorescence emission of **3c** (50 μM) and Fe^{3+} (2 equiv.) in the presence of 5 equiv. of different cations (brown bar); **3c** and other metal ions only (5 equiv.) (green bar) in DMSO/H_2O (2:8, v/v) HEPES buffer solution (pH = 7.4) (λ_{ex} = 306 nm , λ_{em} =343 nm)

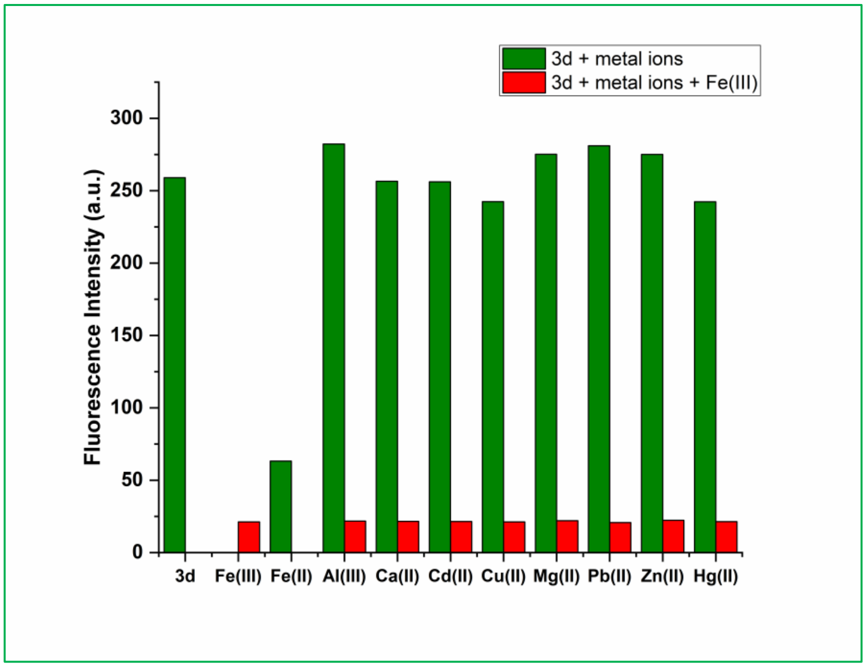

Figure100. Selective quenching of fluorescence emission of **3d** (50 μM) and Fe^{3+} (2 equiv.) in the presence of 5 equiv. of different cations (red bar); **3d** and other metal ions only (5 equiv.) (green bar) in DMSO/H_2O (2:8, v/v) HEPES buffer solution (pH = 7.4) (λ_{ex} = 367 nm , λ_{em} = 435 nm)

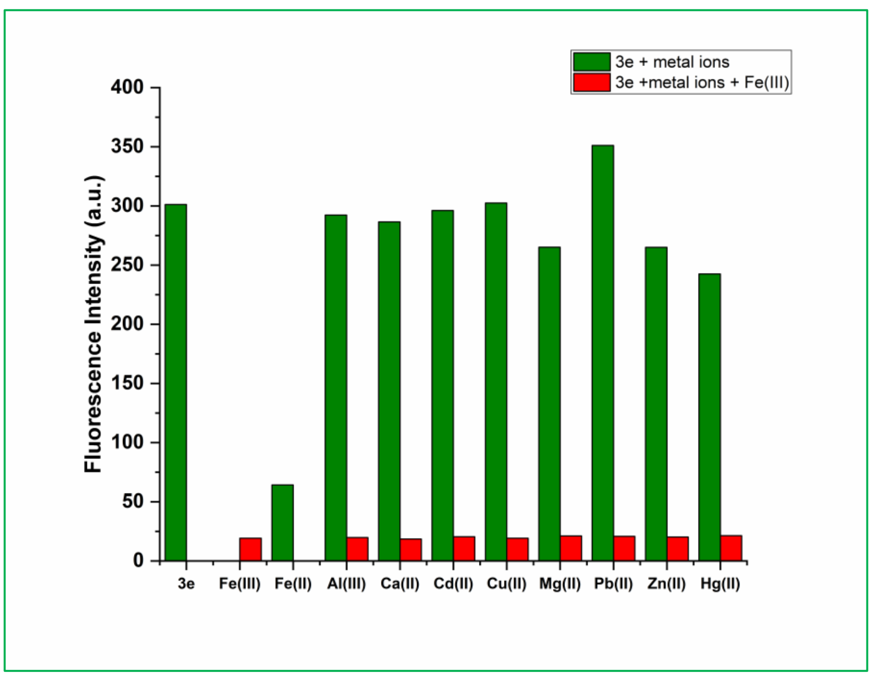

Figure 101. Selective quenching of fluorescence emission of **3e** (50 μM) and Fe^{3+} (2 equiv.) in the presence of 5 equiv. of different cations (red bar); **3e** and other metal ions only (5 equiv.) (green bar) in DMSO/H_2O (2:8, v/v) HEPES buffer solution (pH = 7.4) (λ_{ex} = 286 nm , λ_{em} =343 nm)

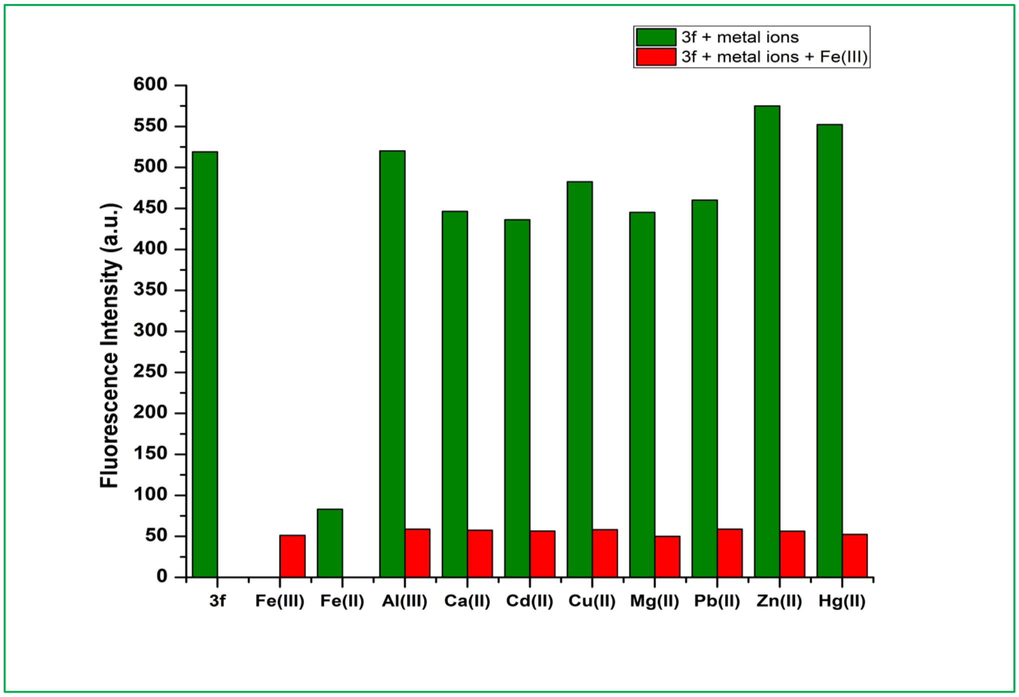

Figure 102. Selective quenching of fluorescence emission of **3f** (50 μM) and Fe^{3+} (2 equiv.) in the presence of 5 equiv. of different cations (red bar) ; **3f** and other metal ions only (5 equiv.) (green bar) in $DMSO/H_2O$ (2:8, v/v) HEPES buffer solution (pH = 7.4) (λ_{ex} = 372 nm , λ_{em} = 434 nm).

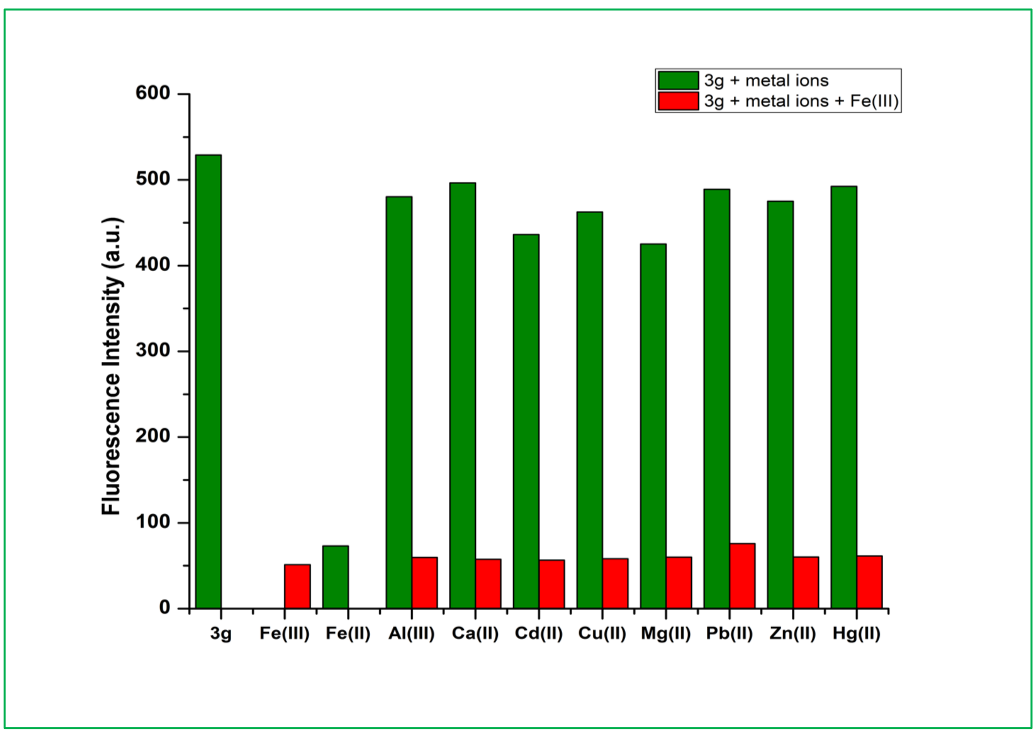

Figure 103. Selective quenching of fluorescence emission of **3g** (50 μM) and Fe^{3+} (2 equiv.) in the presence of 5 equiv. of different cations (red bar) ; **3g** and other metal ions only (5 equiv.) (green bar) in $DMSO/H_2O$ (2:8, v/v) HEPES buffer solution (pH = 7.4) (λ_{ex} = 305 nm , λ_{em} = 405 nm).

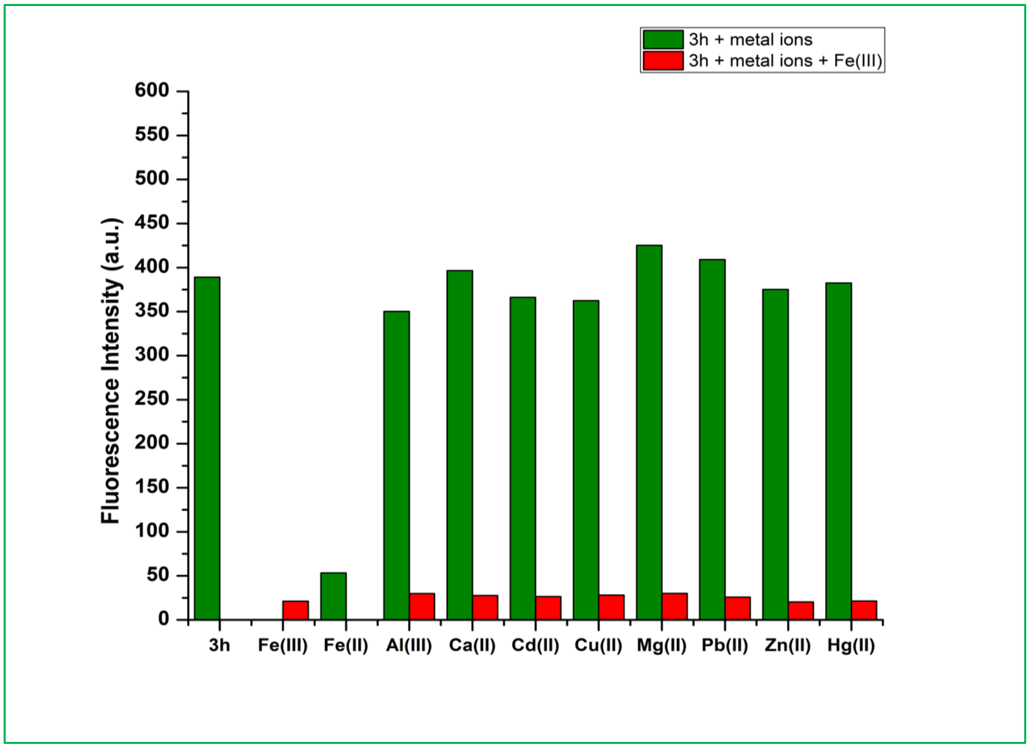

Figure 104. Selective quenching of fluorescence emission of **3h** (50 μM) and Fe^{3+} (2 equiv.) in the presence of 5 equiv. of different cations (red bar) ; **3h** and other metal ions only (5 equiv.) (green bar) in DMSO/H_2O (2:8, v/v) HEPES buffer solution (pH = 7.4) (λ_{ex} = 360 nm , λ_{em} = 410 nm).

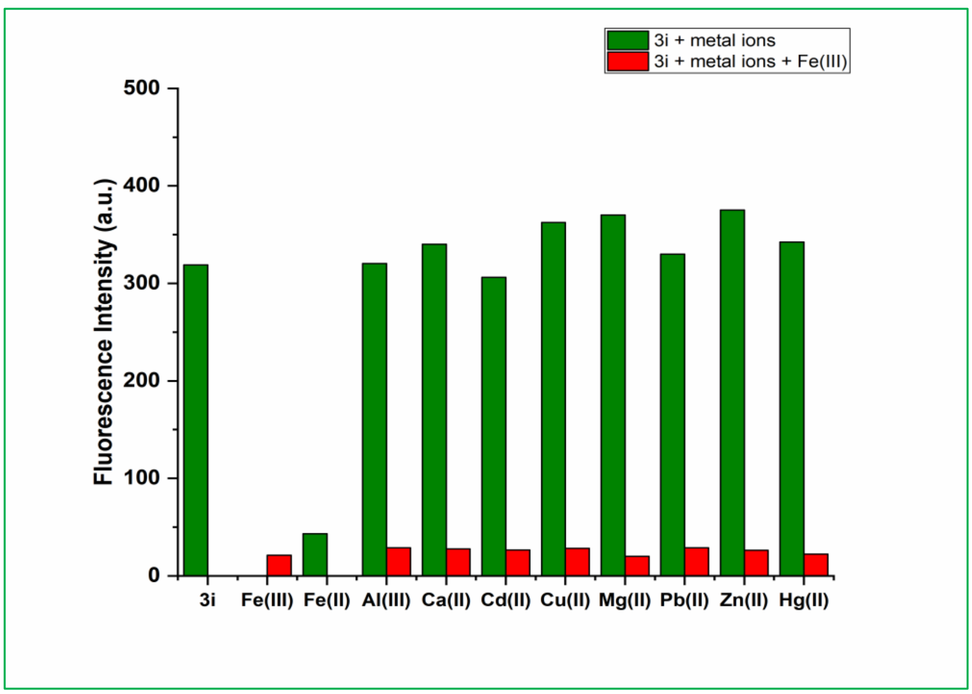

Figure 105. Selective quenching of fluorescence emission of **3i** (50 μM) and Fe^{3+} (2 equiv.) in the presence of 5 equiv. of different cations (red bar) ; **3i** and other metal ions only (5 equiv.) (green bar) in DMSO/H_2O (2:8, v/v) HEPES buffer solution (pH = 7.4) (λ_{ex} = 365 nm , λ_{em} = 434 nm).

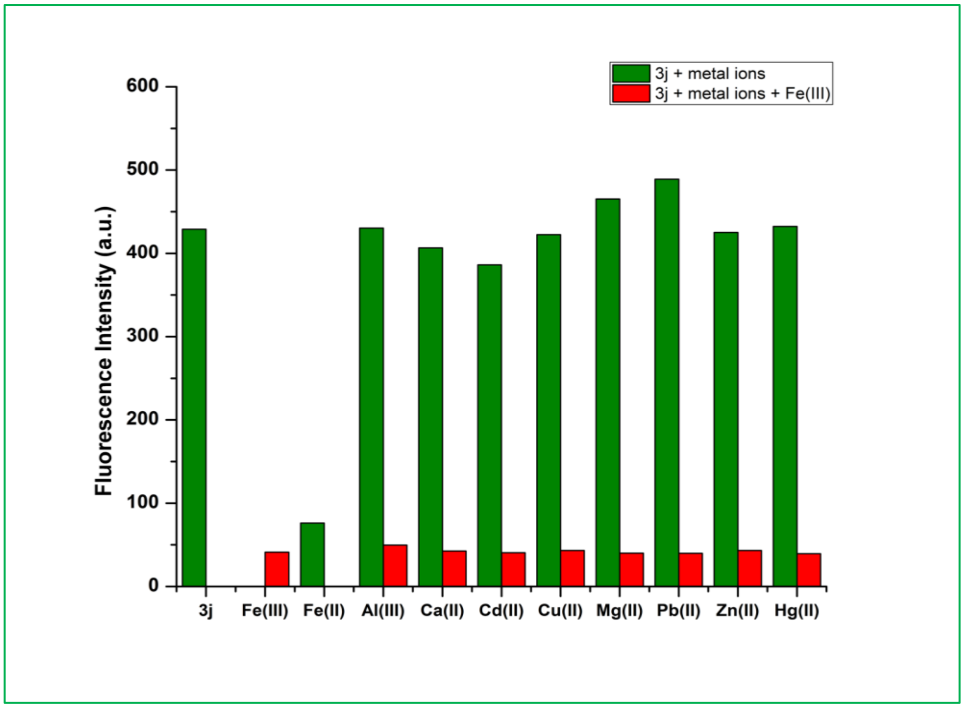

Figure 106. Selective quenching of fluorescence emission of **3j** (50 μM) and Fe^{3+} (2 equiv.) in the presence of 5 equiv. of different cations (red bar) ; **3j** and other metal ions only (5 equiv.) (green bar) in DMSO/H_2O (2:8, v/v) HEPES buffer solution (pH = 7.4) (λ_{ex} = 390 nm , λ_{em} = 435 nm).

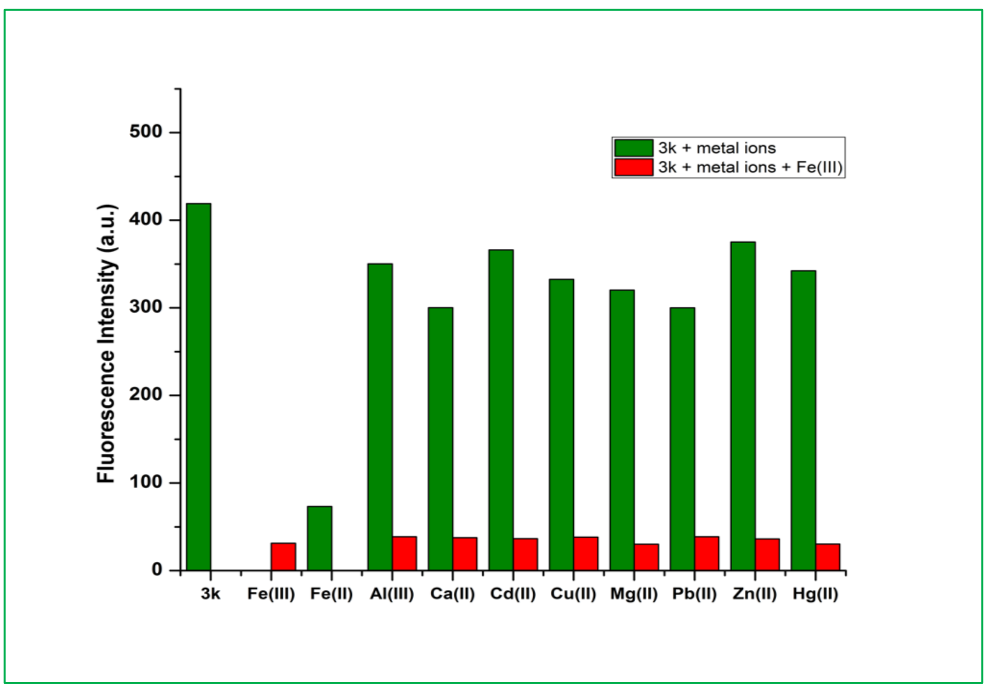

Figure 107. Selective quenching of fluorescence emission of **3k** (50 μM) and Fe^{3+} (2 equiv.) in the presence of 5 equiv. of different cations (red bar) ; **3k** and other metal ions only (5 equiv.) (green bar) in DMSO/H_2O (2:8, v/v) HEPES buffer solution (pH = 7.4) (λ_{ex} = 360 nm , λ_{em} = 430 nm).

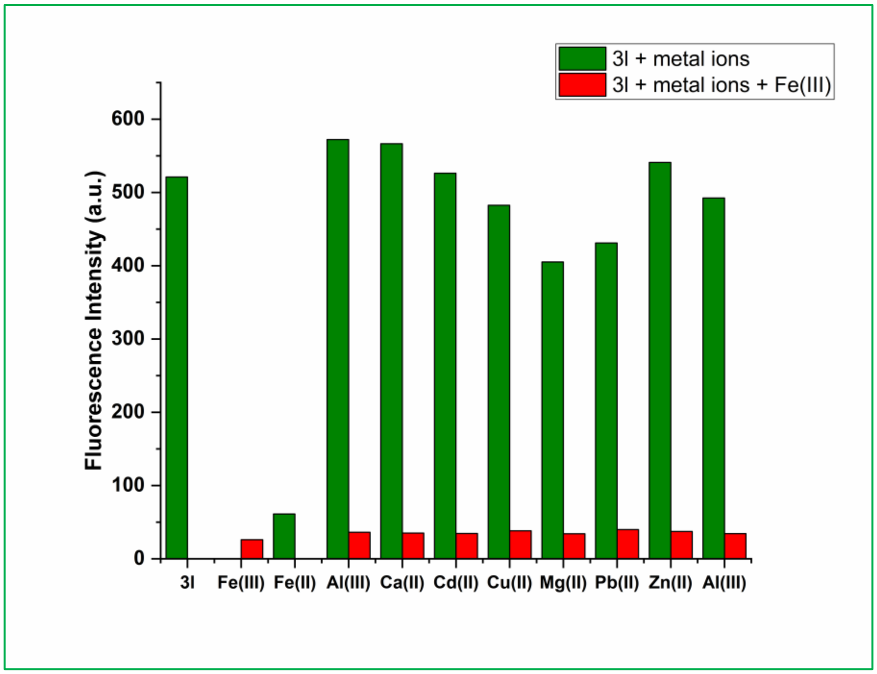

Figure 108. Selective quenching of fluorescence emission of **3l** (50 μM) and Fe^{3+} (2 equiv.) in the presence of 5 equiv. of different cations (red bar); **3l** and other metal ions only (5 equiv.) (green bar) in DMSO/H_2O (2:8, v/v) HEPES buffer solution (pH = 7.4) (λ_{ex} = 284 nm , λ_{em} = 345 nm)

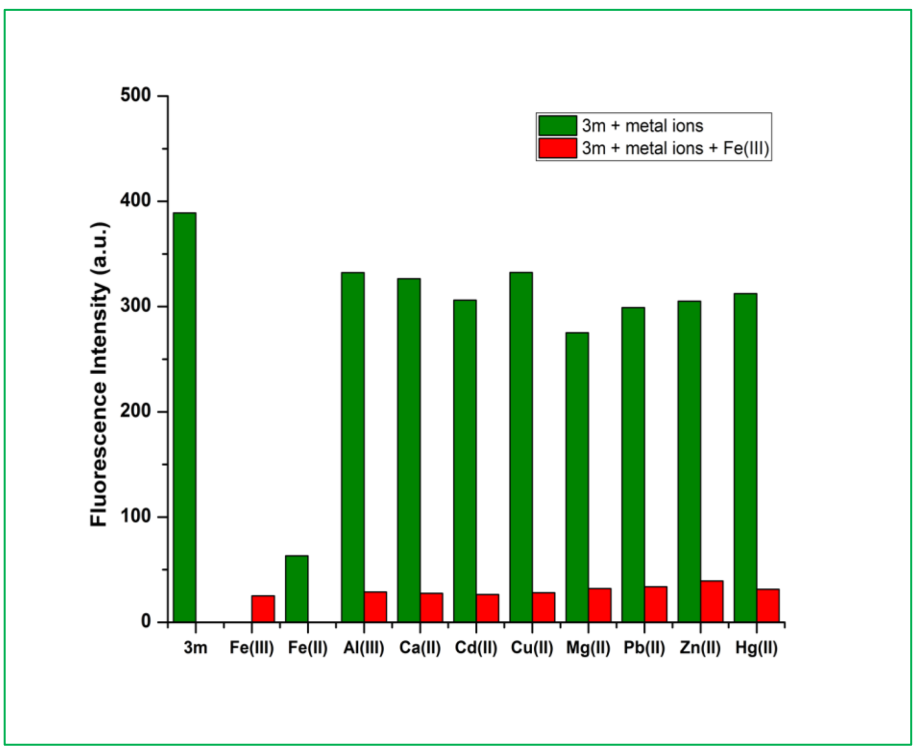

Figure 109. Selective quenching of fluorescence emission of **3m** (50 μM) and Fe^{3+} (2 equiv.) in the presence of 5 equiv. of different cations (red bar) ; **3m** and other metal ions only (5 equiv.) (green bar) in DMSO/H_2O (2:8, v/v) HEPES buffer solution (pH = 7.4) (λ_{ex} = 360 nm , λ_{em} = 435 nm).

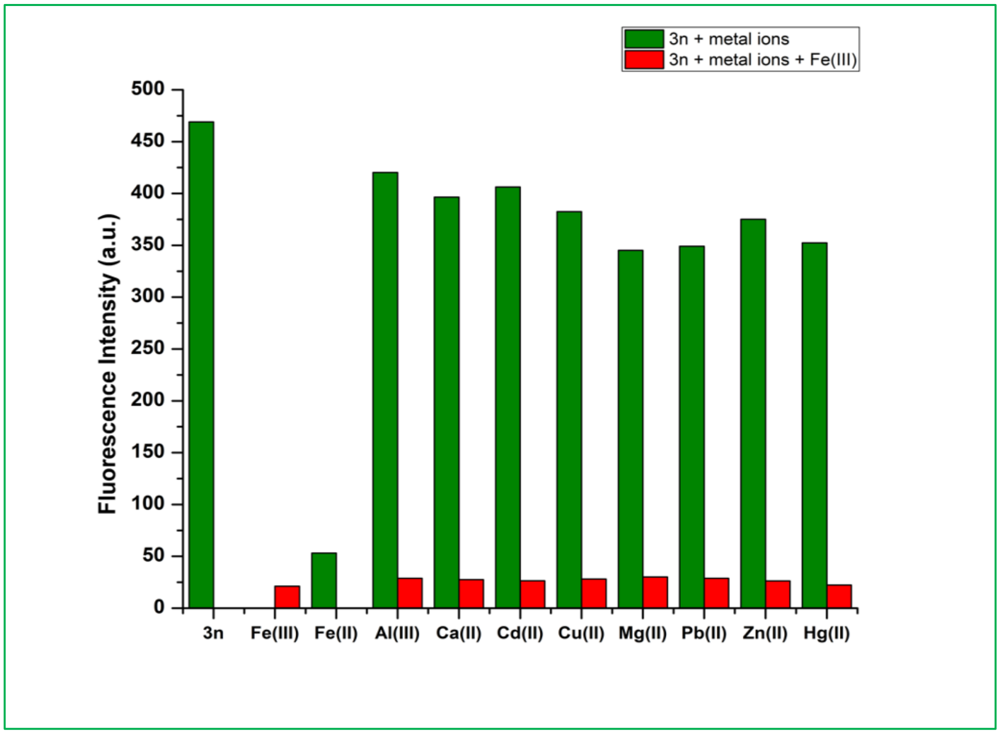

Figure 110. Selective quenching of fluorescence emission of **3n** (50 μM) and Fe^{3+} (2 equiv.) in the presence of 5 equiv. of different cations (red bar) ; **3n** and other metal ions only (5 equiv.) (green bar) in DMSO/H_2O (2:8, v/v) HEPES buffer solution (pH = 7.4) (λ_{ex} = 350 nm , λ_{em} = 434 nm).

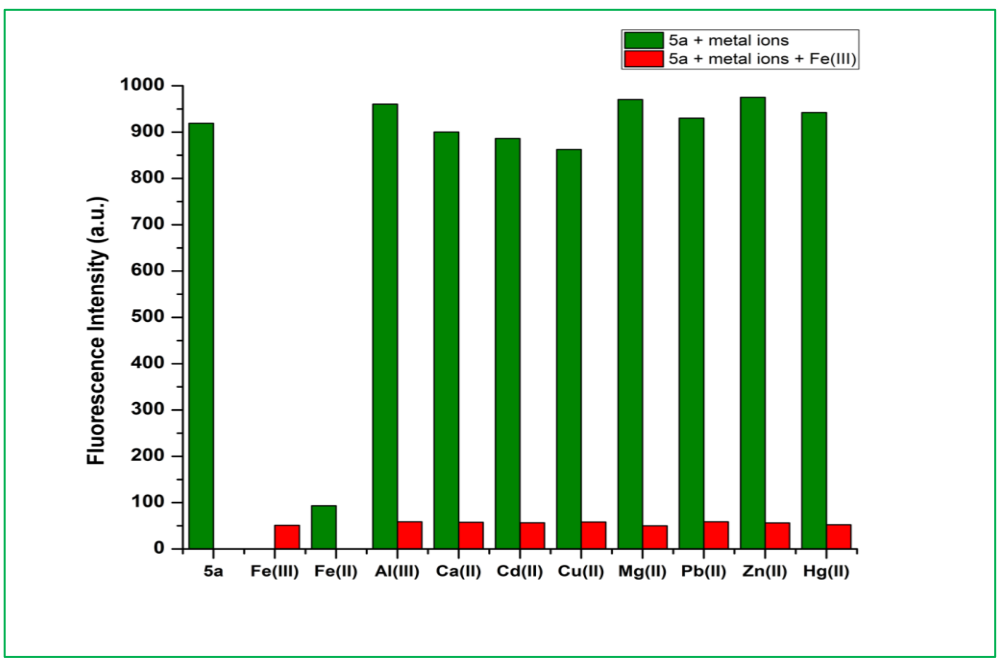

Figure 111. Selective quenching of fluorescence emission of **5a** (50 μM) and Fe^{3+} (2 equiv.) in the presence of 5 equiv. of different cations (red bar) ; **5a** and other metal ions only (5 equiv.) (green bar) in DMSO/H_2O (2:8, v/v) HEPES buffer solution (pH = 7.4) (λ_{ex} = 380 nm , λ_{em} = 420 nm).

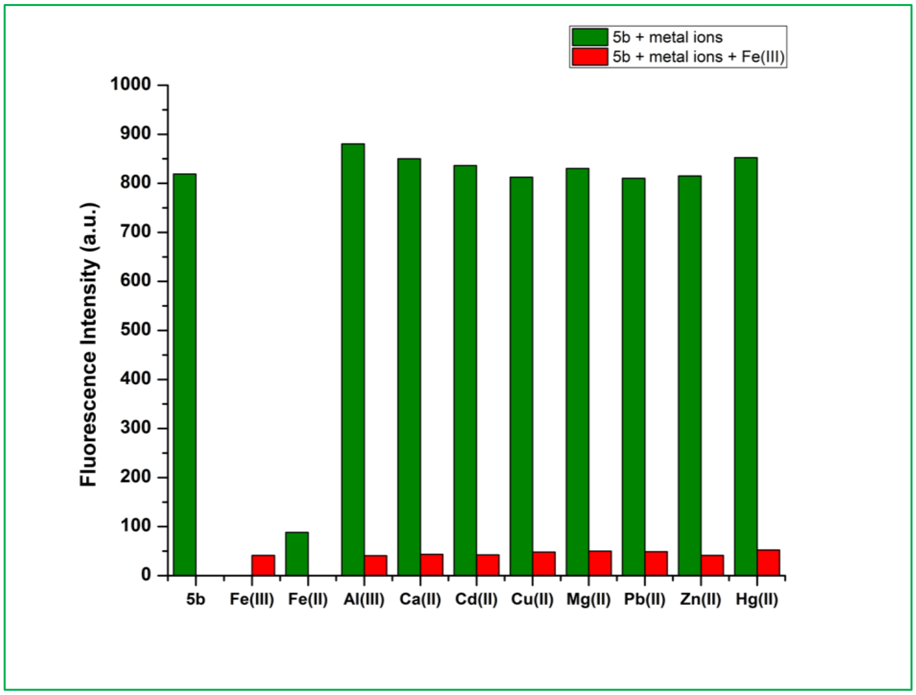

Figure 112. Selective quenching of fluorescence emission of **5b** (50 μM) and Fe^{3+} (2 equiv.) in the presence of 5 equiv. of different cations (red bar) ; **5b** and other metal ions only (5 equiv.) (green bar) in DMSO/H_2O (2:8, v/v) HEPES buffer solution (pH = 7.4) (λ_{ex} = 365 nm , λ_{em} = 435 nm).

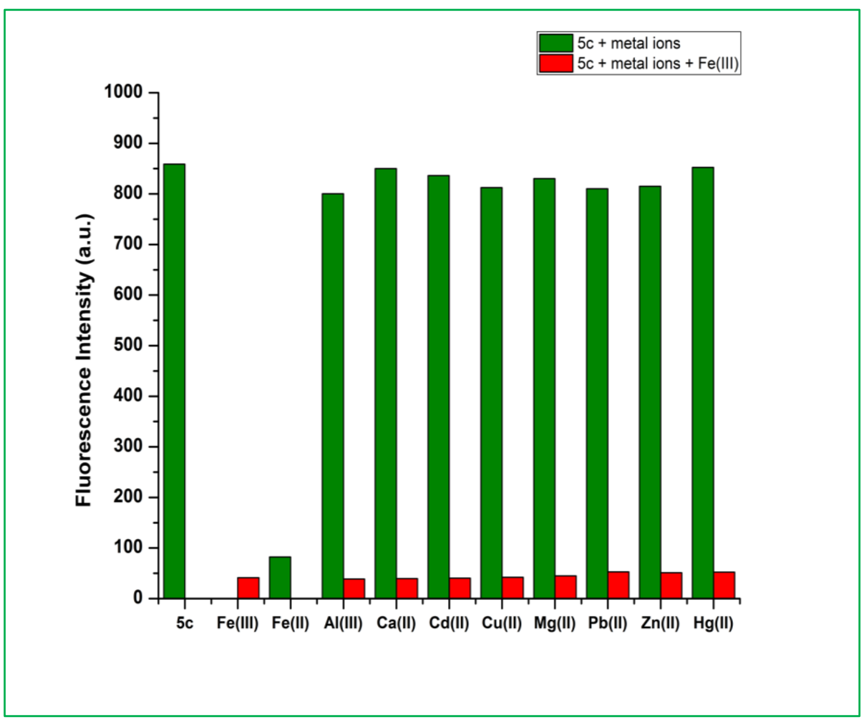

Figure 113. Selective quenching of fluorescence emission of **5c** (50 μM) and Fe^{3+} (2 equiv.) in the presence of 5 equiv. of different cations (red bar) ; **5c** and other metal ions only (5 equiv.) (green bar) in DMSO/H_2O (2:8, v/v) HEPES buffer solution (pH = 7.4) (λ_{ex} = 380 nm , λ_{em} = 436 nm).

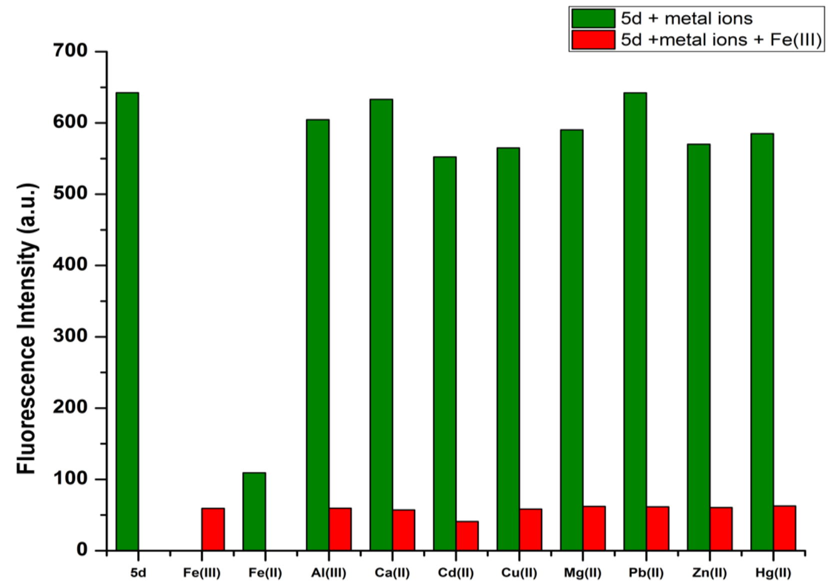

Figure 114. Selective quenching of fluorescence emission of **5d** (50 μM) and Fe^{3+} (2 equiv.) in the presence of 5 equiv. of different cations (red bar) ; **5d** and other metal ions only (5 equiv.) (green bar) in DMSO/H_2O (2:8, v/v) HEPES buffer solution (pH = 7.4) (λ_{ex} = 380 nm , λ_{em} = 425 nm).

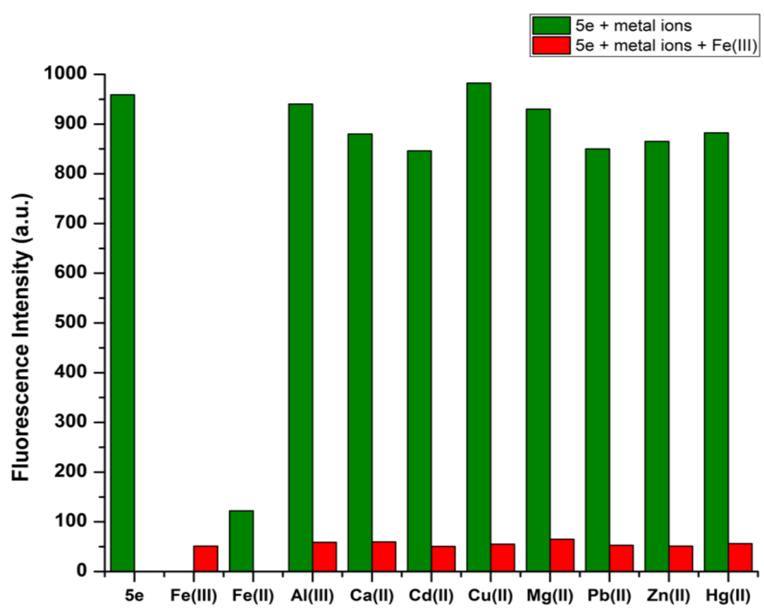

Figure 115. Selective quenching of fluorescence emission of **5e** (50 μM) and Fe^{3+} (2 equiv.) in the presence of 5 equiv. of different cations (red bar) ; **5e** and other metal ions only (5 equiv.) (green bar) in DMSO/H_2O (2:8, v/v) HEPES buffer solution (pH = 7.4) (λ_{ex} = 380 nm , λ_{em} = 425 nm).

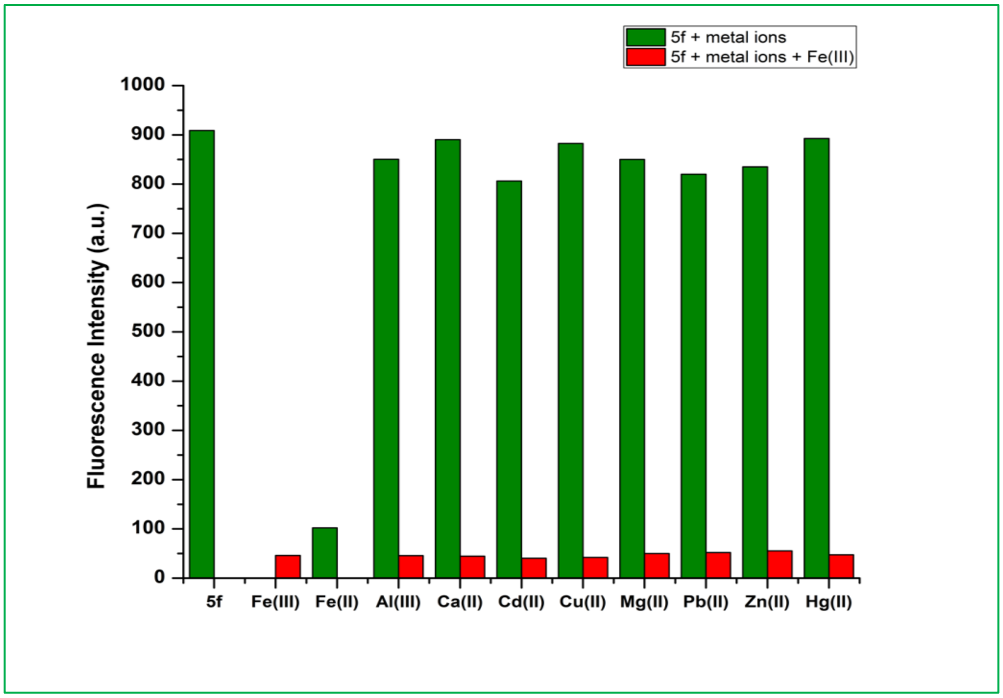

Figure 116. Selective quenching of fluorescence emission of **5f** (50 μM) and Fe^{3+} (2 equiv.) in the presence of 5 equiv. of different cations (red bar) ; **5f** and other metal ions only (5 equiv.) (green bar) in DMSO/H_2O (2:8, v/v) HEPES buffer solution (pH = 7.4) (λ_{ex} = 380 nm , λ_{em} = 435 nm).

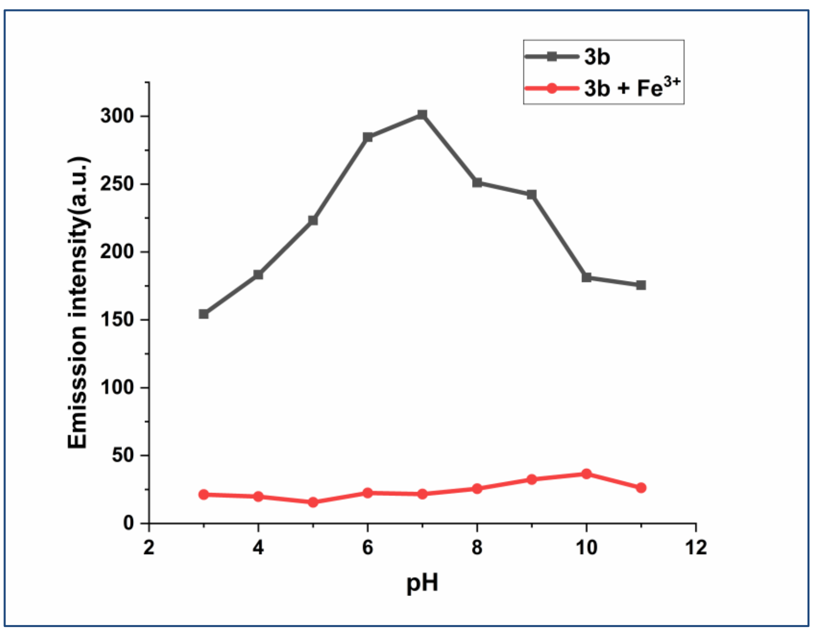

Figure 117. Emission intensity of compounds **3b** in absence and in presence of Fe^{3+} at different pH values in aqueous DMSO solution.

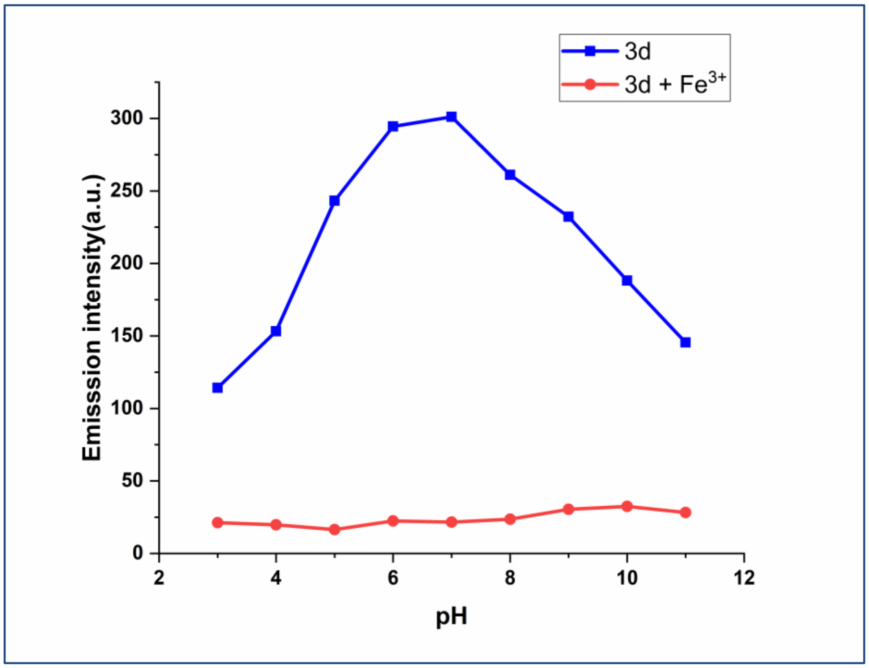

Figure 118. Emission intensity of compounds **3d** in absence and in presence of Fe^{3+} at different pH values in aqueous DMSO solution.

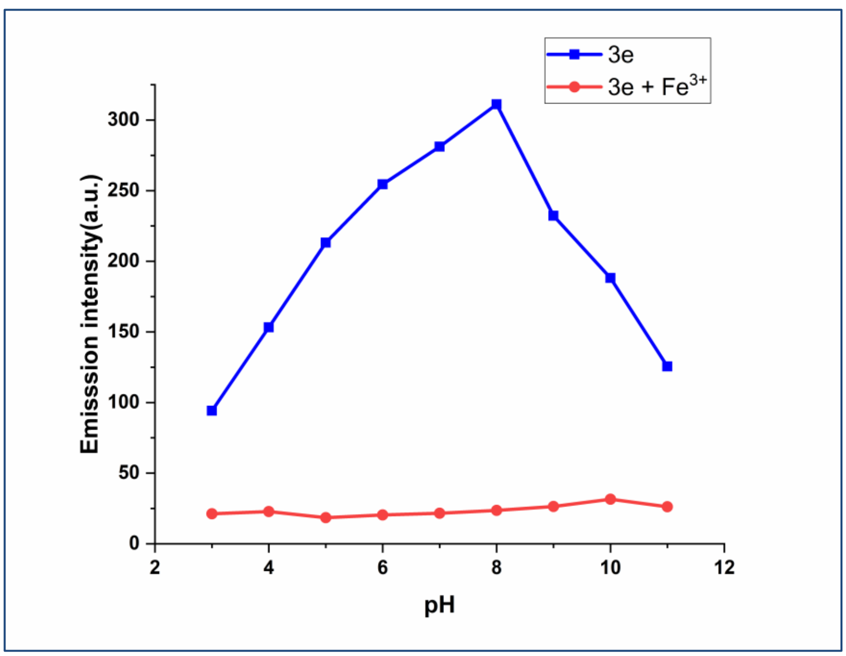

Figure 119. Emission intensity of compounds **3e** in absence and in presence of Fe^{3+} at different pH values in aqueous DMSO solution.

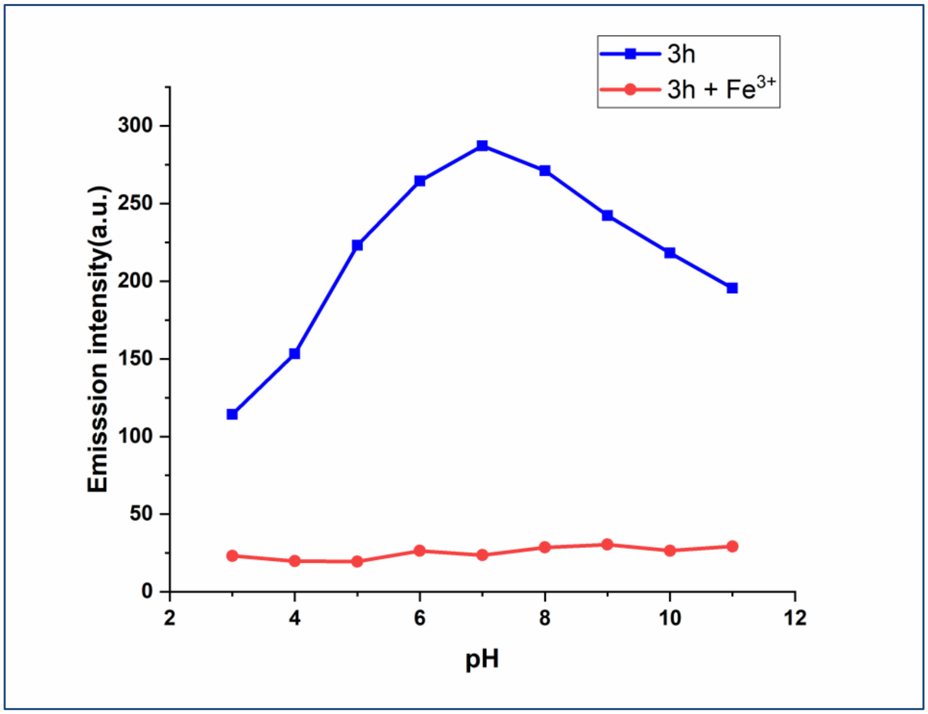

Figure 120. Emission intensity of compounds **3h** in absence and in presence of Fe^{3+} at different pH values in aqueous DMSO solution.

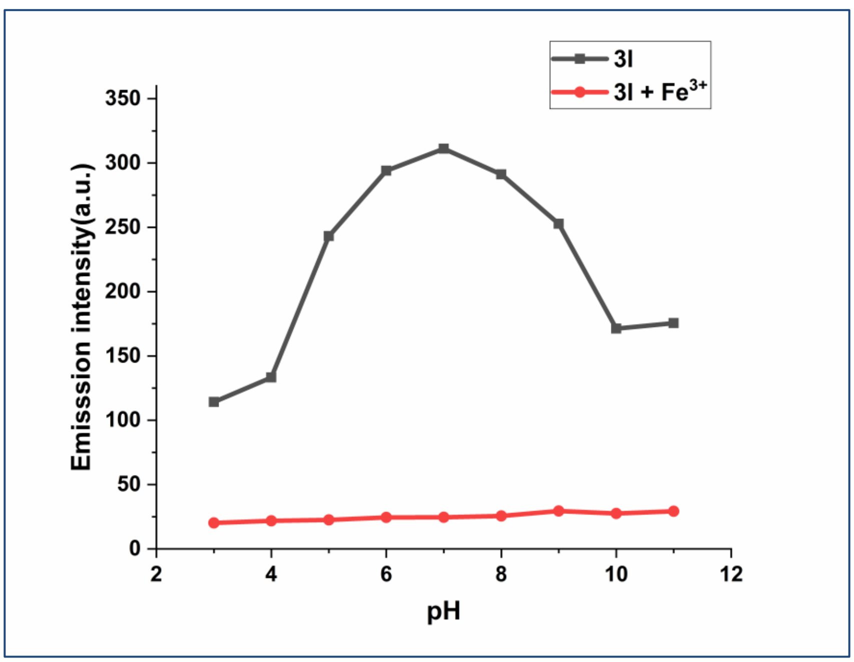

Figure 121. Emission intensity of compounds **3l** in absence and in presence of Fe^{3+} at different pH values in aqueous DMSO solution.

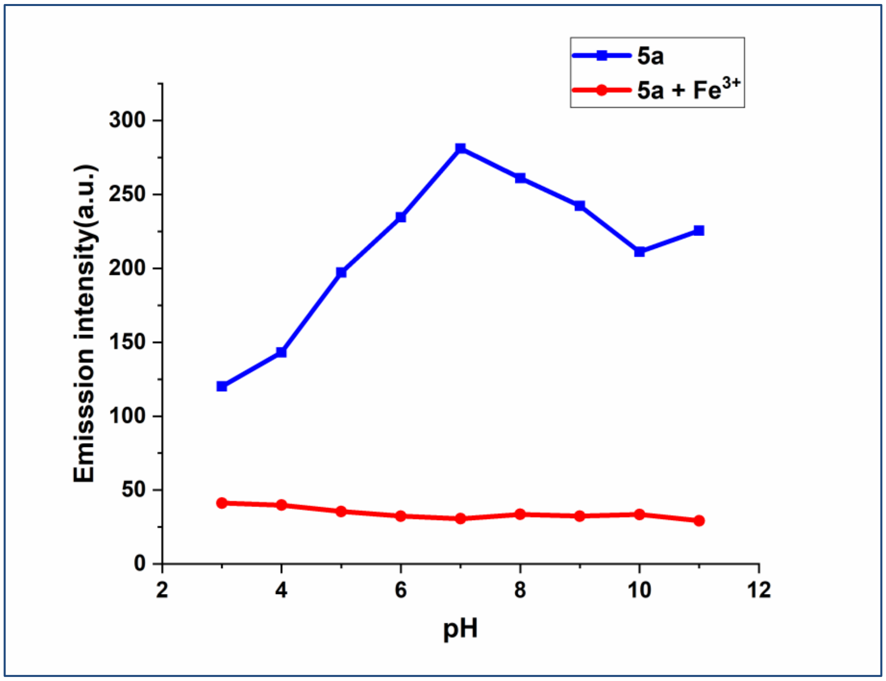

Figure 122. Emission intensity of compounds **5a** in absence and in presence of Fe^{3+} at different pH values in aqueous DMSO solution.

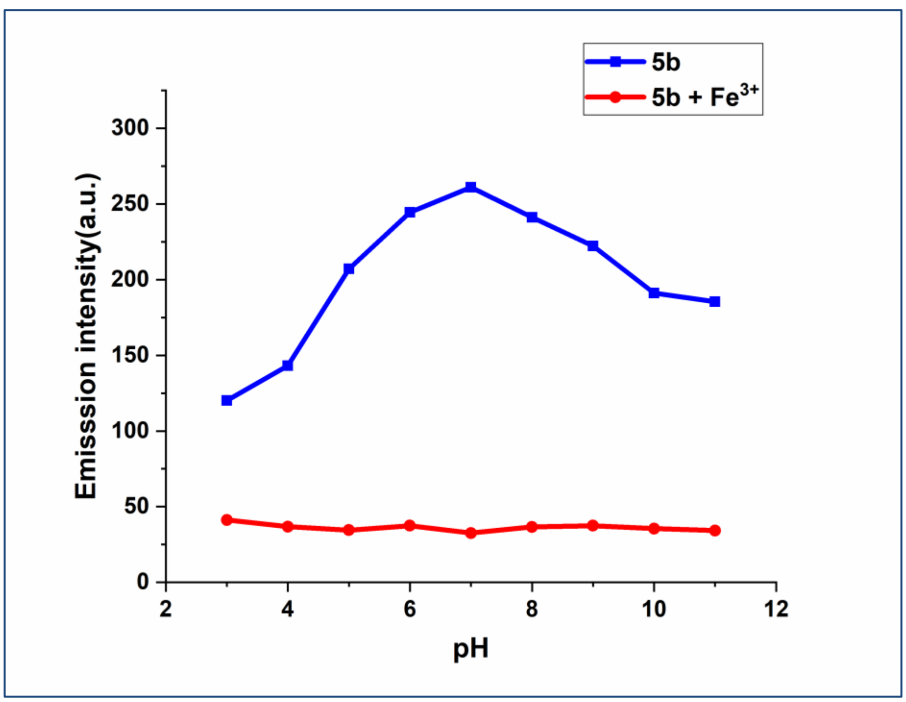

Figure 123. Emission intensity of compounds **5b** in absence and in presence of Fe^{3+} at different pH values in aqueous DMSO solution.

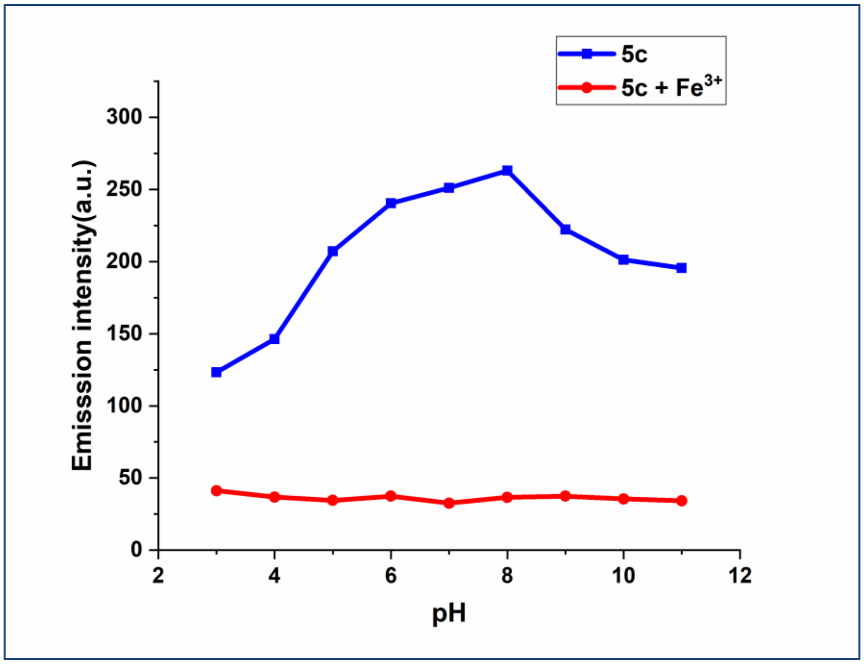

Figure 124. Emission intensity of compounds **5c** in absence and in presence of Fe^{3+} at different pH values in aqueous DMSO solution.

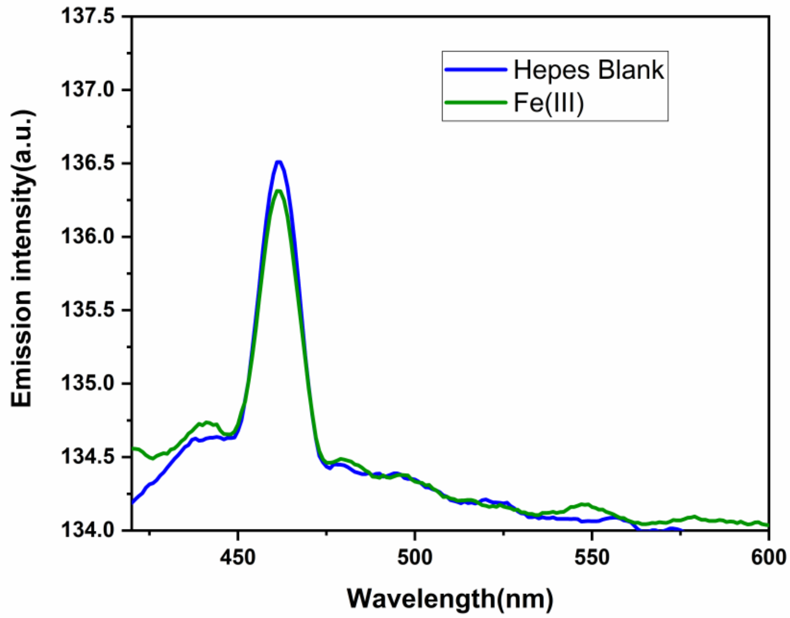

Figure 125. Fluorescence spectra of blank HEPES and Fe (III) (λ_{ex}= 400 nm, λ_{em}= 460 nm)

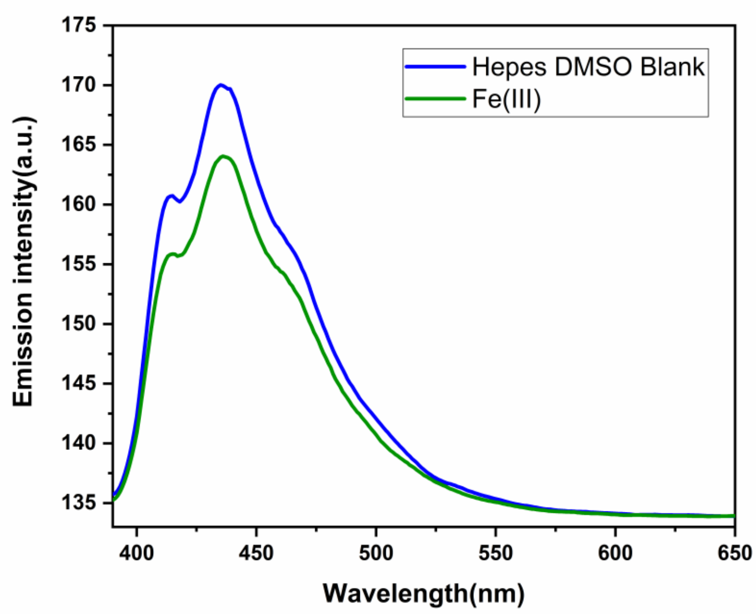

Figure 126. Fluorescence spectra of blank HEPES-DMSO and Fe (III) (λ_{ex}= 380 nm, λ_{em}= 436 nm)

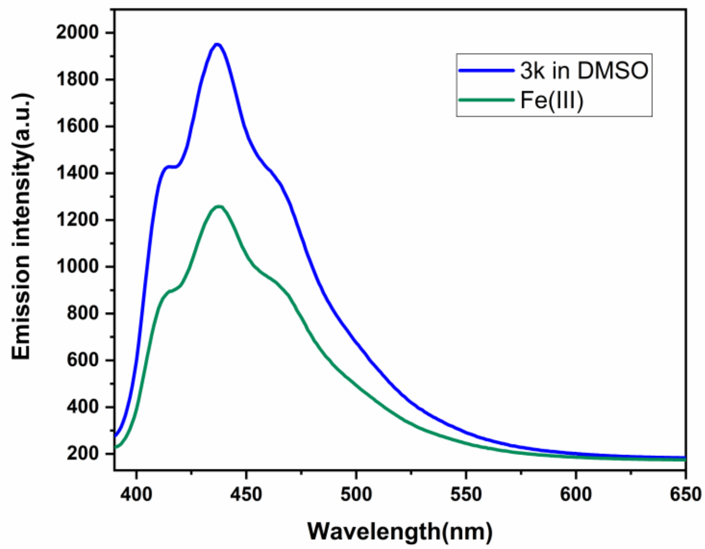

Figure 127. Fluorescence spectra of **3k** and **3k** + Fe (III) in DMSO(λ_{ex}= 380 nm, λ_{em}= 438 nm)

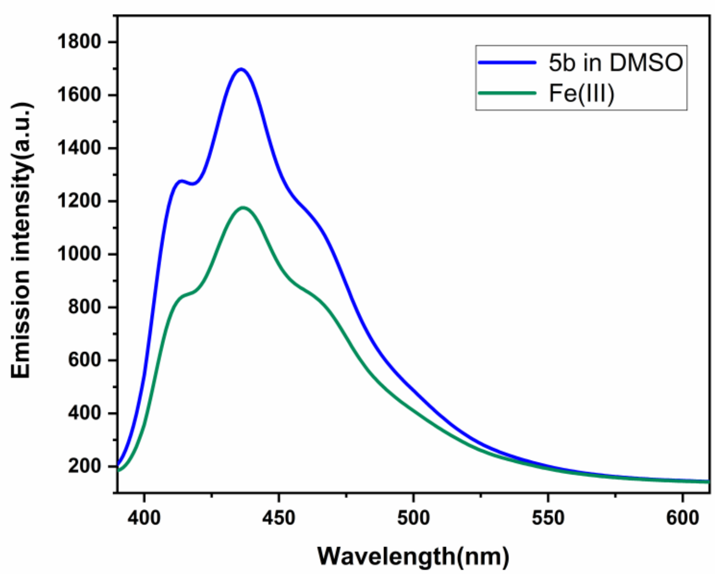

Figure 128. Fluorescence spectra of **5b** and **5b** + Fe (III) in DMSO (λ_{ex}= 375 nm, λ_{em}= 438 nm)

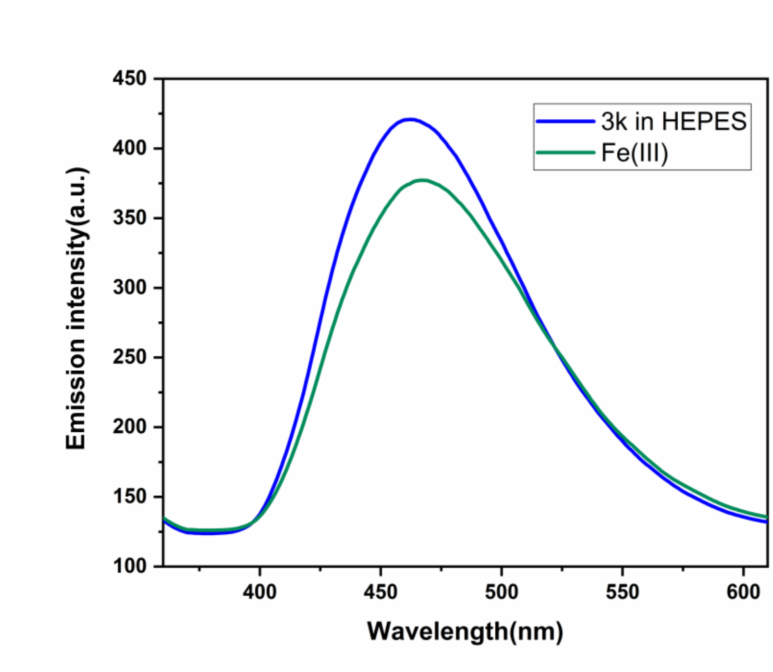

Figure 129. Fluorescence spectra of **3k** and **3k** + Fe (III) in HEPES(λ_{ex}= 370 nm, λ_{em}= 463 nm)

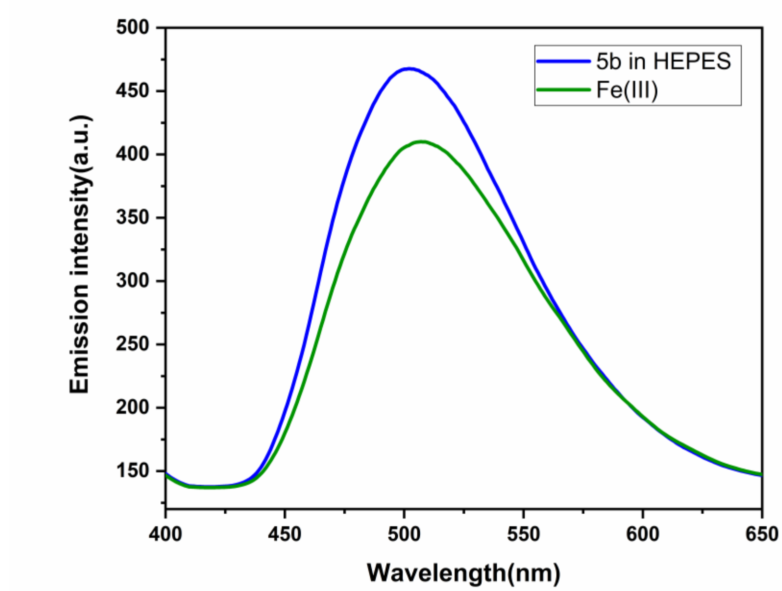

Figure 130. Fluorescence spectra of **5b** and **5b** + Fe (III) in HEPES (λ_{ex}= 400 nm, λ_{em}= 461 nm)

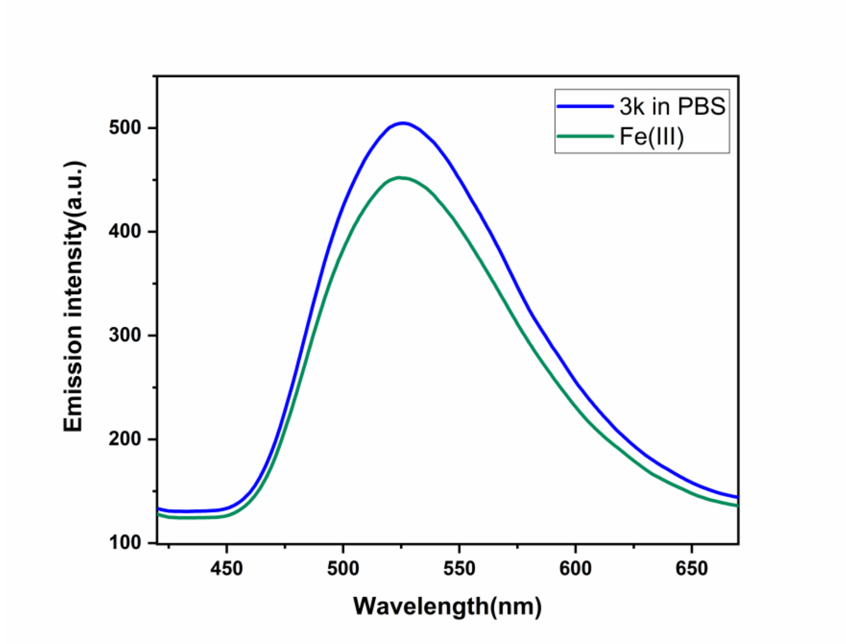

Figure 131. Fluorescence spectra of **3k** and **3k** + Fe (III) in PBS (λ_{ex}= 405 nm, λ_{em}= 528 nm)

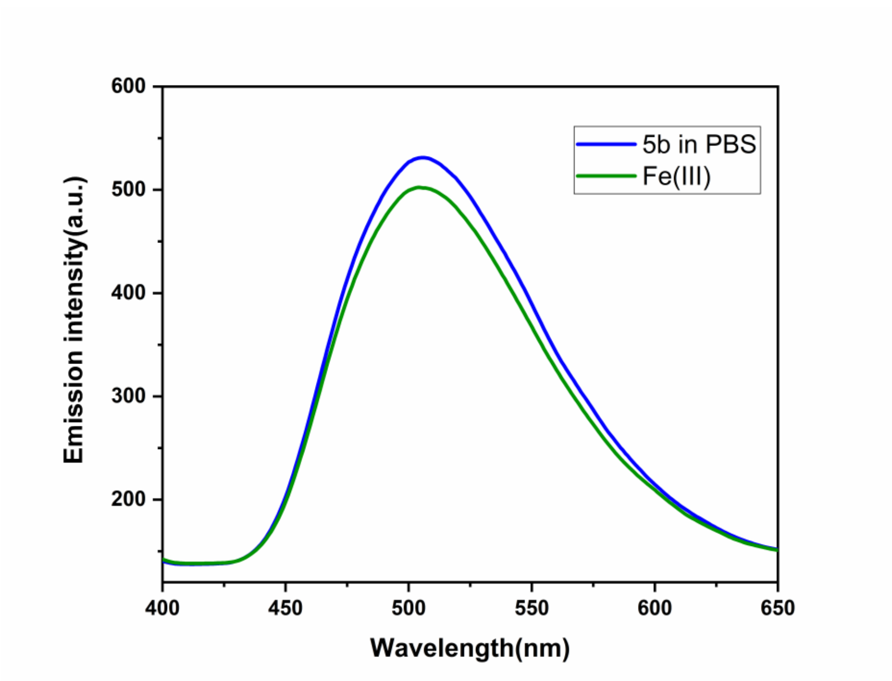

Figure 132. Fluorescence spectra of **5b** and **5b** + Fe (III) in PBS(λ_{ex}= 390 nm, λ_{em}= 505 nm)

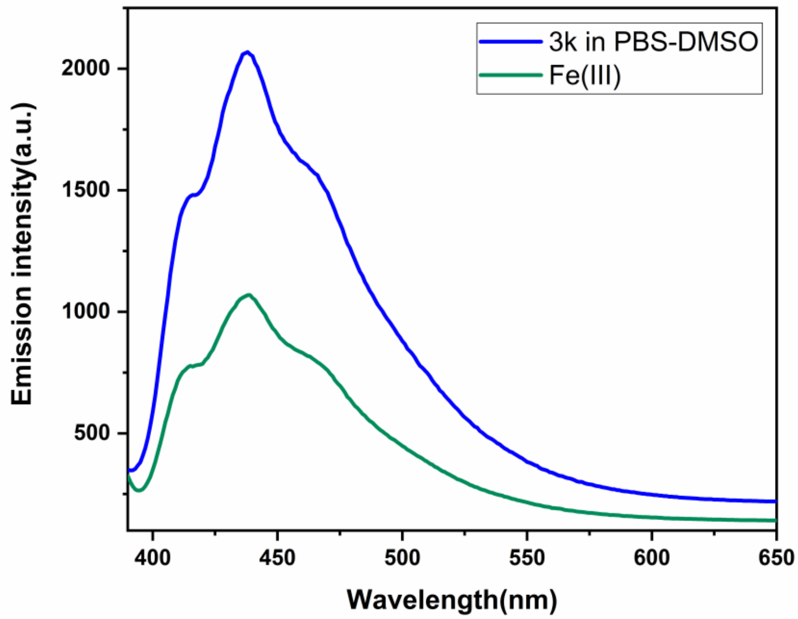

Figure 133. Fluorescence spectra of **3k** and **3k** + Fe (III) in PBS-DMSO (2: 8, v/v) (λ_{ex}= 380 nm, λ_{em}= 438 nm)

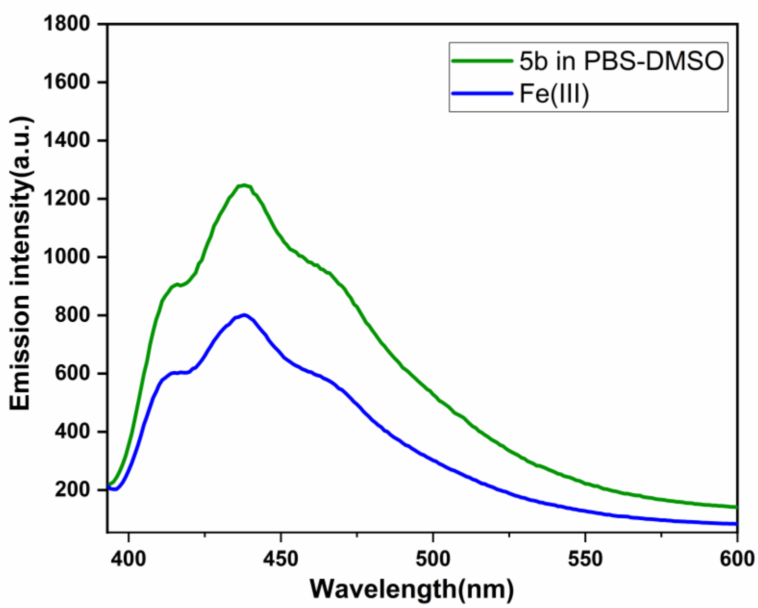

Figure 134. Fluorescence spectra of **5b** and **5b** + Fe (III) in PBS-DMSO (2: 8, v/v)(λ_{ex}= 380 nm, λ_{em}= 438 nm)

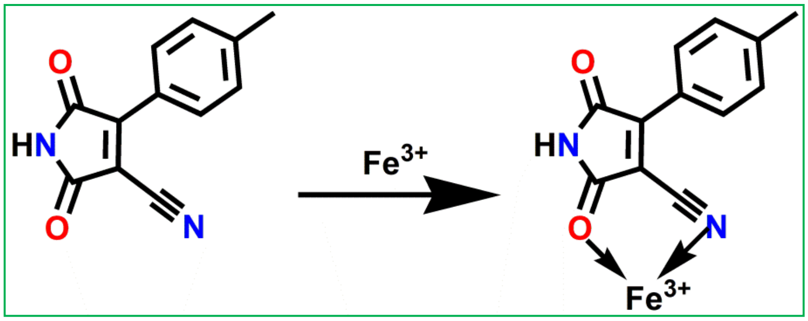

Figure 135. Probable binding of the probe **3b** with Fe^{3+}

Table 2. Summary of photophysical properties of compounds **3a** – **n** and **5a** – **f** studied in various solvents

Compound	λ_{ex} (nm)	λ_{em}(nm)	$\Delta\lambda = [\lambda_{ex} - \lambda_{em}]$ (nm)	Quantum yield (ϕ_f)
DMSO				
3a	360	408	48	0.37
3b	282	340	58	0.43
3c	295	338	43	0.42
3d	362	430	68	0.40
3e	280	340	60	0.47
3f	375	430	55	0.41
3g	348	401	53	0.50
3h	355	407	52	0.57
3i	360	430	70	0.45
3j	382	428	46	0.49
3k	380	440	60	0.45
3l	280	342	62	0.42
3m	358	430	72	0.49
3n	355	430	75	0.44
5a	370	412	42	0.60
5b	375	438	63	0.52
5c	368	425	57	0.54
5d	375	420	45	0.47
5e	372	420	48	0.48
5f	375	430	55	0.51
DMF				
3a	365	415	50	0.37
3b	295	350	55	0.43
3c	305	350	45	0.42

3d	358	440	82	0.40
3e	390	432	42	0.47
3f	372	422	50	0.41
3g	352	460	53	0.50
3h	358	416	52	0.57
3i	368	412	44	0.45
3j	386	442	56	0.49
3k	358	412	54	0.45
3l	292	350	58	0.42
3m	350	413	63	0.49
3n	359	430	71	0.44
5a	374	412	38	0.60
5b	368	422	54	0.52
5c	378	425	47	0.54
5d	382	424	42	0.47
5e	380	422	42	0.48
5f	370	426	56	0.51
MeCN				
3a	362	430	68	0.37
3b	360	440	80	0.43
3c	355	432	77	0.42
3d	342	412	70	0.40
3e	366	424	58	0.47
3f	375	442	67	0.41
3g	348	436	88	0.50
3h	355	448	93	0.57
3i	360	446	86	0.45
3j	382	440	58	0.49
3k	365	432	67	0.45
3l	366	442	76	0.42
3m	353	430	77	0.49
3n	370	430	60	0.44
5a	380	440	60	0.60
5b	380	442	60	0.52
5c	378	440	62	0.54
5d	372	444	72	0.47
5e	378	452	74	0.48
5f	376	445	69	0.51
MeOH				
3a	376	463	87	0.37
3b	364	462	98	0.43
3c	354	442	88	0.42
3d	363	455	92	0.40

3e	380	471	91	0.47
3f	375	452	77	0.41
3g	376	464	88	0.50
3h	372	454	82	0.57
3i	366	454	88	0.45
3j	370	452	82	0.49
3k	390	488	98	0.45
3l	380	462	82	0.42
3m	375	467	92	0.49
3n	372	466	94	0.44
5a	375	467	92	0.60
5b	380	490	110	0.52
5c	383	472	89	0.54
5d	388	476	88	0.47
5e	383	470	87	0.48
5f	377	459	82	0.51
THF				
3a	378	465	87	0.37
3b	386	470	84	0.43
3c	362	445	83	0.42
3d	362	442	80	0.40
3e	372	452	80	0.47
3f	366	448	82	0.41
3g	370	455	85	0.50
3h	360	456	96	0.57
3i	360	450	90	0.45
3j	362	446	84	0.49
3k	355	438	83	0.45
3l	372	462	90	0.42
3m	368	457	89	0.49
3n	376	463	87	0.44
5a	370	442	72	0.60
5b	364	448	84	0.52
5c	372	463	91	0.54
5d	374	468	94	0.47
5e	370	458	88	0.48
5f	372	470	98	0.51
DCM				
3a	372	456	84	0.37
3b	371	460	89	0.43
3c	365	452	87	0.42
3d	368	462	94	0.40
3e	372	450	78	0.47

3f	370	461	91	0.41
3g	378	467	89	0.50
3h	364	456	92	0.57
3i	362	452	90	0.45
3j	372	466	94	0.49
3k	377	460	83	0.45
3l	382	463	81	0.42
3m	380	465	85	0.49
3n	372	463	91	0.44
5a	386	480	94	0.60
5b	378	466	88	0.52
5c	377	460	83	0.54
5d	370	467	97	0.47
5e	378	462	84	0.48
5f	380	471	91	0.51
$CHCl_3$				
3a	368	452	84	0.37
3b	370	456	86	0.43
3c	366	450	84	0.42
3d	378	466	88	0.40
3e	373	465	92	0.47
3f	381	470	89	0.41
3g	378	458	80	0.50
3h	375	462	96	0.57
3i	366	462	96	0.45
3j	368	462	94	0.49
3k	380	470	90	0.45
3l	379	467	88	0.42
3m	379	474	95	0.49
3n	385	473	88	0.44
5a	376	467	91	0.60
5b	372	460	88	0.52
5c	368	467	99	0.54
5d	376	460	84	0.47
5e	375	452	77	0.48
5f	376	464	88	0.51

References

1. H. A. Benesi, J. H. Hildebrand, *J. Am. Chem. Soc.*, **1949**, *71*, 2703-2707.